EFFECTS OF HIGH LEVELS OF STEAM ADDITION ON NO_x REDUCTION IN LAMINAR OPPOSED FLOW DIFFUSION FLAMES

by

Linda G. Blevins

Thesis submitted to the Faculty of the

Virginia Polytechnic Institute and State University

in partial fulfillment of the requirements for the degree of

MASTER OF SCIENCE

in

Mechanical Engineering

APPROVED:

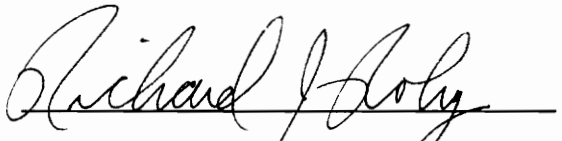

R.J. Roby, Chairman

L.A. Roe

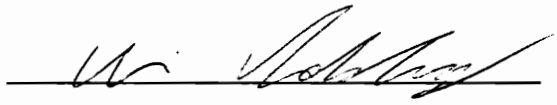

U. Vandsburger

May, 1992

Blacksburg, Virginia

EFFECTS OF HIGH LEVELS OF STEAM ADDITION ON NO_X REDUCTION IN LAMINAR OPPOSED FLOW DIFFUSION FLAMES

by

Linda G. Blevins

Committee Chairman: Richard J. Roby
Mechanical Engineering

(ABSTRACT)

A "leveling off" trend in NO_X emissions with high amounts of steam addition has been observed in industrial gas turbine diffusion flame combustors. Experiments were performed to try to reproduce this trend in a laminar, opposed flow diffusion flame burner. Experiments were performed with CH_4, C_2H_4, CO, CO/H_2 (1:1), and CO/H_2 (1:2) as fuels. Both hydrocarbon fuels and non-hydrocarbon fuels were tested to study the contribution of the Fenimore mechanism to the "leveling off" trend. Probe sampling with chemiluminescent analysis was used to find NO_X concentrations; Pt/PtRh thermocouples corrected for radiation losses were used to measure flame temperatures.

The experiments reproduced the "leveling off" of NO_X emissions, but a "leveling off" of temperatures also occurred. There were no significant differences in the results from the hydrocarbon and non-hydrocarbon fuels. The "leveling off" of NO_X emissions is attributed to the "leveling off" of temperatures in the burner. It is not necessary to invoke the Fenimore mechanism to explain this trend. At least 55% of the NO_X was eliminated from the flames using steam injection, which implies that at least 55% of the NO_X was formed by the Zeldovich mechanism. Evidence of Fenimore NO was provided by the fact that the existence of hydrocarbon coking on the fuel nozzle encouraged NO_X production in all flames.

ACKNOWLEDGEMENTS

I am proud to acknowledge Dr. Rick Roby for his guidance and leadership on this project. I would especially like to thank Rick for giving me the opportunity to travel to many technical meetings, where I made professional contacts which will be priceless during my career. I would like to acknowledge the National Science Foundation for their financial support.

I would also like to thank my parents, Martha and Lonnie Akers, and my sister, Vicki Akers, for the love and support that they gave me. My family will be proud that I "kept my chin up" and survived.

Thanks to the two undergraduate assistants assigned to this project, Mike Foust and Ben Tritt. I hope that observing me hasn't frightened them away from graduate school. Thanks to the machinists, especially Jerry Lucas and Johnny Cox. Thanks also to the helpful employees in the instrumentation shop, Ben Poe, Frank Caldwell, Randy Smith, and Billy Shepherd. Also, thanks to Willie Hylton for all of her help.

I want to thank the graduate students of 117 Randolph Hall, Dan Gottuk, Jim Hunderup, Michelle Peatross, Doug Wirth, and James Reaney, for the lively conversation and help on my project. I also appreciate the input given to me by the members of the combustion group at Virginia Tech. I hope that the Wednesday afternoon seminars continue to be successful in the years to come.

Finally, I thank my happy hour buddies, past and present. Happy hours kept me sane and kept me laughing. The most important of these people were Allen Clem, Patrick Jessee, Eric Albright, Jeff Stastny, Sandy Poliachik, Emily Scott, Tina Handlos, Jim Hunderup, Barry Williams, and Michelle Peatross. Cheers to all of you.

LIST OF FIGURES

LIST OF TABLES

TABLE OF CONTENTS

CHAPTER 1: INTRODUCTION

1.1. Background

Nitrogen oxides (NO_X) are difficult to eliminate from industrial gas turbine diffusion flame combustors. The constituents of NO_X are nitric oxide (NO), nitrogen dioxide (NO_2), and nitrous oxide (N_2O). Nitrogen oxides are eye and lung irritants, and they can be fatal if inhaled in large concentrations. They may also lead to the formation of photochemical smog and acid rain. Because of these negative effects of NO_X, the United States Environmental Protection Agency (EPA) and several state and regional authorities restrict the amount of NO_X which can be emitted by an industrial gas turbine. Currently, the most common way of meeting requirements for NO_X emissions is to inject water or steam into the combustion chambers of the turbines [1].

Traditionally, water injection has worked very well to reduce NO_X emissions to government required levels [2,3,4]. Older combustors have been successfully retro-fitted with water injection systems to meet emissions requirements. However, recently even more stringent regulations on NO_X emissions have been enacted or proposed in several states, and the EPA is considering tougher national standards.

Many gas turbine operators are now finding that water or steam injection alone does not suppress NO_X concentrations to the new lower required levels [5]. In these cases, NO_X concentrations initially decline with water addition, but reach a minimum at high amounts of water addition. Profiles of NO_X concentration as a function of water flow rate "level off" at this minimum. This "leveling off" is shown qualitatively in Fig. 1. Toof [6] presented experimental results obtained from a field test of a 25-MW combustion turbine which showed this "leveling off".

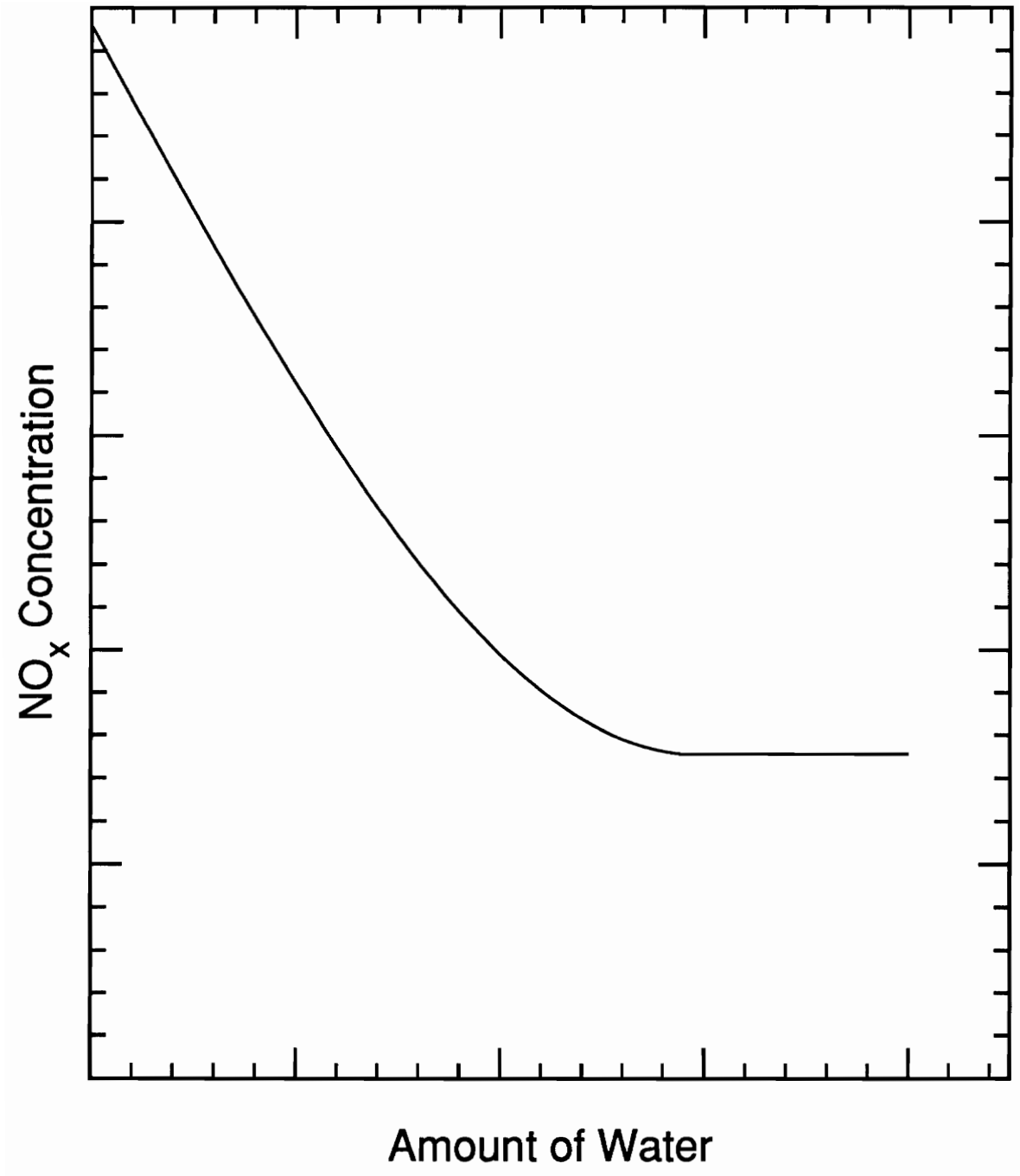

Figure 1. Qualitative "leveling off" of NO_x concentrations (after Toof [6]).

It is believed that the effects of water injection on NO_X reduction are thermal in nature. Injected water acts as a heat sink, which lowers flame temperatures. This reduces the amount of NO_X formed.

Past studies have not directly addressed the "leveling off" of NO_X emissions in industrial gas turbine diffusion flame combustors. There are several possible reasons for the behavior of NO_X emissions with high amounts of water injection. One possibility is that the water may begin to participate chemically in the combustion reactions. Another theory is that some of the water injected may bypass the flame front. A third potential reason is that some of the NO_X may be formed by a chemical mechanism which is insensitive to temperature suppression. Research is needed to find out why high amounts of water are ineffective at reducing NO_X emissions. Investigation of this problem requires knowledge of two of the chemical mechanisms responsible for the formation of NO_X.

1.2. NO Formation

1.2.1. Zeldovich NO

Most of the NO_X formed in industrial gas turbine combustors is formed as nitric oxide (NO). Traditionally, the main source of NO formation in diffusion flame combustors was believed to be the Zeldovich mechanism, which begins when an oxygen atom (O) combines with a nitrogen molecule (N_2). The Zeldovich mechanism consists of the following reactions [7]:

$$O + N_2 = N + NO \tag{1.1}$$

$$N + O_2 = O + NO \tag{1.2}$$

A third reaction thought to be important in fuel rich areas of flames follows [8]:

$$N + OH = H + NO \tag{1.3}$$

The rate constants for the Zeldovich reactions are well known. The overall rate of NO production from this mechanism has been shown to be a strong function of temperature.

Touchton [9], in a study of low to moderate amounts of water addition, concluded that the effects of water were entirely thermodynamic. Touchton compared data obtained from several gas turbine combustors incorporating water addition with predictions from both an equilibrium chemical thermodynamics model and a chemical kinetics model. His comparisons showed that the experimental data was best predicted by the equilibrium calculations. However, Touchton's experiments used water addition levels below those necessary to achieve current and proposed NO_X emissions requirements. Thus, he did not study the conditions where NO_X emissions begin to "level off."

1.2.2. Fenimore NO

One possible explanation for the "leveling off" is that the water or steam participates chemically in the combustion reactions. Miyauchi et. al. [10] performed a study of the effects of steam injection into methane-air premixed flames. In their experiments, temperature was held constant over a range of steam injection rates. Miyauchi found that steam does have a chemical kinetic effect on NO reduction which is independent of the temperature suppression effect. NO concentrations were reduced with increasing steam injection, even though temperatures were kept constant. Miyauchi suggested that some of the NO in their premixed flames was formed by the "prompt NO" mechanism.

"Prompt NO" was first discovered by C.P. Fenimore [11], and hence will be called Fenimore NO. Fenimore studied both hydrocarbon and non-hydrocarbon premixed flames. He found that profiles of NO_x concentrations versus residence time in hydrocarbon flames could not be extrapolated to zero ppm at zero time. However, NO_x concentration in non-hydrocarbon flames did extrapolate to zero ppm at zero time. Fenimore proposed that the "intercept NO" which was predicted at zero time in the hydrocarbon flames was formed very rapidly in the reaction zone by reactions involving hydrocarbon fuel fragments (CH, CH_2, etc.).

Fenimore NO formation is initiated when a hydrocarbon fuel fragment reacts with a nitrogen molecule (N_2). Typical Fenimore reactions follow [12]:

$$CH + N_2 = HCN + N \tag{1.4}$$

$$CH_2 + N_2 = HCN + NH \tag{1.5}$$

$$C_2H + N_2 = HCN + CN \tag{1.6}$$

$$C_2 + N_2 = CN + CN \tag{1.7}$$

The nitrogen species created by these reactions are rapidly converted to NO. Miyauchi hypothesized that adding steam to their premixed flames increased hydroxyl (OH) radical concentrations, which promoted hydrocarbon fragment oxidation. This kept the hydrocarbon fragments from forming Fenimore NO. Thus, there was a reduction of NO due to the chemical effect of adding the steam.

1.2.3. Fenimore NO in Premixed Flames

Many studies of Fenimore NO have been performed using premixed flames. Most research has shown that Fenimore NO is important only in fuel rich premixed flames

[11,13,14]. However, some studies have predicted that it will possibly form in fuel lean premixed flames [15,16].

The importance of the Fenimore NO mechanism was questioned by Bowman [8] and Sarofim and Pohl [17]. Both of these studies concluded that the rapid formation of flame front NO could be explained by the Zeldovich mechanism if the existence of superequilibrium oxygen atom (O) concentration was considered. However, several researchers have found that the O atom concentrations would have to be unreasonably in excess of equilibrium amounts to account for the rapid formation of NO formed in the flame front [13,15,18,19].

One study which provides convincing evidence of Fenimore NO was performed by Hayhurst and Vince [12]. They compared NO formation in premixed $H_2/O_2/N_2$ flames with NO formation in the same flames with 1% added acetylene (C_2H_2). They saw a sharp increase in the flame front NO formation rate with the added hydrocarbon. This indicated the formation of Fenimore NO. Hayhurst and others have tried to determine which reactions are most important in the Fenimore mechanism and to obtain expressions for the rates of these important reactions [12,20,21,22]. However, the rates of the Fenimore mechanism are not as well known as those of the Zeldovich mechanism.

All of these past investigations have been performed using premixed flames. The importance of the Fenimore NO mechanism in diffusion flames has not been studied as extensively.

1.2.4. NO in Turbulent Diffusion Flames

Results from several studies of NO formation in turbulent diffusion flames have been published. These studies dealt with the dependence of NO formation on fluid

mechanics quantities, such as the Froude number, the Reynolds number, and the turbulent length scales [23,24,25,26]. Emphasis has been placed on the effects of superequilibrium radical concentrations on NO formation by the Zeldovich mechanism [27]. Results from much of the work have been distorted by probe difficulties [23,27].

Very little emphasis has been placed on studying Fenimore NO in turbulent diffusion flames. However, Takagi et al. [25] suggested that Fenimore NO may be more important in diffusion flames than it is in premixed flames. Takagi found that HCN concentrations were higher for hydrocarbon diffusion flames than for hydrocarbon premixed flames. He hypothesized that hydrocarbon fragments survive for longer periods of time in diffusion flames than they do in premixed flames. These hydrocarbon fragments participate in the Fenimore mechanism to produce NO. Thus, Takagi concluded that the Fenimore mechanism may be significant in turbulent diffusion flames.

1.2.5. NO in Laminar Diffusion Flames

Turbulent diffusion flames are difficult to study experimentally and theoretically. As a result, many researchers study laminar diffusion flames. Information from laboratory laminar diffusion flames can be used to analyze turbulent diffusion flames. One theory which has been proposed is the "laminar flamelet theory" [28]. The laminar flamelet theory is based upon the assumption that laminar, counterflow diffusion flames exhibit the same scalar behavior as some turbulent diffusion flames. Laminar flamelet theory involves studying scalar parameters of a laminar, counterflow flame, or "flamelet." The theory involves applying these scalar parameters to a turbulence model by predicting the probability that these flamelets will occur in a turbulent diffusion flame. The scalars used to describe the flamelet are the mixture fraction and the instantaneous scalar dissipation rate. Thus, the "laminar flamelet theory" uses information obtained

from laminar diffusion flames to model and understand turbulent diffusion flames. Some success has been achieved with the laminar flamelet theory by Drake et. al.[29]. Extrapolation of data from laminar diffusion flames must be done carefully, as the laminar flamelet theory does not always apply.

Counterflow diffusion flames have been discussed thoroughly and classified by Tsuji [30]. A laminar, opposed flow diffusion flame consists of opposing streams of fuel and oxidizer. A flame is established on the oxidizer side of the stagnation plane where the two streams meet. The fluid mechanics and chemistry of this type of flame have been successfully modeled [31]. The model uses potential flow assumptions and well-known chemical mechanisms.

Counterflow diffusion flames are useful for fundamental diffusion flame chemistry studies. Drake and Blint used modeling and experiments with laminar, opposed flow diffusion flames to evaluate the relative importance of the Zeldovich and Fenimore NO formation pathways in diffusion flames [32]. They concluded that more than two-thirds of the NO formed in their diffusion flames was a result of the Fenimore NO mechanism. Based on this conclusion, Drake and Blint suggested that the Fenimore mechanism may also be very important in turbulent diffusion flames.

1.2.6. Comparison of Zeldovich and Fenimore NO

It is important to contrast the Zeldovich mechanism with the Fenimore mechanism. These two mechanisms are very different. Zeldovich NO is formed in the hot post-flame gases. The amount of Zeldovich NO is a strong function of the peak temperature and residence time in these post-flame gases. Fenimore NO, however, is formed very rapidly in the flame front of hydrocarbon flames. Zeldovich NO requires only air at high temperatures, while Fenimore NO requires the presence of fuel fragments and air.

Zeldovich NO is a function of peak temperature; Fenimore NO is dependent on the hydrocarbon content of the fuel.

The past studies of Touchton [9] and Drake and Blint [32] have addressed the relative importance of these two NO formation mechanisms. The conclusions of these two studies seem to contradict each other. Touchton found that water injection worked entirely by a thermodynamic effect. He concluded that the Zeldovich mechanism was very important in diffusion flames. However, Drake and Blint concluded that the Fenimore mechanism was very important in their diffusion flames. Touchton would not predict the "leveling off" of NO_X emissions with increasing amounts of water; Drake and Blint would predict that the "leveling off" is due to the existence of Fenimore NO. Because of this conflict, additional research is needed to discover which of these studies best predicts the behavior of diffusion flames using high amounts of water injection.

1.3. Scope of the Current Work

The overall objective of this project is to determine if water injection can be used to meet new, lower NO_X emissions requirements, or if the "leveling off" of NO_X emissions with increased water addition represents a fundamental limit for NO_X reduction by water addition. This project will involve comparison of experimental results with chemical kinetic modeling results. This particular thesis deals with the experimental portion of the project.

The scope of this thesis is to report on experiments which were performed to try to reproduce the "leveling off" of NO_X concentrations in diffusion flames with high levels of steam injection in a laboratory burner. One focus of this investigation was to try to resolve the apparent conflict between the conclusion of Touchton that the Zeldovich mechanism is most important in turbulent diffusion flames and the conclusion of Drake

and Blint that the Fenimore mechanism is most important in diffusion flames. Since Fenimore NO will only form in hydrocarbon flames, the experiments presented in this thesis involved injecting steam into both hydrocarbon and non-hydrocarbon diffusion flames. Results from hydrocarbon flames and non-hydrocarbon flames with steam addition will be compared to determine if the "leveling off" of NO_x concentrations is a result of the Fenimore NO mechanism.

CHAPTER 2: EXPERIMENTAL APPARATUS AND PROCEDURE

2.1. Introduction

The opposed flow diffusion flame burner and steam generator are described in the first two sections of this chapter. The next section describes the instrumentation used for collecting data in the experiments. The final section describes the procedure followed for performing experiments.

2.2. Experimental Apparatus

2.2.1. Burner Design

The experimental apparatus used for this study was a laminar, opposed flow diffusion flame burner. Detailed shop sketches and drawings of the parts of the burner are shown in Appendix A. A schematic of the burner is shown in Fig. 2. The burner included flow straighteners for both the fuel and air streams, and thus produced a "Type II" flame, according to the classification by Tsuji [30]. Air flowed in the upward direction, fuel flowed in the downward direction, and a flame was established on the air side of the stagnation plane.

The air side of the burner consisted of a 32 cm diameter sheet metal housing. The contents of the housing were flow straightening devices separated and held in place by pieces of 32 cm diameter poly-vinyl chloride (PVC) pipe. The outer diameter of the PVC pipe was machined to a size slightly smaller than the inner diameter of the housing, so that the pieces of pipe fit right into the housing. The arrangement of the flow straighteners is shown in Fig. 3.

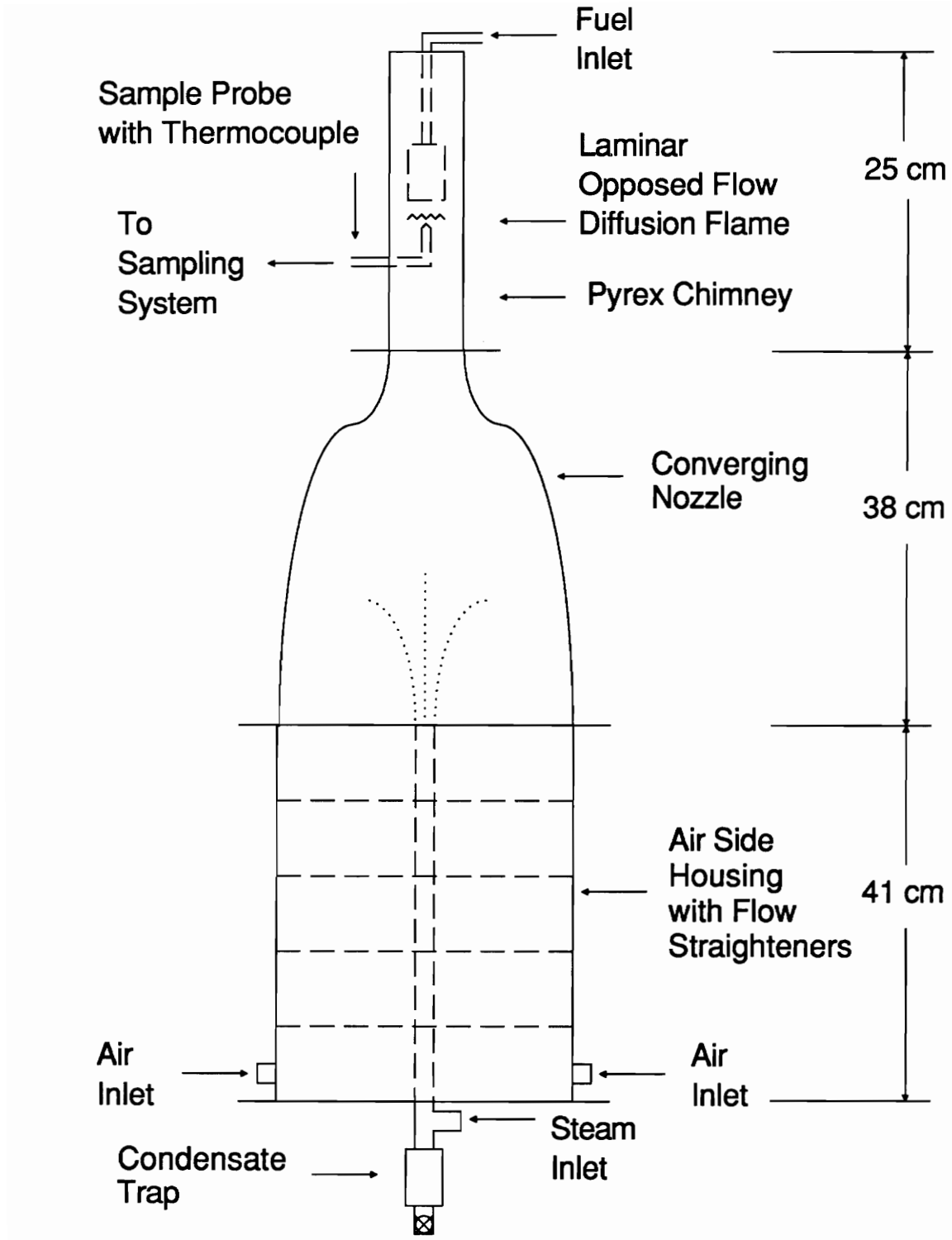

Figure 2. Schematic of opposed flow diffusion flame burner.

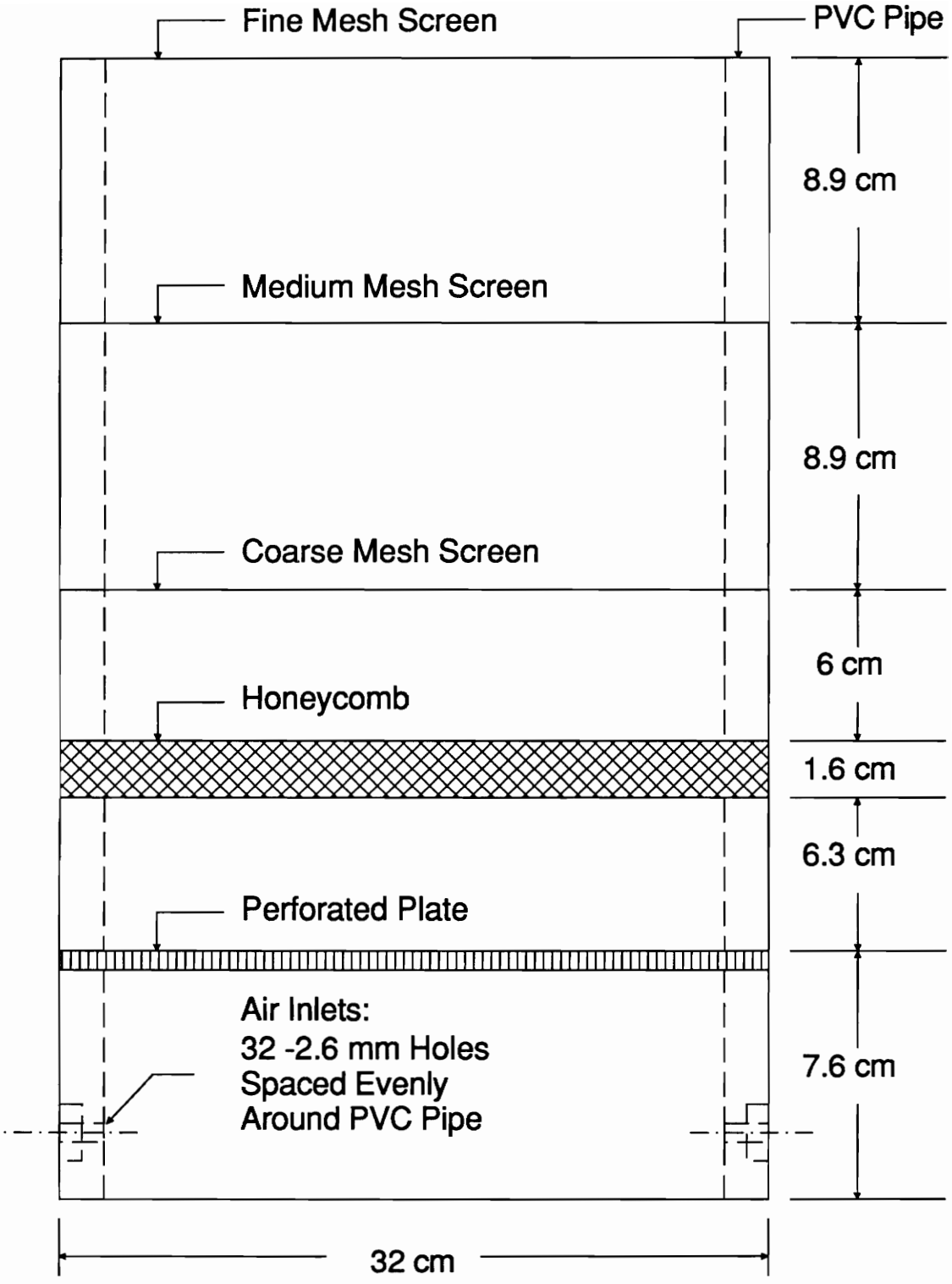

Figure 3. Arrangement of flow straighteners on air side of burner.

There were four 10 mm air inlets, spaced evenly around the radius of the lower portion of the housing. A piece of PVC pipe was placed in the bottom of the burner. A groove was machined around the outside of the pipe, with 32 holes of 2.6 mm diameter drilled in this groove. The purpose of this pipe was to distribute the four large incoming air streams into 32 tiny evenly spaced air streams.

The air side housing also contained perforated plate, honeycomb, and coarse, medium, and fine mesh stainless steel screens. These items were cut into circular pieces which were 32 cm in diameter. The stainless steel perforated plate was 3 mm thick with 3.8 mm holes drilled at evenly spaced locations, while the honeycomb was 16 mm thick.

The coarse, medium, and fine screens were stretched across and attached with screws to pieces of PVC pipe. Felt gaskets were placed between all of the pieces of PVC pipe to seal the air side of the burner. The inner diameter of the PVC pipe matched the inner diameter of the next piece of flow straightening equipment, the converging nozzle.

The fiberglass converging nozzle was mounted on top of the air side housing using nuts and bolts, with a felt gasket used as a seal. The function of the converging nozzle was to smoothly reduce the diameter of the air flow stream from 32 cm to 7 cm. The nozzle was constructed by shaping fiberglass over a wooden mold. The mold was formed by glueing several poplar planks together, and then machining the poplar to the proper shape. Finally, several coatings of polyurethane lacquer were applied to keep the surface of the mold smooth. The fiberglass was then formed over the mold, creating a smooth inner surface of the burner to prevent flow disturbance. The inner diameter of the converging nozzle was matched to the next section in the air stream, the Pyrex chimney.

The chimney was made of a 25.4 cm long, Pyrex tube with a 7.5 cm outer diameter and a 7 cm inner diameter. The Pyrex chimney sat in a groove in an aluminum flange.

The flange was mounted with nuts and bolts to a flange on top of the converging nozzle. A 13 mm diameter O-ring was used to seal the connection. The groove on the flange was sized slightly larger than the chimney, so that the chimney could be easily removed. The lip of the groove was tall enough to keep the chimney from falling off of the burner.

A vertical slot was cut into the side of the Pyrex chimney. The approximate dimensions of the slot were 0.4 cm by 10.3 cm. The purpose of this slot was to provide an opening for inserting a sample probe and a thermocouple. Due to limited glass cutting facilities, the slot had to be cut much longer than necessary. This was the only way to make the slot wide enough to hold the probe. In order to prevent entrainment of room air or flow disturbance through this long slot, a piece of duct tape was placed over the portion of the slot which was not occupied by the probe and thermocouple.

A fuel nozzle was suspended into the Pyrex chimney using a 5 mm stainless steel tube. The fuel was delivered to the nozzle through this tube. A schematic of the fuel nozzle is shown in Fig. 4. The fuel nozzle consisted of an uncooled stainless steel cylinder that was 38 mm in diameter. The fuel exited the nozzle through 147 evenly spaced, 1.6 mm diameter holes in the flat end of the cylinder. This produced 147 tiny jets which combined to create a flat, uniform fuel supply. The cylinder was filled with 100 stainless steel beads of 2.6 mm diameter. The purpose of these beads was to create plug flow rather than Poisselle flow exiting the fuel nozzle.

2.2.2. Steam Generator

The method of water addition used in these experiments was steam injection. A schematic of the steam generator setup is shown in Fig. 5. The steam generator consisted of a 5.4 cm diameter cylindrical stainless steel chamber which contained a heating coil. The lower half of the heating coil was designed to heat water; the upper half was

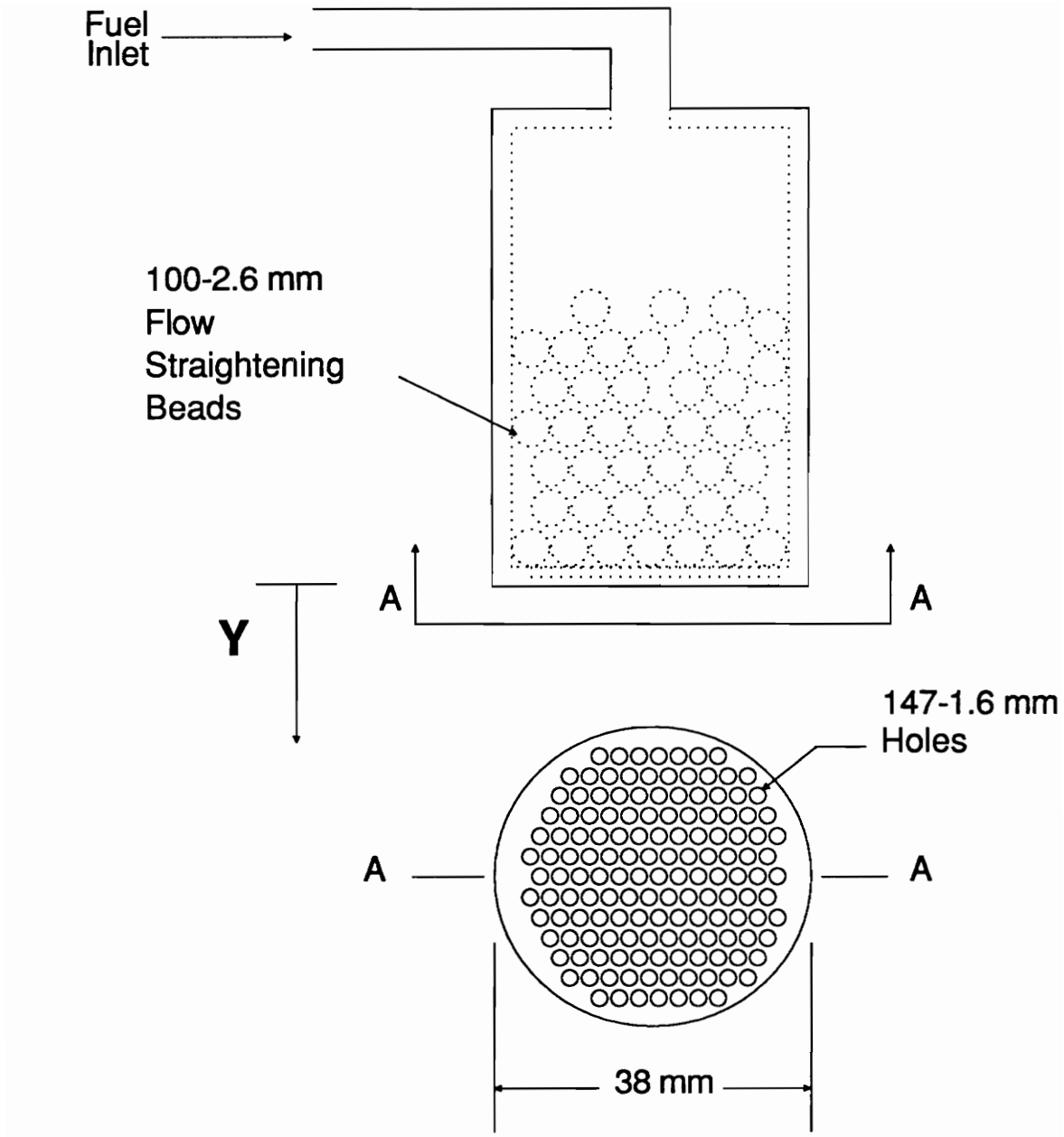

Figure 4. Schematic of fuel nozzle.

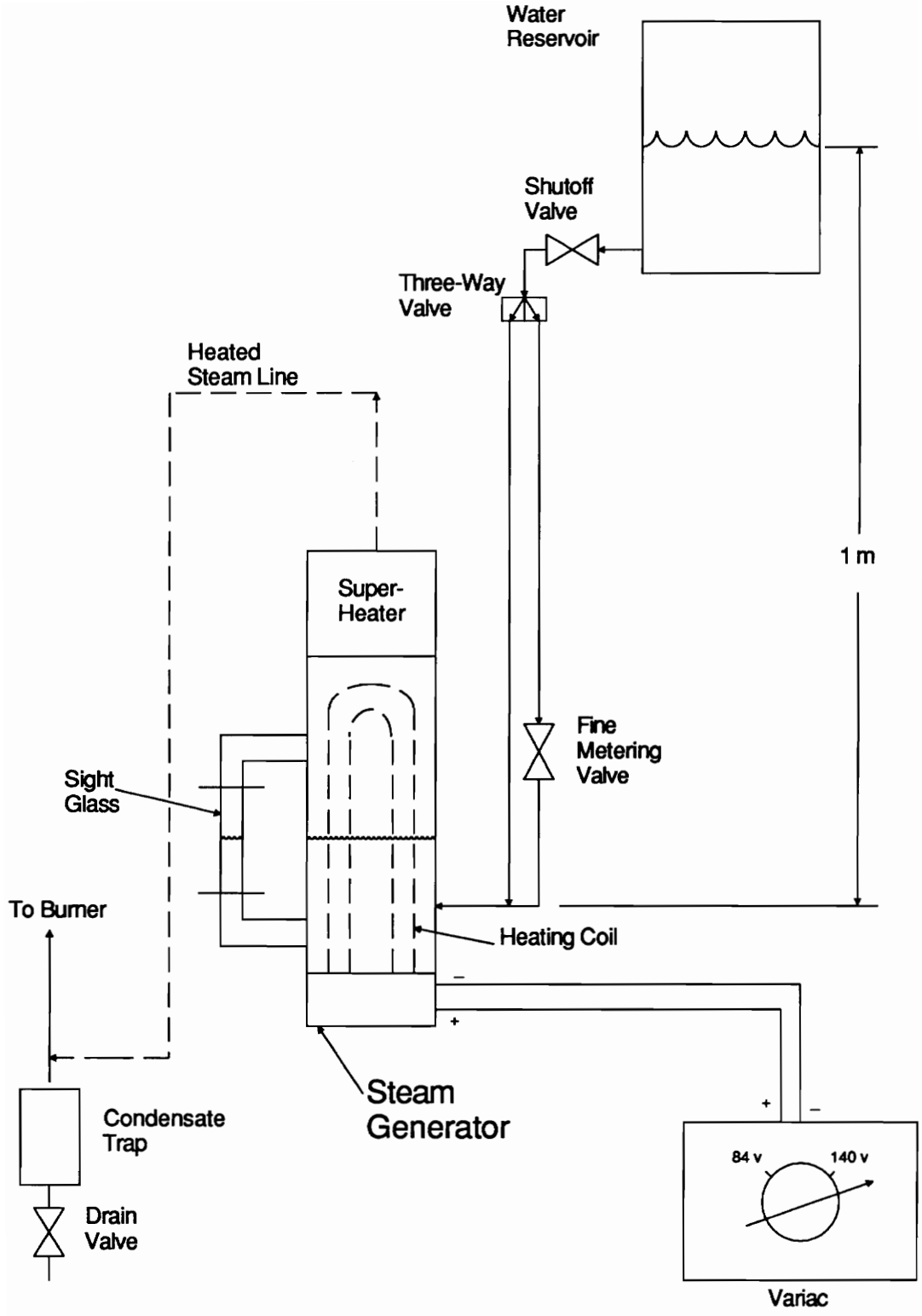

Figure 5. Schematic of steam generator setup.

designed to heat steam. The steam generator was equipped with a sight glass for visual observation of the water level. The steam flow rate was controlled by using a variac to change the amount of heat input to the steam generator. A small superheater was mounted at the exit of the steam generator.

Distilled water was fed by gravity through 5 mm polyethylene tubing to the steam generator. The feedwater reservoir was a 400 ml glass beaker. The water in the reservoir was refilled periodically to keep the water at the 200 ml level in the beaker, which corresponded to a height of about 1 m above the point of entry into the boiler. The water flow rate was controlled using a NUPRO fine metering valve, part number SS-SS4-A, with a NUPRO vernier handle, part number NY-2M-K6.

The fine metering valve was calibrated using a 10 ml graduated cylinder and a stopwatch. For each position of the vernier handle, the water flowing through the valve was allowed to drip into the graduated cylinder. The dripping was timed using a stopwatch, and the mass flow rate of the water was calculated. A calibration curve of water flow rate as a function of the number of turns of the vernier handle is shown in Appendix B.

Once the fine metering valve was calibrated, the variac could be calibrated. For each setting of the variac, ranging from 84 V to 140 V, the position of the fine metering valve was varied until a point was reached when the water level in the steam generator sight glass remained constant. This assured that the water flow into the boiler matched the steam flow out of the boiler. Thus, since the water flow rate was known, the steam flow rate was also known. A calibration curve of steam flow rate as a function of variac setting is shown in Appendix B.

For this experiment, variac settings from 84 V to 140 V were used. The reason that the lower limit for the variac was 84 V was that this was the lowest setting of the variac for which steam could be generated. The upper limit was chosen because, at settings above 140 V, the steam entering the burner contained large amounts of liquid water.

Steam was delivered to the burner in a heated, 8 mm stainless steel tube. The tube was heated by Thermolyne silicone rubber heating tape (Fisher Scientific part number 11-463-54B). There was a condensate trap at the lowest point in the steam line. This trap was a 4.1 cm diameter steel cylinder with a drain valve.

Steam was injected on the air side of the burner, after the flow straightening screens but before the converging nozzle. The steam was injected in this location to avoid condensation on the flow straightening screens. Steam flowed from the heated tube into the center of the bottom of the air side housing. An unheated tube extended from the bottom of the housing to the entrance of the converging nozzle. Holes were cut in the center of the flow straightening devices so that the tube could be inserted into the burner. Once the steam exited this unheated tube, it was entrained into the air stream. Visual observation of the steam and air with a laser sheet proved that the steam and air were well mixed before they contacted the flame front.

2.3. Instrumentation

A schematic of the entire experimental setup is shown in Fig. 6. Five cylinders of breathing air were used simultaneously as the air supply for the burner. The breathing air was mixed at an Airco facility from O_2 and N_2. The specifications of this mixture were that it contained from 19.5% to 23.5% O_2, and that it contained no more than 3 ppm of moisture. The outlets from the five cylinders were combined into one stream with stainless steel pigtails (Airco part number PF-346) and a brass manifold (Airco part

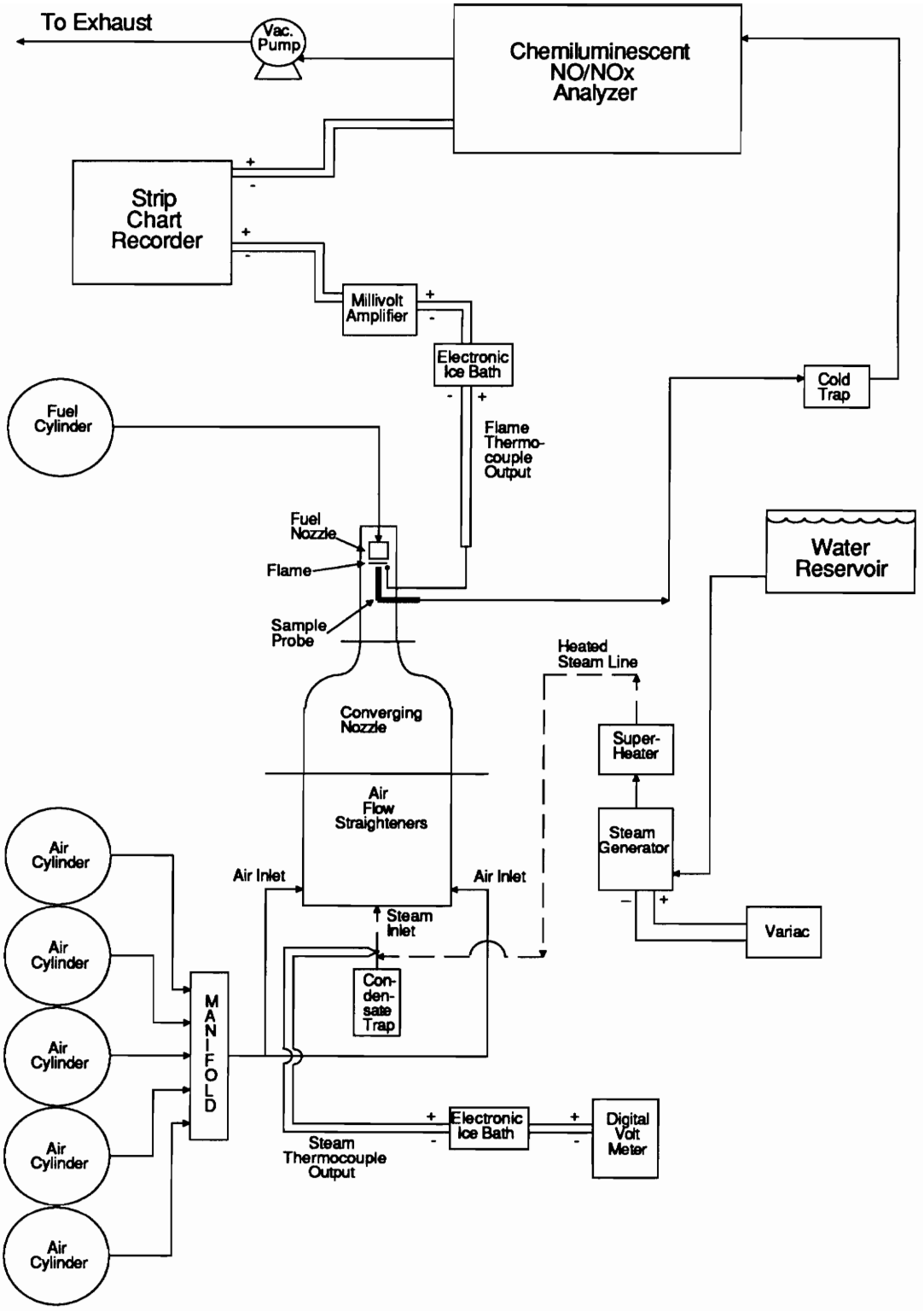

Figure 6. Schematic of experimental setup.

number MB-346). Air flow rate was measured using a Matheson 605 series rotameter tube. The air was delivered to the rotameter at 550 KPa. Air flow rate was controlled using a Matheson size 9 utility metering valve on the exit of the rotameter tube. Air was delivered to the burner in 8 mm polyethylene tubing.

The fuels burned in these experiments were methane (CH_4), ethylene (C_2H_4), carbon monoxide (CO), 50 mol% carbon monoxide with 50 mol% hydrogen (CO/H_2, 1:1), and 33 mol% carbon monoxide with 67 mol% hydrogen (CO/H_2, 1:2). The CH_4 used was Airco Grade 1.3, which is 93% pure. The C_2H_4 used was Airco Grade 2.5 which is 99.7% pure. The CO used was Airco Grade 2.3, which is 99.3% pure. The H_2 used was Airco Commercial Grade, which is 99.8% pure. As a safety precaution, small CO detectors (Sporty's Pilot Shop #4116A) were placed around the laboratory. These detectors are designed to change color when the concentration of CO in the air becomes dangerous.

The two hydrocarbon fuels and three non-hydrocarbon fuels chosen for these tests were used because Fenimore NO only forms in hydrocarbon flames. Thus, contrasting the NO trends of hydrocarbon flames with those of non-hydrocarbon flames would provide information about whether or not the achieved minimum NO concentrations were a result of the Fenimore mechanism. There were two reasons that the mixtures of CO and H_2 were chosen for these tests. First, the CO/H_2 (1:2) mixture was used to create a non-hydrocarbon fuel with the same ratio of H atoms to C atoms as the hydrocarbon fuel of CH_4. Second, the mixtures of CO and H_2 were chosen to simulate the products of coal gasification, since gasified coal is now being used as a fuel in some industrial gas turbines [33].

Methane and C_2H_4 were delivered at 280 KPa to a Matheson 602 series rotameter tube. Both of these fuel flow rates were controlled with Matheson high accuracy HA-3 metering valves. Carbon monoxide was delivered at 140 KPa to a Matheson 602 series rotameter tube, and the flow rate was controlled with a Matheson size 7-LOW metering valve. Hydrogen was delivered at 140 KPa to a Matheson 602 series rotameter tube, and the flow rate was controlled with a Matheson high accuracy HA-3 metering valve. Carbon monoxide and H_2 were mixed after the rotameters using a Swagelok tee. All fuels were delivered to the burner in 5 mm polyethylene tubing.

All rotameters were calibrated using a dry gas meter (DGM) and a stopwatch. For each setting of the rotameter, the time that it took for a known volume to pass through the DGM was recorded. The volumetric flow rates could then be calculated. These flow rates were corrected for standard temperature and pressure. Calibration curves for this experiment are given in Appendix B.

An uncooled quartz probe was chosen for these experiments because conversion of NO to NO_2 is less likely to happen in uncooled quartz probes than it is to happen in other types of probes [27]. A schematic of the 3 mm uncooled quartz sample probe used in these experiments is shown in Fig. 7. The sample was pulled through the probe into a stainless steel section of 5 mm tubing, and then through polyethylene tubing to a condensate trap. The condensate trap consisted of an Erlenmeyer flask with an inlet through a hole in a rubber stopper on top and an outlet through a nipple on the side. The flask was submerged in a bath of ice water. The sample flowed into the top of the flask, the water condensed out, and the dry gases flowed out of the nipple.

After the sample left the condensate trap, it was introduced into a Thermo-Environmental Model 10 Chemiluminescent NO-NO_2-NO_x analyzer. A Sargent-Welch

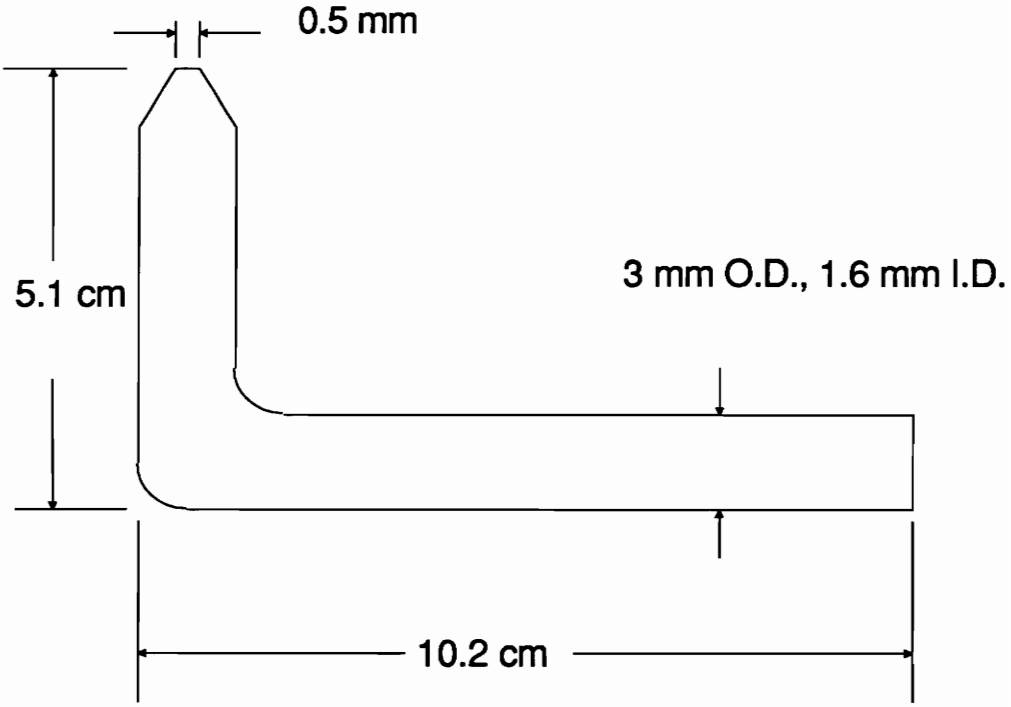

Figure 7. Schematic of quartz sample probe.

Model 399 vacuum pump pulled the sample gases through the analyzer. The NO_X analyzer was zeroed with room air and calibrated with a certified Airco mixture of 240 parts per million (ppm) NO in N_2 background. The same cylinder of span gas was used for all calibrations. The 0-10 V output of the NO_X analyzer was recorded on channel 1 of an Astro-Med DASH II model MT two-channel, thermal-array strip chart recorder (Astro-Med part number 223834220). The gain on channel 1 of the strip chart recorder was set at 0.2 V/div, with a 50 division grid. The strip chart recorder was zeroed and spanned using the zero and full scale settings on the NO_X analyzer. An uncertainty analysis revealed that NO and NO_X measurements were accurate to within 1.4%. The uncertainty analysis is shown in Appendix D.

Uncoated Platinum-Platinum 10% Rhodium (Pt/Pt10%Rh, Type S) fine wire thermocouples (OMEGA #P10R-005-7) were used to measure flame temperature. The thermocouple wires were 0.13 mm in diameter. Two different thermocouples were used for these experiments. The bead diameters of the thermocouples were measured with a photomicroscope, and were found to be 0.34 mm and 0.37 mm. An electronic ice bath, OMEGA type MCJ-S, was used to simulate the ice bath junction.

The thermocouple was mounted on the sample probe with the bead very close to the location of sampling. This provided a spatially consistent temperature measurement. The thermocouple was attached to the probe by threading the 0.13 mm wires of the thermocouple through pieces of 0.72 mm outer diameter quartz tubing. These pieces of tubing were then attached to the quartz sample probe using Aremco alumina ceramic putty #600. A schematic of the thermocouple and sample probe combination is shown in Fig. 8. Since the fine thermocouple wires were not long enough to reach the cold junction compensator, they were welded to 0.25 mm extension wires (Pt-OMEGA #SPPL-010, Pt10%Rh-OMEGA #SP10RH-010).

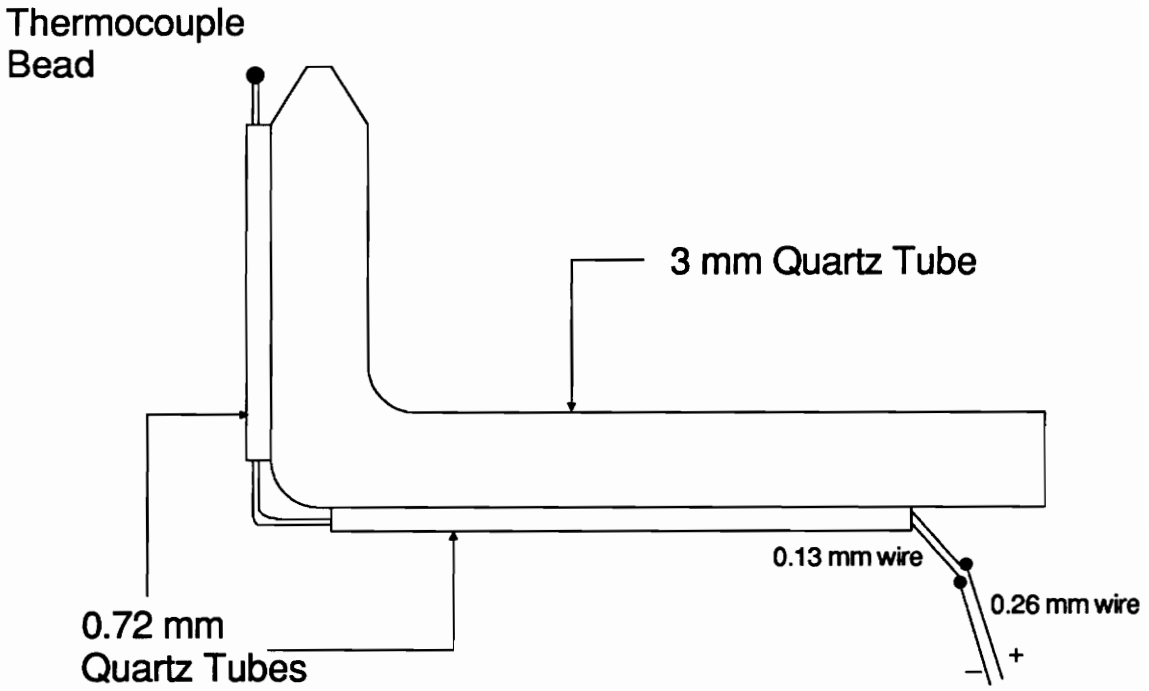

Figure 8. Schematic of thermocouple mounted on sample probe.

The sample probe and thermocouple were attached to a Unislide series A2500 X-Z translation stage. The translation stage was mounted on an optical table. The probe and thermocouple were inserted into the slot in the side of the chimney. Sampling was done vertically along the stagnation plane of the flame, as shown in the location denoted by the black square in Fig. 9. There were no differences in the trends in data collected from this flame front location and data collected in the post flame region. The only difference in the two sampling locations was that the NO_X concentration signals were stronger from the flame front location than from the post flame region. Thus, sampling was performed in the flame front location.

Output from the thermocouple was amplified using an OMEGA model OMNI II-A millivolt amplifier. Typical flame temperatures produced 0-20 mV output from the thermocouple. The gain on the amplifier was set at five, so that its output was 0-100 mV. The amplified thermocouple signal was recorded on channel 2 of the Astro-Med strip chart recorder. The gain for channel 2 of the strip chart recorder was set at 2 mV/div with a 50 division grid. The uncertainty analysis shown in Appendix D revealed that temperature measurements were accurate to within 2.8%.

Since the millivolt amplifier was not completely linear, a calibration was made using a variable voltage source and two voltmeters. For each input voltage to the amplifier, the actual output voltage was recorded. A calibration curve of input voltage versus measured output voltage was generated, and is shown in Appendix B. A sketch of the circuit used to create the variable voltage source is shown in Fig. 10. This circuit was also used to zero and span the strip chart recorder.

The flame temperature thermocouple readings were corrected for radiation losses using a FORTRAN program obtained from Sandia National Laboratories [34]. The

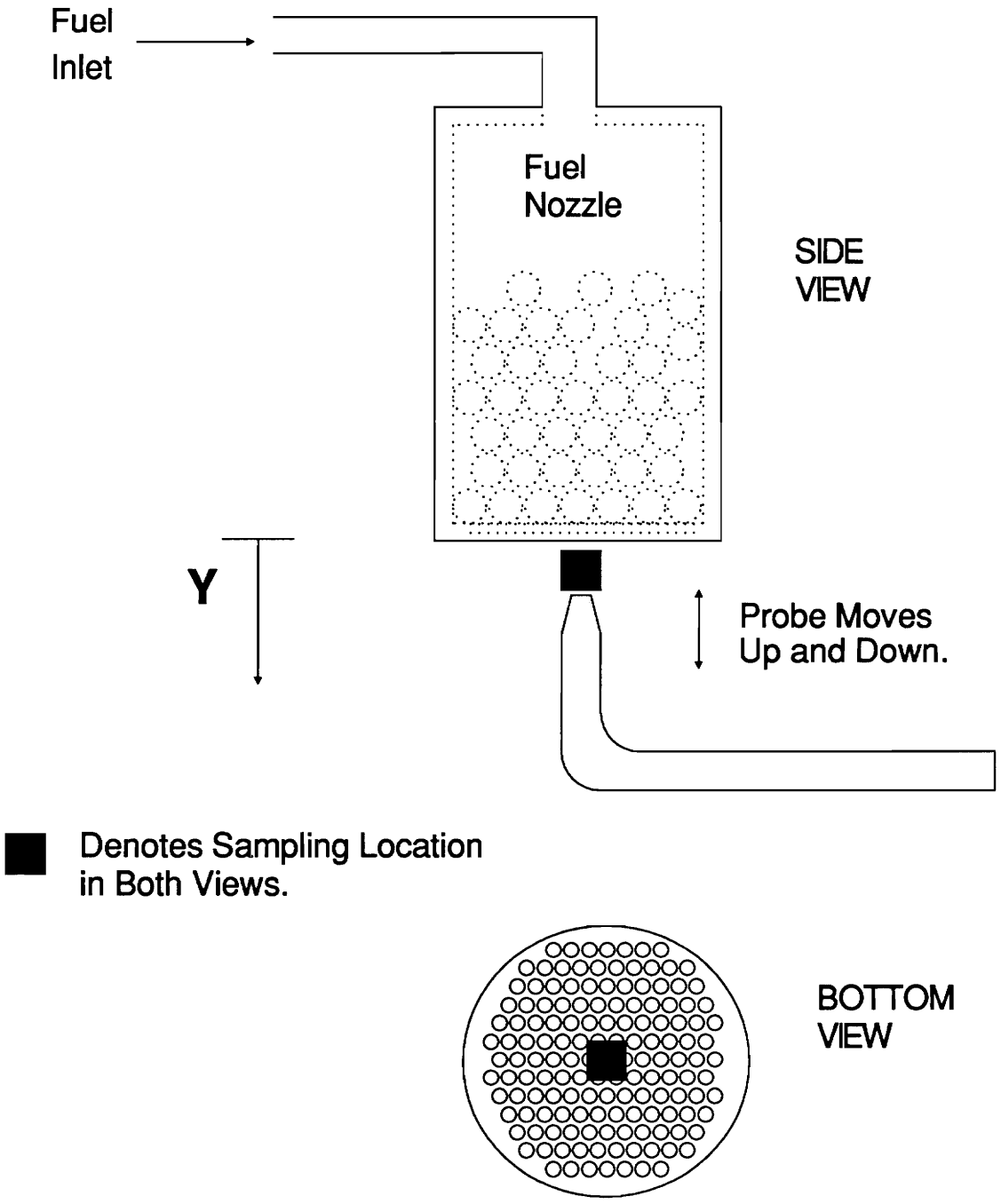

Figure 9. Schematic of sampling location.

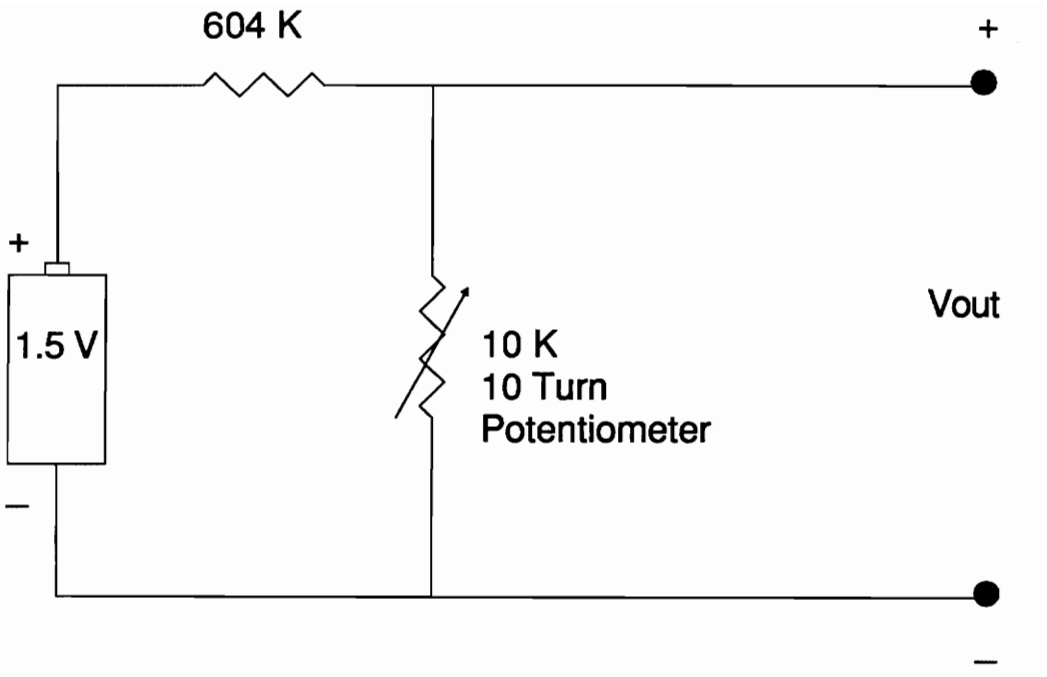

Figure 10. Sketch of variable voltage circuit used for calibrations.

computer program was modified to create the data files needed for these experiments. The program is listed in Appendix C.

A Chromel-Alumel (Type K) thermocouple probe with a stainless steel sheath (OMEGA #KQSS-18G-12) was inserted into the steam line just before the steam entered the burner. An OMEGA type MCJ-K cold junction compensator was used to simulate the ice bath. Output from the thermocouple was visually read from a digital voltmeter. The temperature of the steam before it entered the unheated section of tubing was typically in the range of 378 K to 398 K.

2.4. Experimental Procedure

Different flow rates were used for the five different fuels. These flow rates varied, depending on the stability limits of the fuel in the opposed flow burner. The only exception to this was C_2H_4. The C_2H_4 flow rate was limited by excessive soot formation. The different fuel flow rates are shown in Table 2.1.

In past studies, a common way to operate opposed flow burners was to inject N_2 on the fuel side of the burner [32, 35]. This created higher fuel velocities, which caused the flames to stabilize far away from the fuel nozzle. This made the flames more adiabatic. Thus, injecting N_2 with the fuel produced more stable flames by eliminating the heat losses to the fuel nozzle. However, N_2 was not injected with the fuel in the experiments presented in this thesis so that the N_2 chemistry of the fuel-air diffusion flame would not be disturbed. Thus, the flames in this study stabilized close to the stainless steel fuel nozzle, and were often difficult to stabilize.

The air flow rate was kept constant at 94 sl/min or 121 g/min for all experiments. This was to keep the radial strain rate constant. The average velocity of the air in the

Table 2.1. Fuel Flow Rates

Fuel	Volumetric Flow Rate (sl/min)	Mass Flow Rate (g/min)	Lower Heating Value (MJ/kg)	Maximum Heat Release Rate (KW)
CH_4	0.77	0.55	50	0.46
C_2H_4	0.29	0.36	50	0.30
CO	1.13	1.40	10.1	0.24
CO/H_2 (1:1)				0.31
CO	0.80	1.0	10.1	0.17
H_2	0.80	0.07	120	0.14
CO/H_2 (1:2)				0.22
CO	0.40	0.50	10.1	0.08
H_2	0.80	0.07	120	0.14

chimney was 0.5 m/s. The Reynolds number of the air stream was 2200. The radial strain rate was 13 s^{-1}. The strain rate, "a," was calculated assuming axisymmetric plug flow [36]. The following relationship was used:

$$a = U / 2R \tag{2.1}$$

In this equation, U is the air stream velocity, and R is the radius of the fuel nozzle.

The overall steam flow rates used in these experiments ranged from 2 g/min to 12 g/min. Steam flow measurements were estimated to be accurate to within 1 g/min. As mentioned previously, the air and steam were well mixed when they contacted the flame front. Since the fuel nozzle occupied 30% of the area of the chimney, the assumption was made that 30% of the steam contacted the flame front. Using this assumption, the corrected steam flow rates were 0.6 g/min to 3.6 g/min.

The first step in preparing to collect data was to zero and span the Astro-Med strip chart recorder. Next, the NO_X analyzer was calibrated. For these experiments, the strip chart recorder was operated at 1 mm/s. The flame was ignited and allowed to burn for a few minutes so that the burner could get heated up and the flame could reach steady state. Care was taken to make sure the sample probe was positioned over the center hole at the exit of the fuel nozzle.

During data collection, temperature was measured at 0.5 mm increments through the flame; NO and NO_X were measured in 1 mm increments. An error analysis shown in Appendix D indicated that the distance from the fuel nozzle was known to within 0.5 mm. The first step in collecting data was to move the sample probe up into the flame until it was touching the fuel nozzle. This location corresponded to Y = 0 mm. Both flame temperature and NO concentration were recorded on the strip chart recorder. The

time response of the thermocouple was much quicker than the time response of the NO analyzer. Thus, data collection involved waiting for the NO reading to reach a steady value. Visual monitoring of the strip chart recorder was used to determine when the NO reading reached steady state. Once the NO reading was taken, the analyzer was switched to NO_X mode.

After a clear NO_X reading was obtained, the probe was translated down to Y = 0.5 mm. In this location, only a temperature reading was made. Then, the probe was translated down to Y = 1 mm. Temperature, NO, and NO_X were recorded. This procedure continued until sampling was completed at 4 mm or 5 mm away from the fuel nozzle. Experiments performed by translating the probe up from below the flame instead of down from the burner showed no difference in measurements to within experimental accuracy.

Once data had been obtained for the flame without steam injection, the steam generator was turned on. The variac was set at 84 V; the vernier valve handle on the water supply was set at 9.7 turns. The experiment was allowed to run for a few minutes to reach steady state. Then, the condensate trap was drained and a stopwatch was set.

The sampling procedure described for the flame with no steam injection was repeated for the flame with steam injection. The steam thermocouple voltage was manually recorded. When sampling was completed, the steam trap was drained and the stopwatch was turned off. The average condensate flow rate for the run was then calculated and subtracted from the overall steam flow rate to obtain a net steam flow rate.

This procedure was repeated for eight or nine different steam injection amounts. The NO_X analyzer was recalibrated between each run. If the NO_X analyzer calibration

was off by more than 2% of the maximum reading, the data was taken again. The approximate time that it took to run one experiment was five hours.

Each fuel was tested twice. After all of the first experiments were performed once, disassembly of the fuel nozzle revealed heavy coking on the stainless steel beads inside the nozzle. This coking was caused by pyrolysis of fuel in the hot stainless steel nozzle. Several CH_4 and C_2H_4 flames had been burned in the nozzle before testing began. As a result, partially pyrolyzed hydrocarbon fragments were deposited in the nozzle. Therefore, hydrocarbon fragments were available to form Fenimore NO during all of the first experiments, including the ones performed with non-hydrocarbon fuels.

Once this coking was discovered, all the tests were run for a second time. The fuel nozzle and beads were thoroughly cleaned in an ultrasonic cleaner before each subsequent test. This cleaning affected the outcomes of the experiments. The differences in the results from the coked nozzle and the clean nozzle will be discussed in the next section of this paper.

One difference in the first set of experiments performed and the last set of experiments performed was that total NO_x measurements could not be determined during the early experiments. This was because of the existence of certain species in the flame front which cause the catalyst in the NO_2 to NO converter to reduce both NO_2 and NO back to N_2 [16,37]. Some researchers have been able to avoid this problem by operating their NO_2 to NO converter at 400ł C rather than the usual 600ł C [16].

An interesting problem occurred when testing the pure CO flames in the clean nozzle. The CO flame was very unstable, and it continually blew off. Introduction of a very small steam flow rate to the air side of the burner stabilized the flame. The OH radicals introduced by the steam were enough to keep the CO steadily burning in air.

Experiments were performed as described above, but baseline data for the flame with no steam injection could not be obtained.

A probe effect was observed during data collection. As the probe was traversed down through the flame, a point was reached when the flame stabilized on the probe, and was actually pulled down into the probe. This distorted the data by creating a second peak in the NO and NO_X concentration profiles. Although the second peak existed for all flames in this study, the second peak was not considered to be an actual data point because the shape of the flame was distorted by the probe. Thus, although it is important to know that it exists, the second peak will not be presented in this thesis as actual data.

CHAPTER 3: EXPERIMENTAL RESULTS

3.1. Introduction

The first section of this chapter describes the important quantities which are used to compare the results from the different fuels. Graphs of NO_X concentration and temperature as functions of the distance from the fuel nozzle are presented for the hydrocarbon fuels and non-hydrocarbon fuels in the following two sections. The next section compares the results from all of the fuels by presenting graphs of peak temperature, peak NO_X concentration, and the percentage of NO_X removed (RNO_X) as functions of the amount of steam added. Results from the flames burned in the coked nozzle are shown in the final section of this chapter.

3.2. Important Quantities for Comparison of Results

Traditionally, for steam injection studies, NO concentrations have been plotted as functions of the ratio of the mass flow rate of steam to the mass flow rate of fuel. In this study, NO concentrations and temperatures are plotted as functions of the ratio of the mass flow rate of steam to the maximum heat release rate of the fuel. This is a more meaningful quantity for comparing fuels with different heating values. The maximum heat release rate is the product of the fuel flow rate and its lower heating value. Heating values and maximum heat release rates for the flames used in these experiments are shown in Table 2.1. The maximum heat release rate is proportional to the peak temperature that can exist in a flame. Since steam injection studies deal with suppressing this peak temperature by different amounts, the ratio of the mass flow rate of steam to the maximum heat release rate of the fuel is an important quantity for comparison.

It is more important to study the trends in NO_x concentrations than it is to study the trends in NO concentrations. This is because past studies showed that some of the NO in the sample is converted to NO_2 in the probe [38]. Since NO_2 will not form at the high temperatures that exist in the flames, any NO_2 in the sample is formed from NO in the probe [37]. If this is the case, then total NO_x concentration measurements will represent the original amount of NO in the sample. Total NO_x data will be emphasized for the clean nozzle, but NO data will be considered for the coked nozzle since total NO_x measurements were not made with the coked nozzle.

A useful way to look at NO_x with steam injection is to divide the NO_x concentration with steam injection by the NO_x concentration measured in the same flame with no steam injection. This gives a normalized quantity which ranges from zero to one. This quantity is called RNO_x, and it represents the percentage of the original NO_x which remains in the flame with a particular steam injection amount. This study will use both RNO_x and RNO for comparisons.

One error bar is shown on each graph which displays NO concentrations, NO_x concentrations, or temperatures in this section. In some cases, the error bar is not visible on the graph. This is because the error bar is smaller than the symbol used to plot the data. Thus, where error bars are not visible, the symbol size approximates the error.

3.3. NO_x and Temperature Profiles for Hydrocarbon Fuels

3.3.1. Methane

Figure 11(a) and Fig. 11(b) show NO_x concentrations and temperatures, respectively, as a function of distance from the fuel nozzle for CH_4. Concentrations of NO_x are initially in the range of 70 ppm, and are reduced to the range of 40 ppm at large

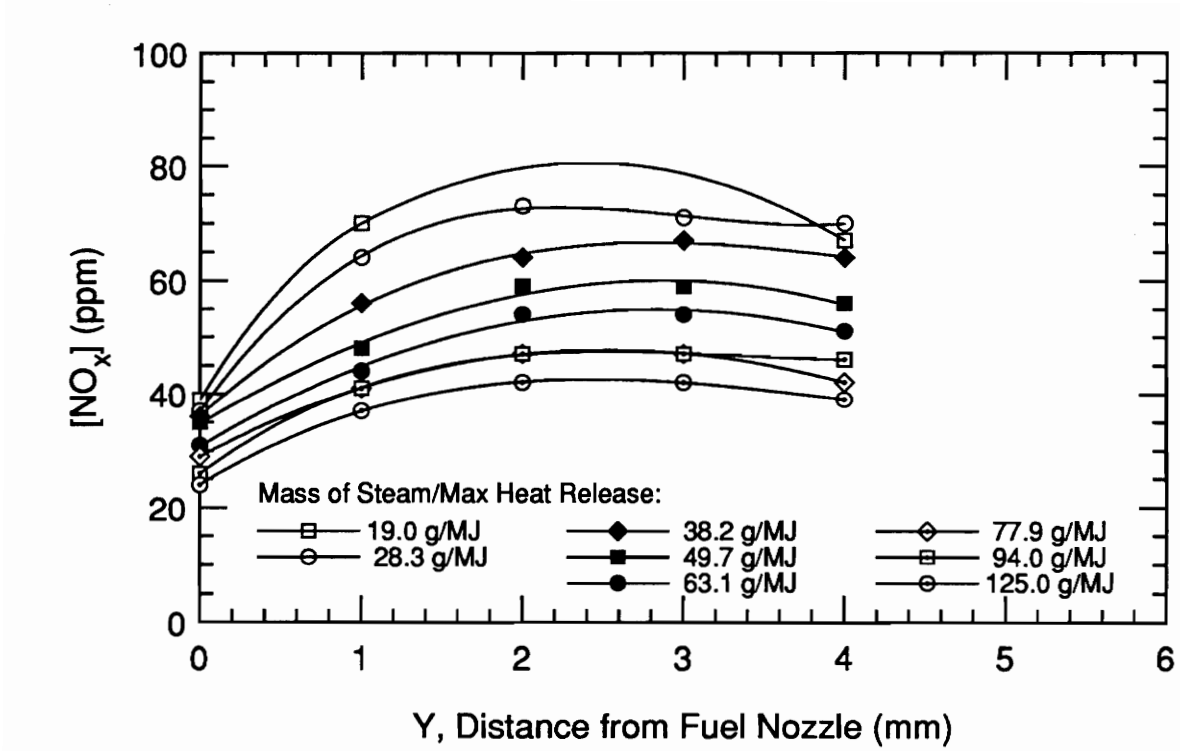

Figure 11(a). NO_x concentration profiles for various amounts of steam, CH_4 as a fuel, using the clean nozzle.

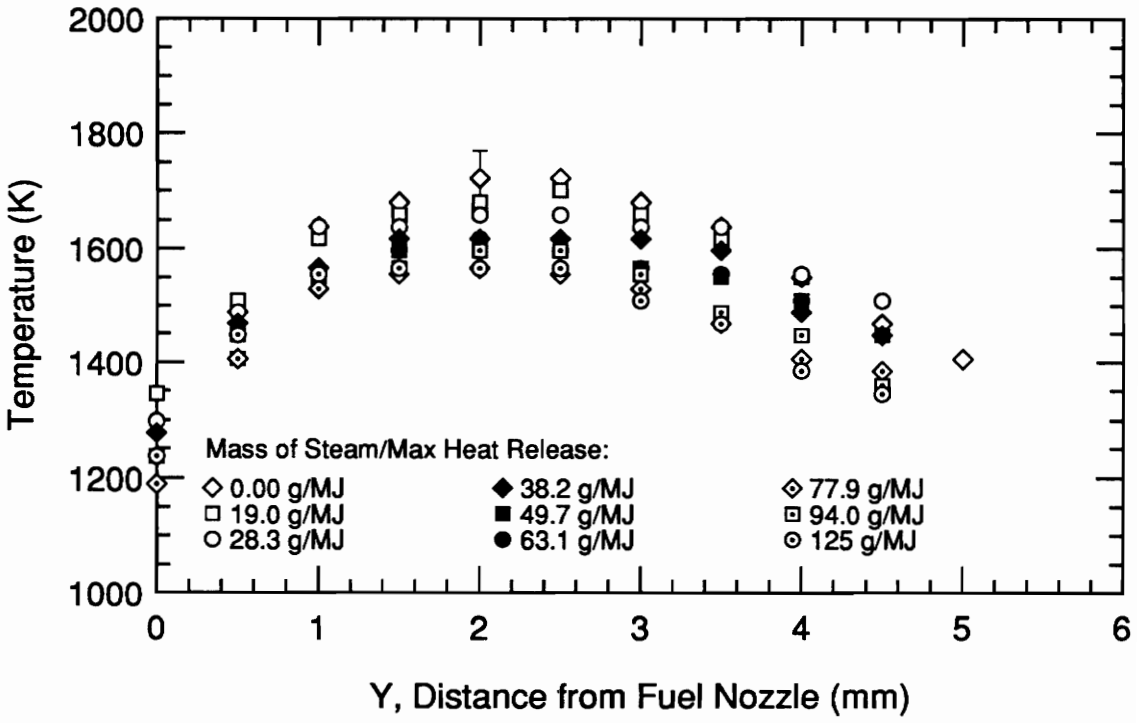

Figure 11(b). Temperature profiles for various amounts of steam, CH_4 as a fuel, using the clean nozzle.

amounts of steam injection. With no steam injection, the temperature peaks at 1722 K, and is reduced to 1570 K. Thus, for this CH_4 flame and for most of the other flames in this study, steam injection suppresses flame temperatures.

Profiles of NO concentration as a function of the distance from the fuel nozzle for the CH_4 flame are shown in Fig. 12. Concentrations of NO are initially in the range of 70 ppm, and are reduced to the range of 20 ppm with large amounts of steam. The NO concentration curves have the same shapes as the NO_X concentration curves for the clean nozzle shown in Fig. 11(a). The only differences in the two sets of profiles are the absolute magnitudes of the concentrations.

Figure 13 provides a closer look at temperature profiles for four amounts of steam addition into the CH_4 flame. With no steam injection, temperature peaks at a distance of 2.3 mm from the fuel nozzle. The profile for the steam amount of 28.3 g/MJ peaks at a distance of 2.1 mm from the fuel nozzle. The profile for the steam amount of 63.1 g/MJ peaks at a distance of 1.9 mm from the fuel nozzle. The profile for the steam amount of 125 g/MJ peaks at a distance of 1.7 mm from the fuel nozzle. This data shows that as the amount of steam injected increases, the peak temperature for CH_4 moves 0.5 mm closer to the fuel nozzle. This verifies the visual observation that the CH_4 flame moved physically closer to the fuel nozzle as steam injection increased. Methane flames were the only flames in this study which noticeably moved in space.

3.3.2. Ethylene

Total NO_X concentration profiles and temperature profiles for the C_2H_4 flame are shown in Fig. 14(a) and Fig. 14(b), respectively. Concentrations of NO_X are initially in the range of 100 ppm, and are reduced to the range of 30 ppm. The peak temperature with no steam injection is 1591 K, and temperatures are suppressed as low as 1489 K.

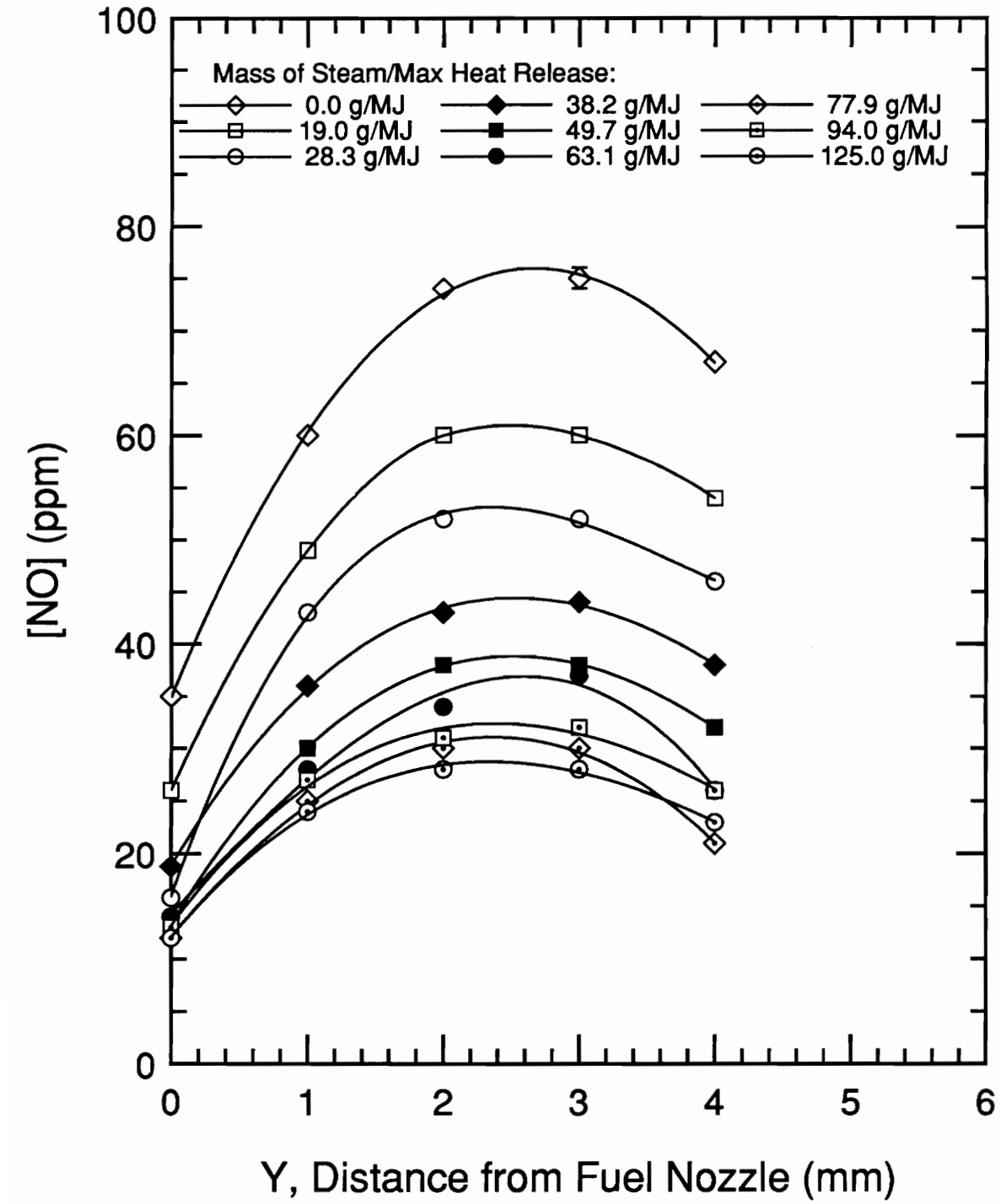

Figure 12. NO concentration profiles for varying amounts of steam, CH_4 as a fuel, using the clean nozzle.

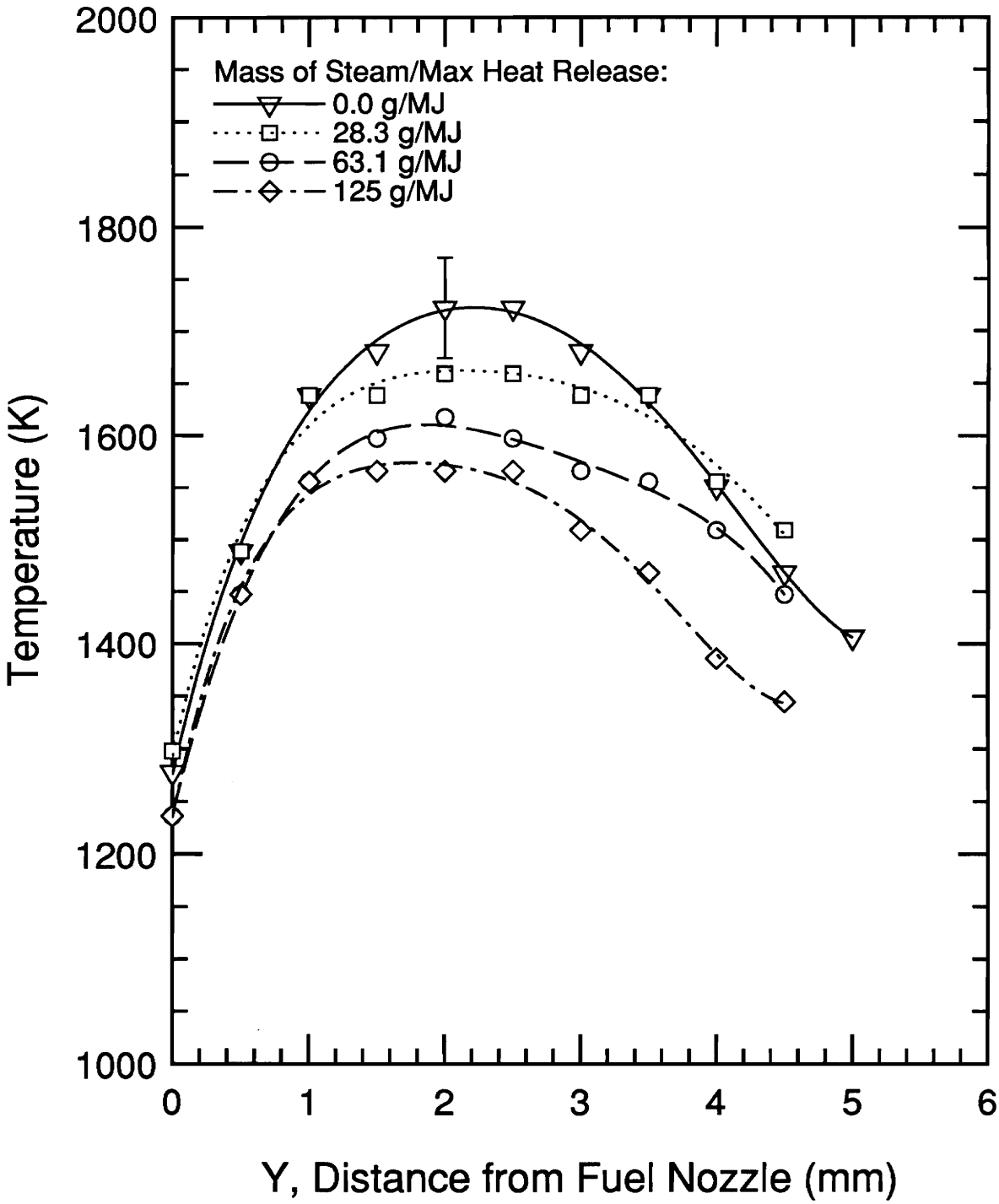

Figure 13. Selected temperature profiles, CH_4 as a fuel, using the clean nozzle.

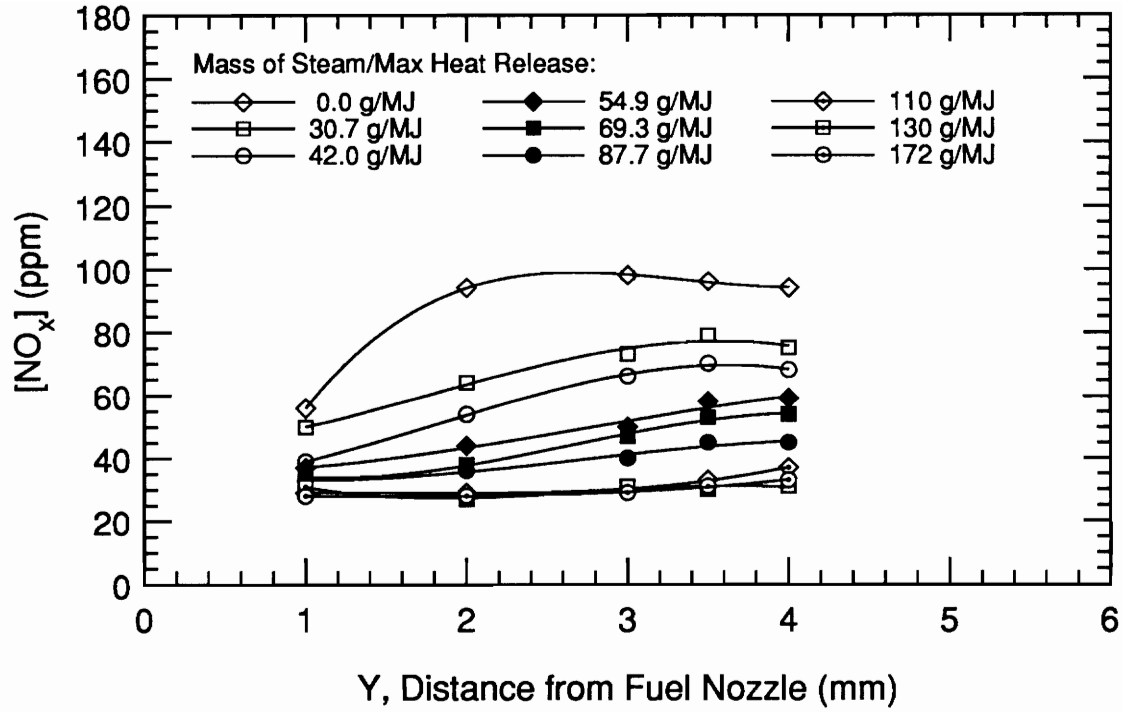

Figure 14(a). NO_x concentration profiles for various amounts of steam, C_2H_4 as a fuel, using the clean nozzle.

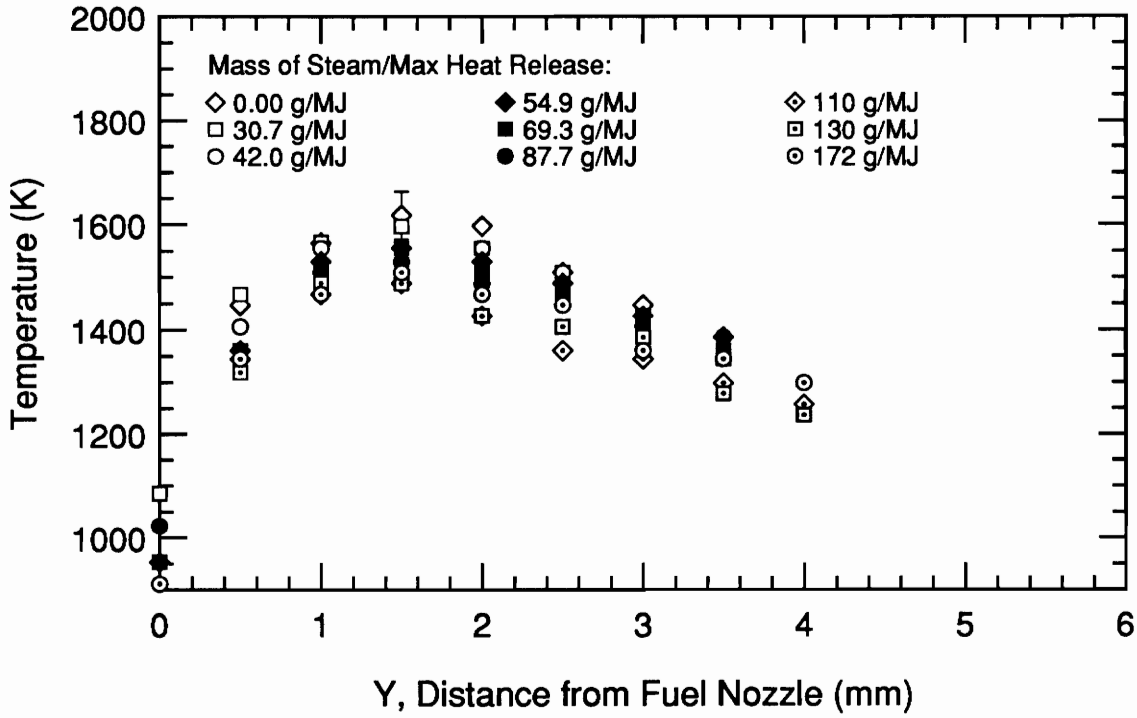

Figure 14(b). Temperature profiles for various amounts of steam, C_2H_4 as a fuel, using the clean nozzle.

Figure 15 shows NO profiles for the C_2H_4 flame. Concentrations of NO are initially in the range of 80 ppm, and are reduced to the range of 10 ppm. These NO profiles exhibit the same basic behavior as the NO_X profiles for the clean nozzle shown in Fig. 14(a).

3.4. NO_X and Temperature Profiles for Non-Hydrocarbon Fuels

3.4.1. Carbon Monoxide

The CO flame with no steam injection could not be stabilized. Thus, data was not obtained for the dry CO flame. Adding a small amount of steam, which corresponded to 43.1 g/MJ, helped with stability. The purpose of adding a small amount of steam was to introduce OH radicals to stabilize the flame.

Total NO_X profiles and temperature profiles for CO flames are shown in Fig. 16(a) and Fig. 16(b), respectively. Concentrations of NO_X are initially in the range of 10 ppm, and are reduced to the range of 4 ppm. Temperature for this CO flame initially decreases but eventually begins to increase with increasing amounts of steam. With the lowest steam amount, the temperature profile peaks at 1065 K. The temperature reaches a minimum of 1023 K, but actually increases to 1086 K at the highest amount of steam addition. Thus, the temperatures of the CO flames decrease with moderate steam addition, and then increase with high amounts of steam addition.

Nitric oxide profiles for the CO flame are shown in Fig. 17. Concentrations of NO are initially in the range of 10 ppm, and are reduced to the range of 3 ppm. These NO profiles exhibit the same basic behavior as the NO_X profiles of Fig. 16(a).

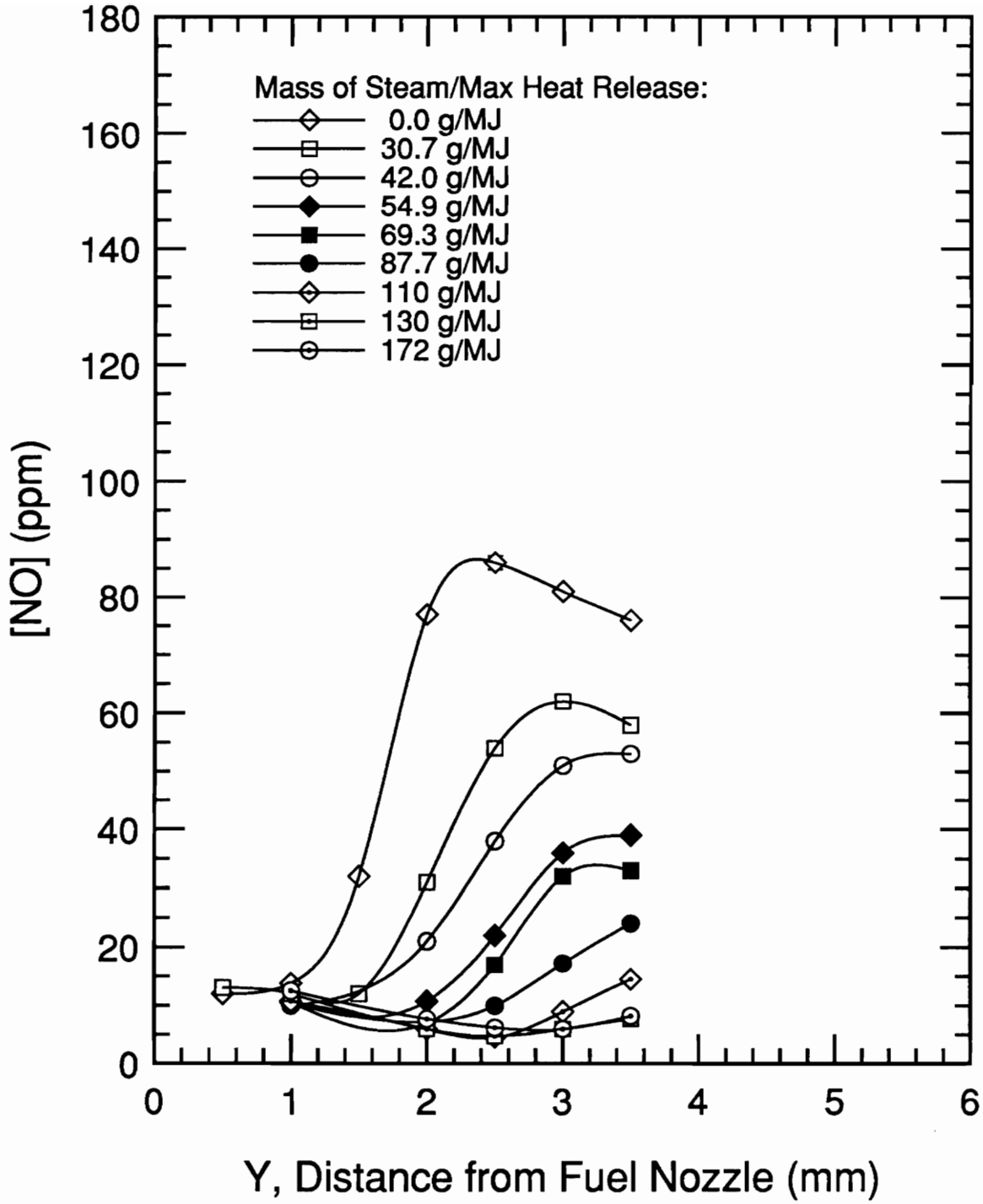

Figure 15. NO concentration profiles with various amounts of steam, C_2H_4 as a fuel, using the clean nozzle.

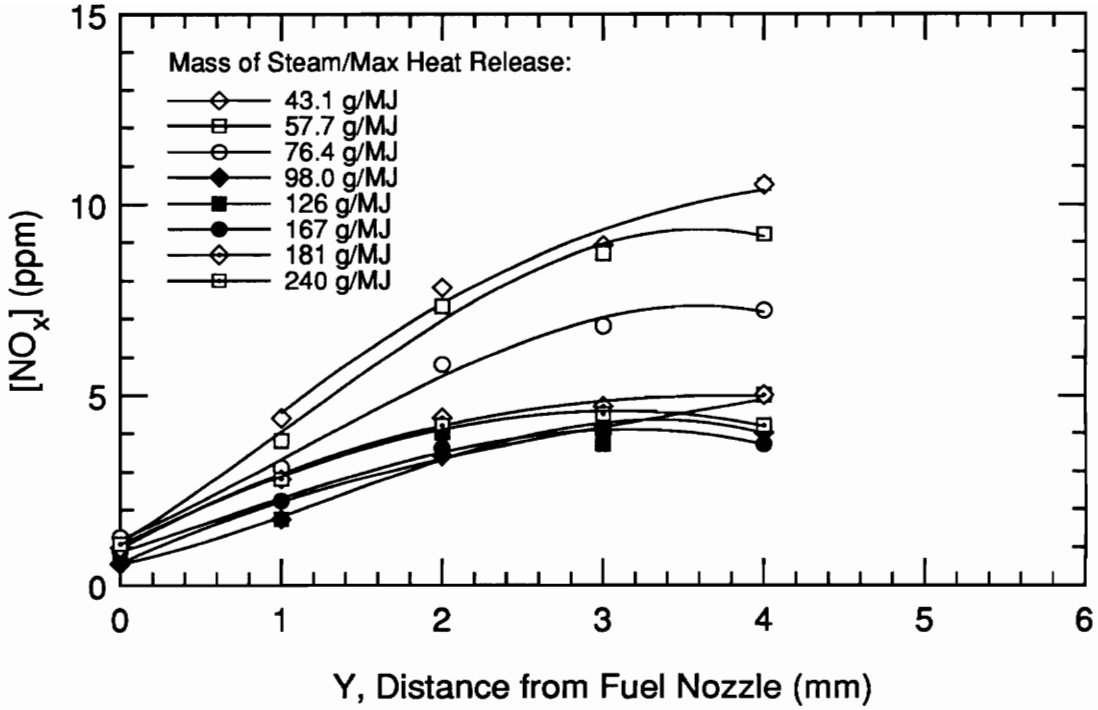

Figure 16(a). NO_x concentration profiles for various amounts of steam, CO as a fuel, using the clean nozzle.

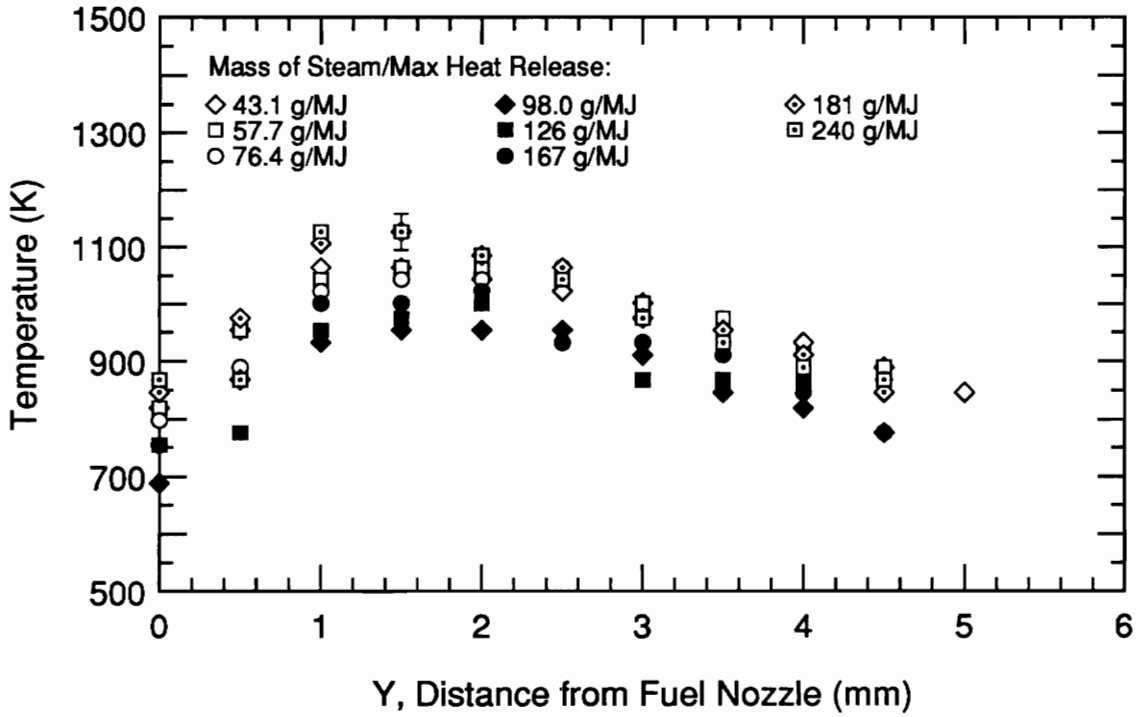

Figure 16(b). Temperature profiles for various amounts of steam, CO as a fuel, using the clean nozzle.

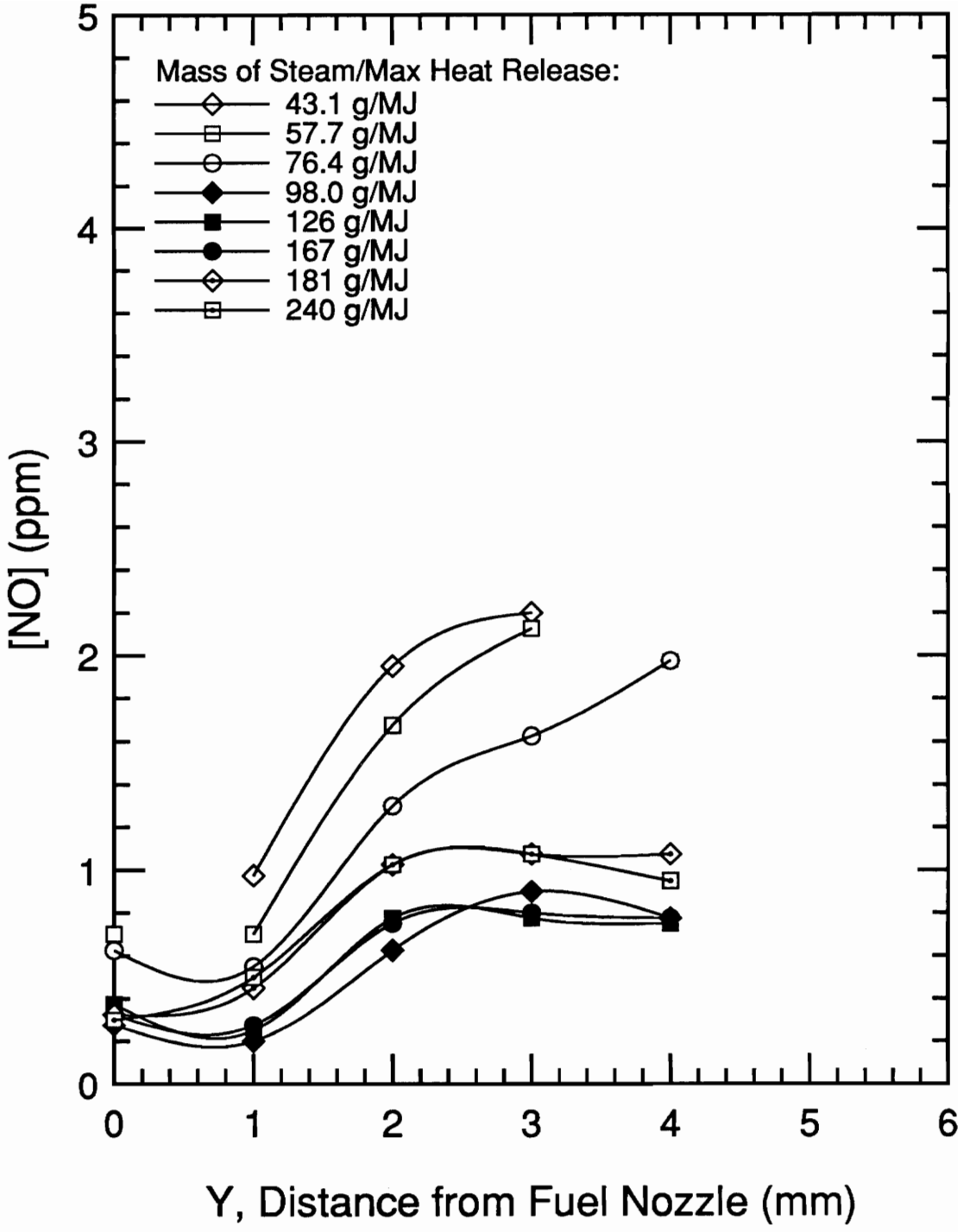

Figure 17. NO concentration profiles for various amounts of steam, CO as a fuel, using the clean nozzle.

3.4.2. Carbon Monoxide with Hydrogen (1:1)

Total NO_X concentration profiles and temperature profiles for CO/H_2 (1:1) are shown in Fig. 18(a) and Fig. 18(b), respectively. Concentrations of NO_X are initially in the range of 40 ppm, and they are reduced to the range of 10 ppm. The peak temperature with no steam injection is 1855 K, and it is suppressed as low as 1834 K. This is a very small amount of temperature suppression. Within experimental accuracy limits, the peak temperature in the CO/H_2 (1:1) flame remains constant.

Nitric oxide concentration profiles for the CO/H_2 (1:1) flame are shown in Fig. 19. Concentrations of NO are initially in the range of 40 ppm, and they are reduced to the range of 10 ppm. These NO profiles have the same basic shapes as the NO_X profiles shown in Fig. 18(a).

3.4.3. Carbon Monoxide with Hydrogen (1:2)

Profiles of NO_X concentration and temperature are shown for the CO/H_2 (1:2) flame in Fig. 20(a) and Fig. 20(b), respectively. Concentrations of NO_X are initially in the range of 8 ppm, and they are reduced to the range of 1 ppm. The peak temperature for no steam injection is 1618 K, and it is suppressed to 1345 K.

Nitric oxide profiles for the CO/H_2 (1:2) flame are shown in Fig. 21. NO concentrations are initially in the range of 4 ppm, and are reduced to the range of 0.1 ppm. The NO profiles exhibit the same basic shapes as the NO_X profiles shown in Fig. 20(a).

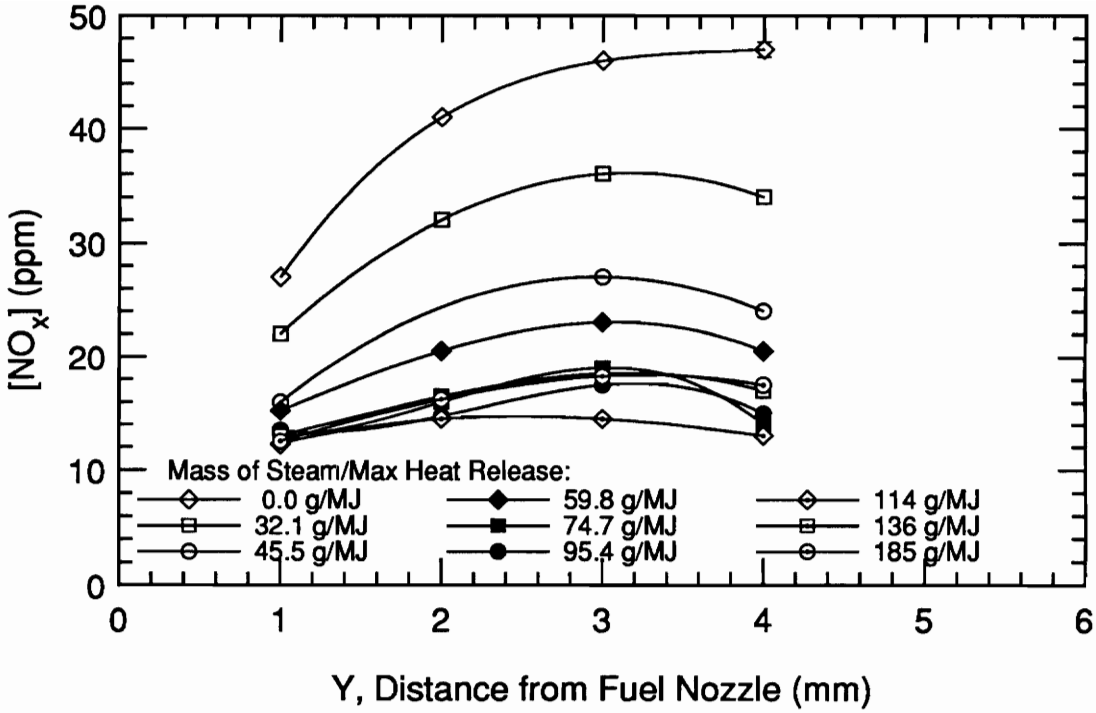

Figure 18(a). NO_x concentration profiles for various amounts of steam, CO/H_2 (1:1) as a fuel, using the clean nozzle.

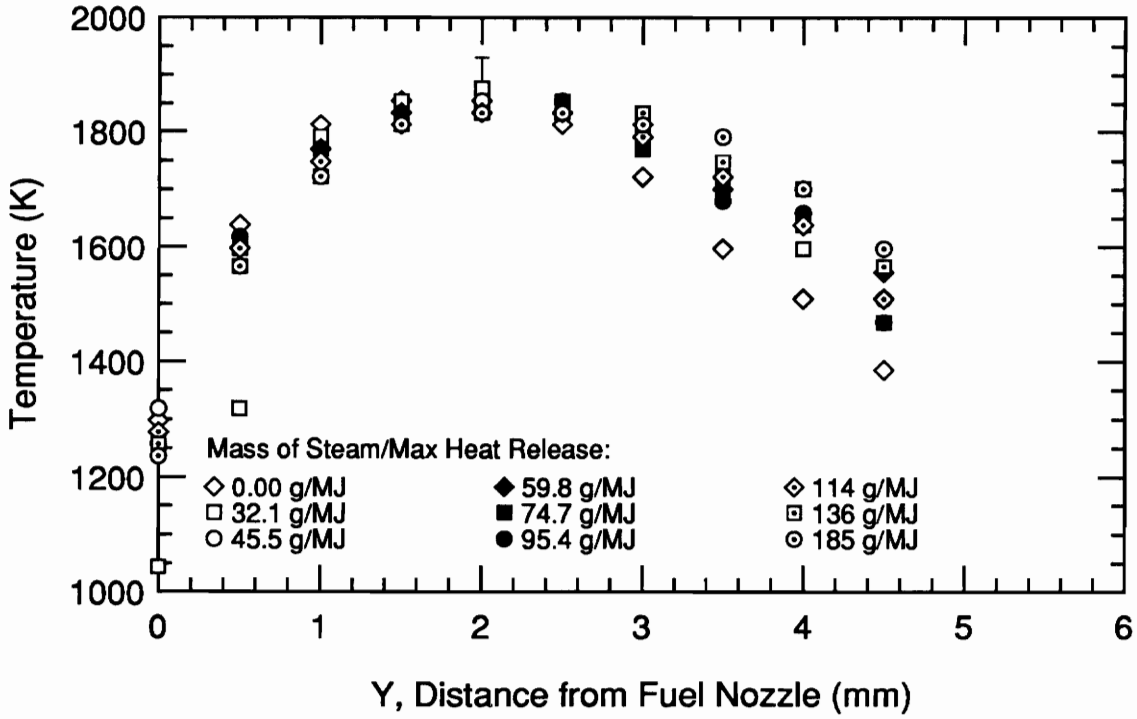

Figure 18(b). Temperature profiles for various amounts of steam, CO/H_2 (1:1) as a fuel, using the clean nozzle.

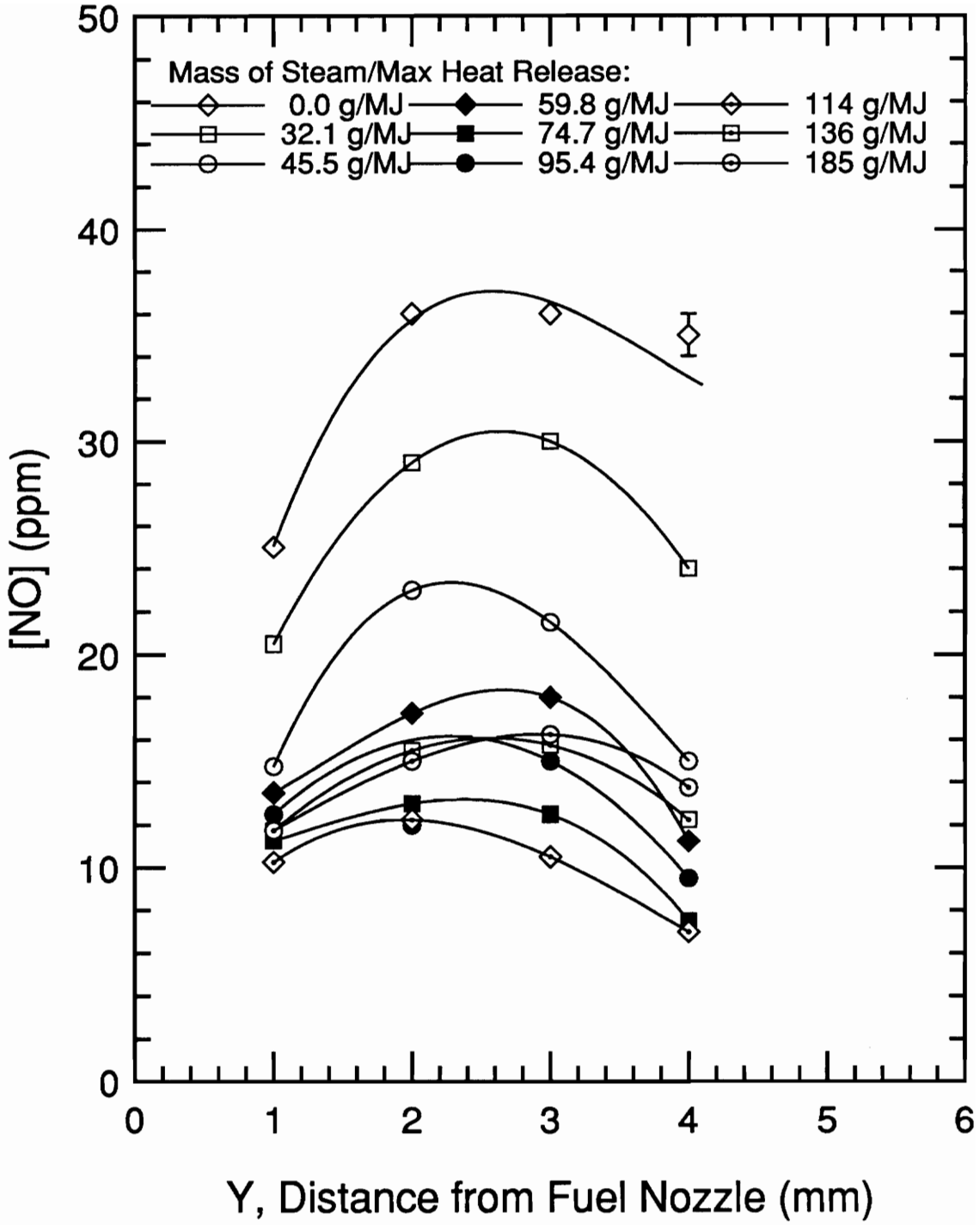

Figure 19. NO concentration profiles for various amounts of steam, CO/H_2 (1:1) as a fuel, using the clean nozzle.

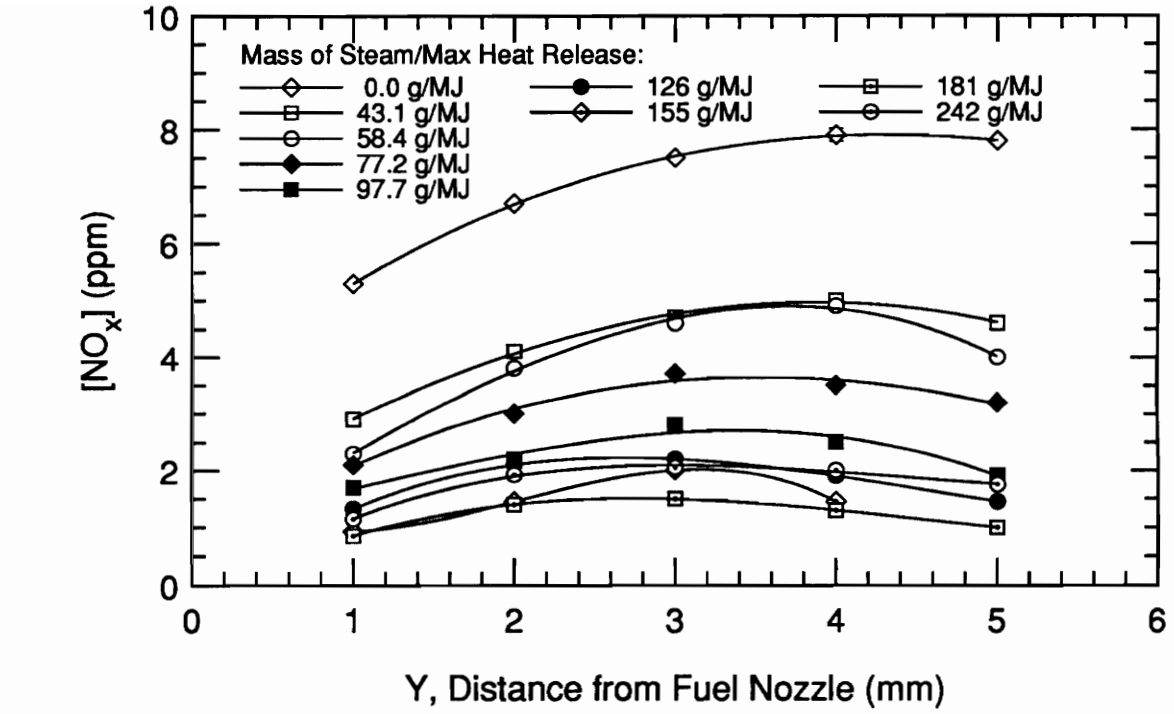

Figure 20(a). NO_x concentration profiles for varying amounts of steam, CO/H_2 (1:2), using the clean nozzle.

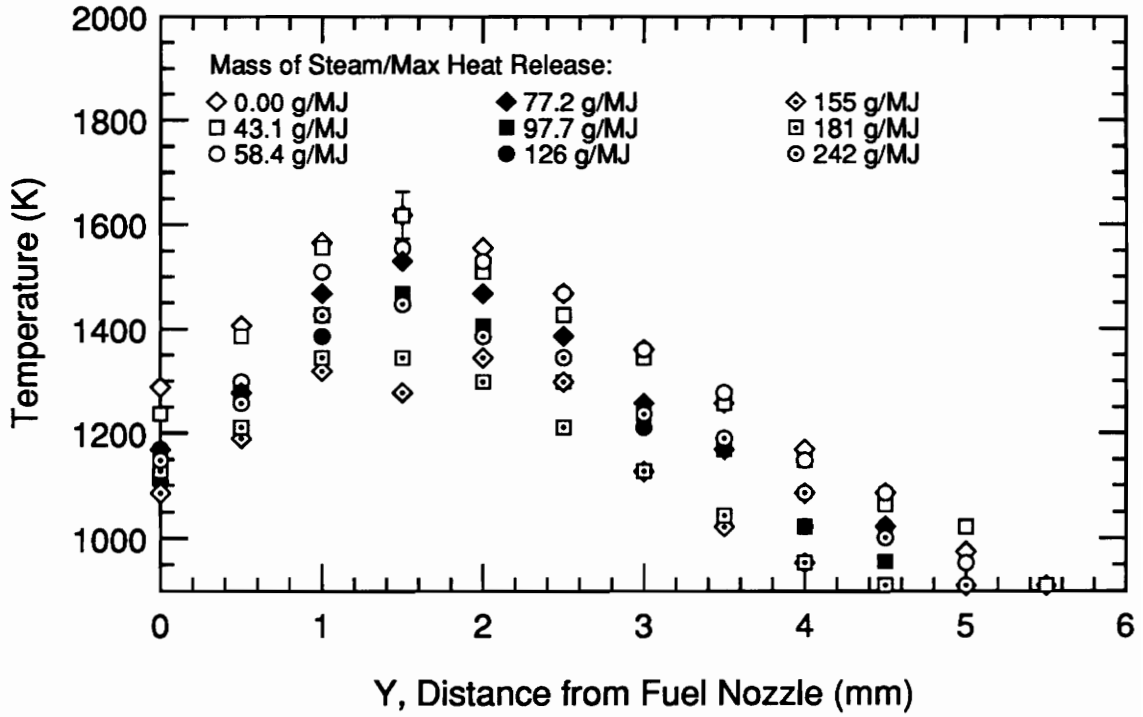

Figure 20(b). Temperature profiles for various amounts of steam, CO/H_2 (1:2) as a fuel, using the clean nozzle.

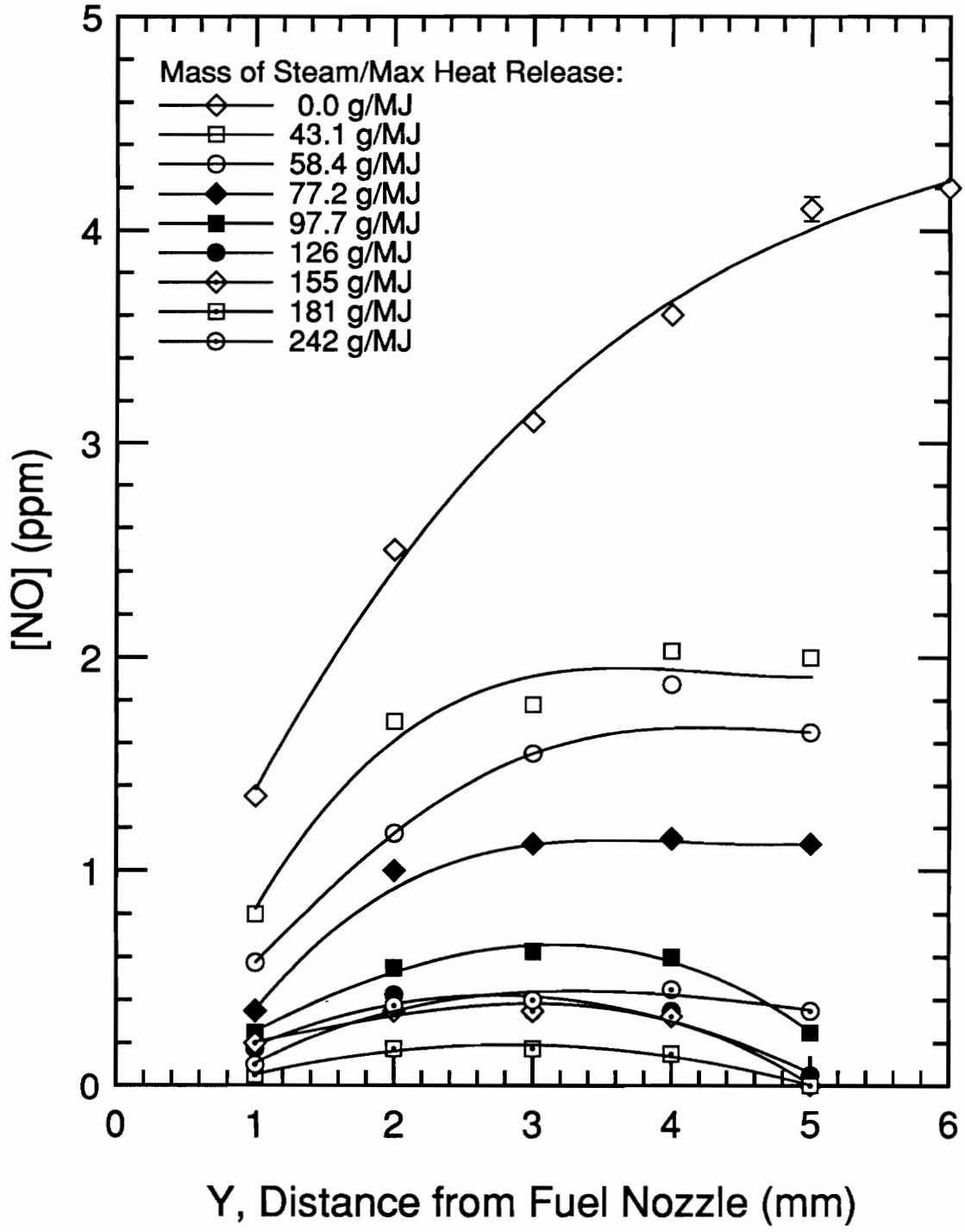

Figure 21. NO concentration profiles with various amounts of steam, CO/H_2 (1:2), using the clean nozzle.

3.5. Comparison of All Fuels

3.5.1. Method of Comparison

Because the flames can move physically in space, an NO_X measurement at 1 mm from the fuel nozzle with no steam injection may not compare with an NO_X measurement at 1 mm from the fuel nozzle with high steam injection. These may be physically two different points in the flame. To compensate for this ambiguity, for each steam amount in a particular flame, the peak NO_X concentration, no matter how far it is located from the nozzle, is chosen for comparison with other peak NO_X concentrations. Likewise, for each steam flow rate, the peak temperatures are chosen for comparison.

3.5.2. Temperature

Graphs of temperature versus the amount of steam addition are presented in this section. In general, temperatures are not suppressed uniformly in these opposed flow diffusion flames with increasing steam addition. Most of the graphs exhibit a "leveling off" trend. For this analysis, the "leveling off" value represents an average of the data points after the point is reached where temperatures no longer decrease.

Peak temperatures as a function of the amount of steam for each fuel are shown in Fig. 22. The temperature curves "level off" for CH_4 and C_2H_4. Temperature in the CH_4 flame starts at 1722 K and "levels off" at 1570 K with a steam amount of about 110 g/MJ. Temperature in the C_2H_4 flame starts at 1618 K and "levels off" at 1497 K with a steam amount of about 150 g/MJ. As mentioned previously, temperature in the CO flame decreases to a minimum and then increases again. Temperature in the CO flame starts at 1065 K, decreases to 1023 K at the steam amount of 100 g/MJ, and then increases to a maximum of 1086 K at a steam injection amount of about 250 g/MJ. In the CO/H_2 (1:1)

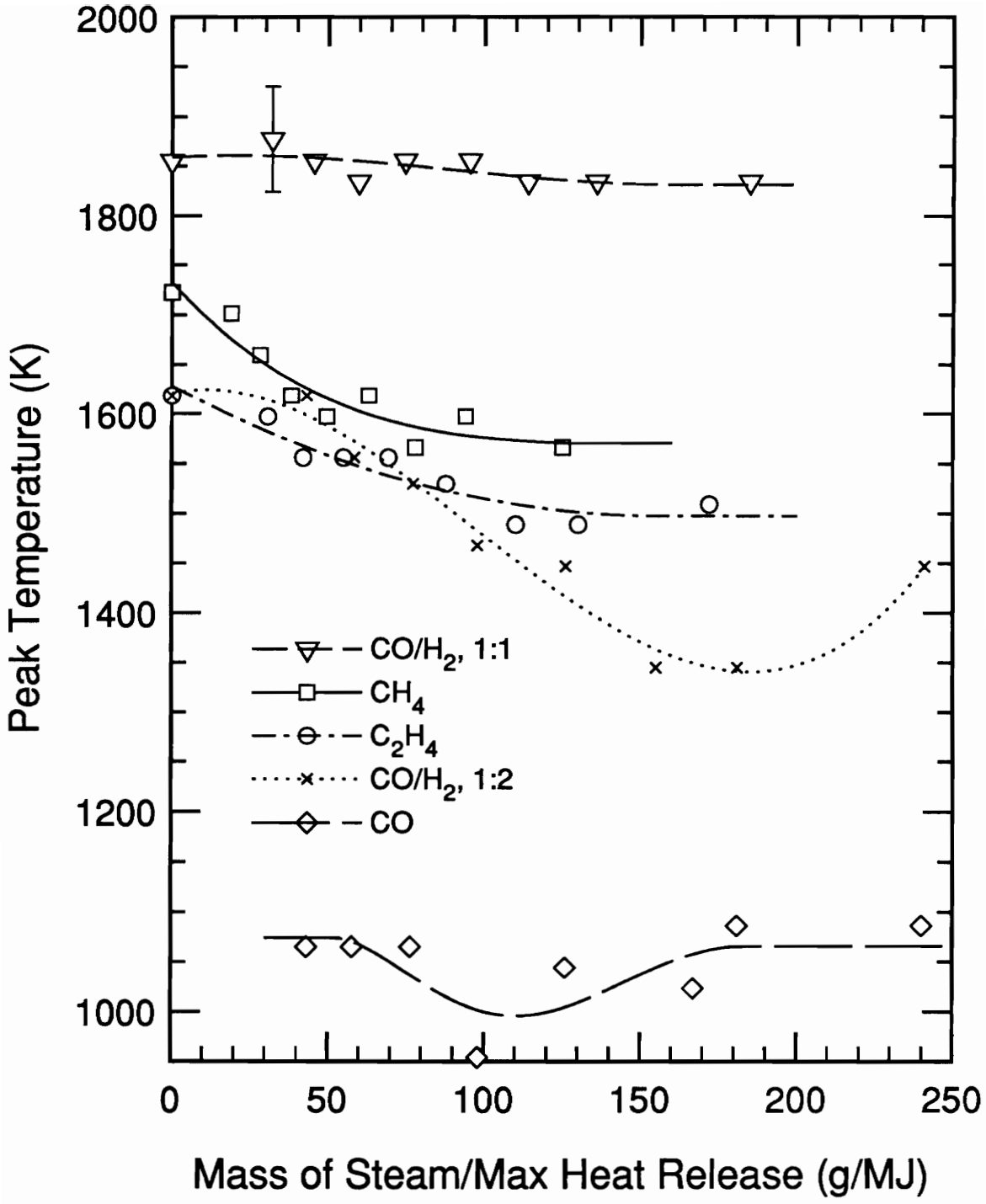

Figure 22. Peak temperatures for all fuels, using the clean nozzle.

flame, temperatures are "level" over the entire range of steam amounts. Temperature in this CO/H_2 (1:1) flame starts at 1855 K and remains essentially constant, dropping only to 1834 K. Temperature in the CO/H_2 (1:2) flame decreases to a minimum and then increases again. This temperature in the CO/H_2 (1:2) flame starts at 1618 K, drops to 1345 K at a steam amount of 150 g/MJ, and increases again to 1447 K at a steam amount of about 250 g/MJ. All temperatures "level off" at a steam amount of 100-150 g/MJ.

3.5.3. NO_X and NO

The "leveling off" of NO_X concentrations observed in gas turbine combustors was reproduced in both the hydrocarbon and non-hydrocarbon laboratory diffusion flames. Graphs of NO_X concentrations and NO concentrations versus the amount of steam injected are presented in this section. All of these graphs exhibit the "leveling off" trend. For this analysis, the "leveling off" value represents an average of the data points after the point is reached where NO_X or NO concentrations no longer decrease.

Figure 23 shows total NO_X concentration as a function of the amount of steam for each fuel. Total NO_X concentrations in the CH_4 flame start at 92 ppm and "level off" at 41 ppm with a steam amount of about 110 g/MJ. Total NO_X concentrations in the C_2H_4 flame start at 98 ppm and "level off" at 30 ppm with a steam amount of about 150 g/MJ. Total NO_X concentrations in the CO flame start at 11 ppm and "level off" at 4.3 ppm with a steam amount of about 130 g/MJ. Total NO_X concentrations in the CO/H_2 (1:1) flame start at 46 ppm and "level off" at 15 ppm with a steam amount of about 120 g/MJ. Total NO_X concentrations in the CO/H_2 (1:2) flame start at 7.9 ppm and "level off" at 1.6 ppm with a steam amount of about 150 g/MJ. All of these NO_X concentration curves "level off" at steam amounts of 100-150 g/MJ. This graph shows that total NO_X concentrations

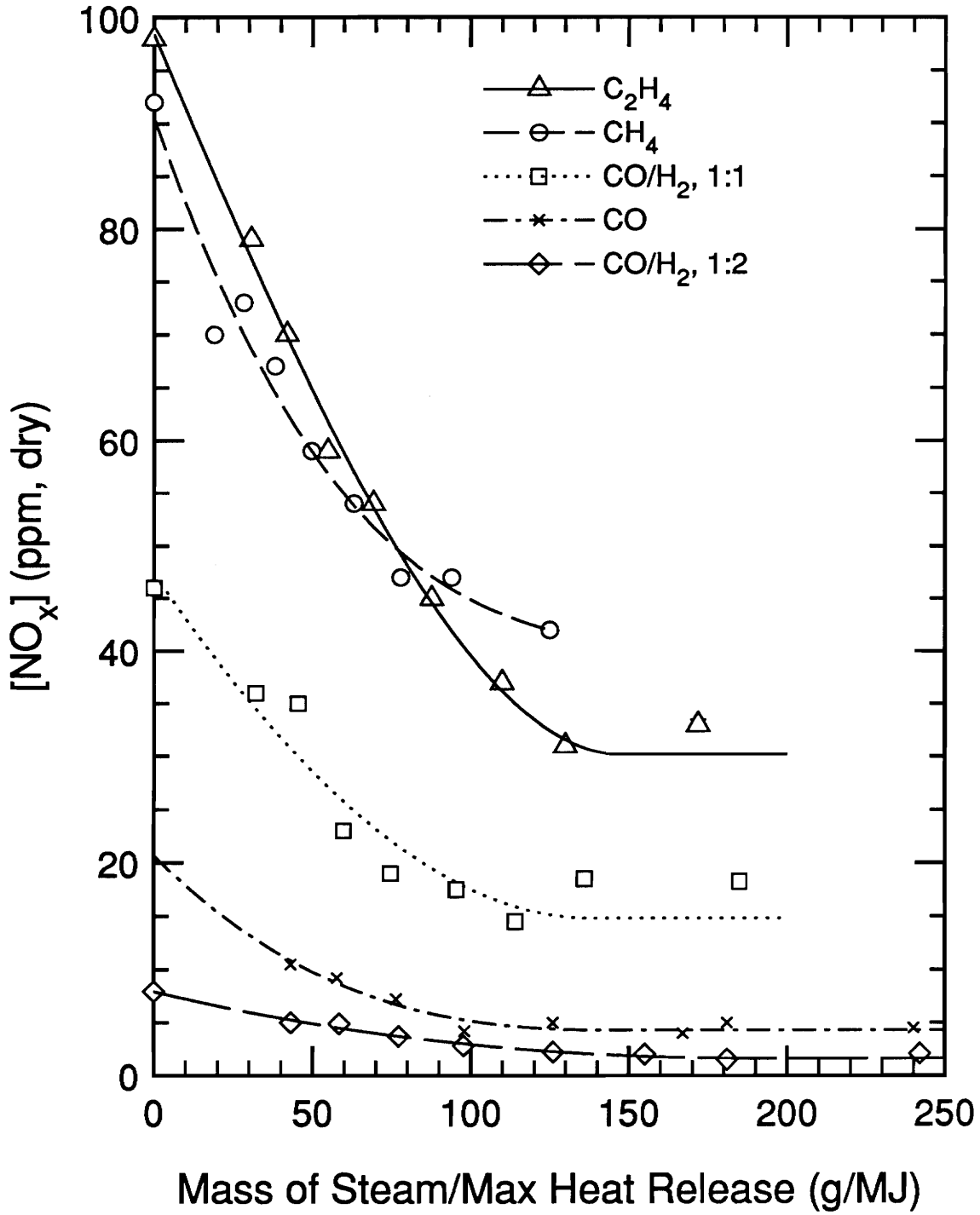

Figure 23. NO_x concentrations for all fuels, using the clean nozzle.

for the hydrocarbon fuels are higher than the total NO_x concentrations for the non-hydrocarbon fuels.

Figure 24 shows NO concentration measurements as a function of steam amount. Comparison of Fig. 24 with Fig. 23 shows that there is a large amount of NO_2 formed in the C_2H_4 flame. The difference between the amount of NO_x and the amount of NO measured at the "leveling off" point of the C_2H_4 flame is 22 ppm, whereas this difference is 12 ppm, 4 ppm, 2 ppm, and 1.5 ppm, for CH_4, CO, CO/H_2 (1:1), and CO/H_2 (1:2), respectively. The excessive amount of NO_2 in the C_2H_4 flame was most likely formed in the sample probe. The existence of hydrocarbons in the probe promote NO to NO_2 conversion. Hori showed that C_2H_4 promotes this conversion more readily than does CH_4 [39].

Table 3.1 summarizes the peak NO_x concentration and the peak temperature for each flame. The locations of these peak quantities are also shown. This data shows that the NO_x concentration peaks on the air side of the location of the peak temperature for all fuels.

3.5.4. RNO_x and RNO

RNO_x represents the percentage of the original NO_x which is removed with steam addition. Graphs of RNO_x versus the amount of steam added are presented in this section. Comparison of RNO_x for different fuels shows the effectiveness of steam for eliminating NO_x in different types of flames.

Figure 25 shows RNO_x as a function of the amount of steam. For all fuels, RNO_x "levels off." For the CH_4 flame, RNO_x "levels off" at 0.46 with a steam amount of 125 g/MJ. For the C_2H_4 flame, RNO_x "levels off" at 0.31 with a steam amount of about 150

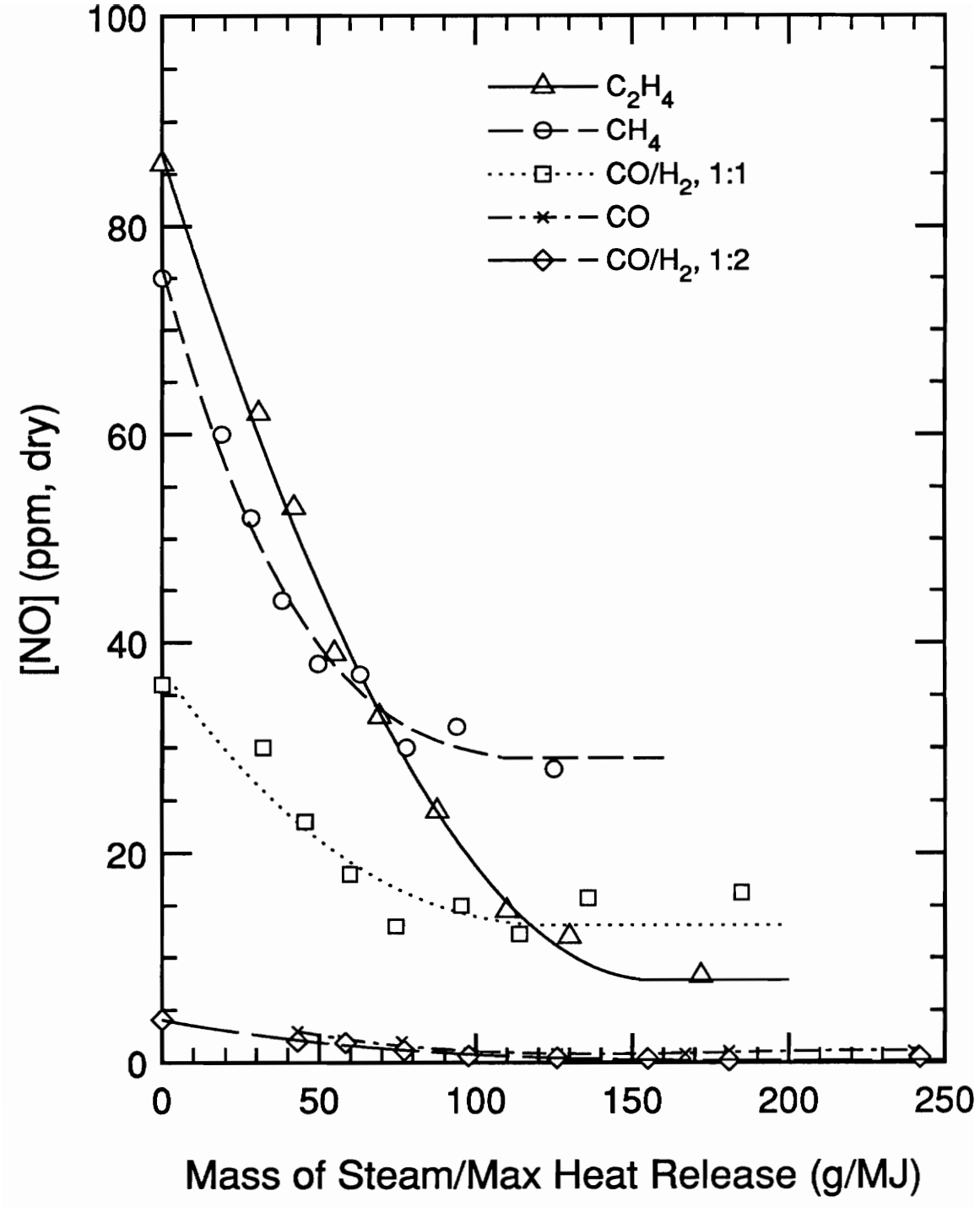

Figure 24. NO concentrations for all fuels, using the clean nozzle.

Table 3.1. Peak Quantities and Their Locations

Fuel	Peak NO_x Concentration (ppm)	Y, Distance from Nozzle (mm)	Peak Temperature (K)	Y, Distance from Nozzle (mm)
CH_4	92	2.5	1722	2.0
C_2H_4	98	2.5	1618	1.5
CO	11	4.0	1065	1.5
CO/H_2 (1:1)	46	3.0	1855	2.0
CO/H_2 (1:2)	7.9	4.0	1618	1.5

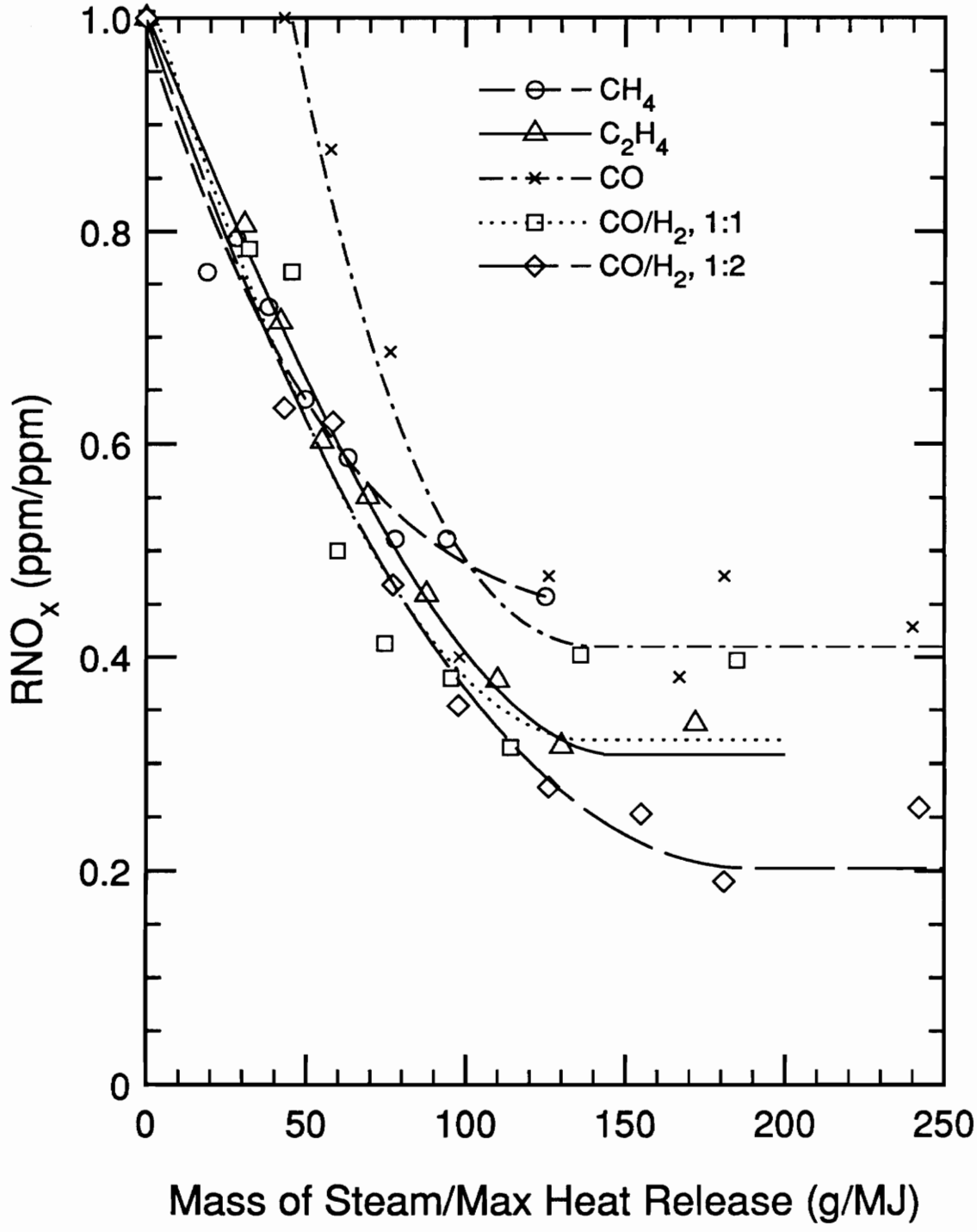

Figure 25. RNO_x for all fuels, using the clean nozzle.

g/MJ. Since the dry CO flame could not be stabilized, RNO_X for the CO flame is defined as the ratio of the NO_X concentration with a certain steam flow rate to the NO_X concentration with the lowest steam amount of 43.1 g/MJ. For the CO flame, RNO_X "levels off" at 0.45 with a steam amount of about 130 g/MJ. For the CO/H_2 (1:1) flame, RNO_X "levels off" at 0.32 with a steam amount of about 120 g/MJ. For the CO/H_2 (1:2) flame, RNO_X "levels off" at 0.20 with a steam amount of about 150 g/MJ. All of these curves "level off" at steam amounts between 100-150 g/MJ. This data shows that steam is most effective at eliminating NO_X in the CO/H_2 (1:2) flame. Steam is less effective at eliminating NO_X from the CO/H_2 (1:1) and C_2H_4 flames, and it is least effective at eliminating NO_X from CH_4 flames.

Figure 26 shows RNO as a function of the amount of steam with the clean nozzle. The "leveling off" values for RNO are quite different from the "leveling off" values for RNO_X. Table 3.2 compares these values. The table shows peak NO concentrations, peak NO_X concentrations, and minimum values of RNO and RNO_X. In general, suppression of total NO_X is not as effective as suppression of NO. However, this NO data may be in error because of NO to NO_2 conversion in the probe. The RNO_X data presented in this section shows that for all flames with the clean nozzle, at least 55% of the NO_X is eliminated using steam injection.

3.6. Results from the Coked Nozzle

3.6.1. NO and Temperature Profiles

Nitric oxide concentrations and temperatures as a function of the distance from the coked fuel nozzle are shown in Figs. 27-31 for all fuels. Although the NO and temperature profiles exhibit many of the same trends seen in the data from the clean

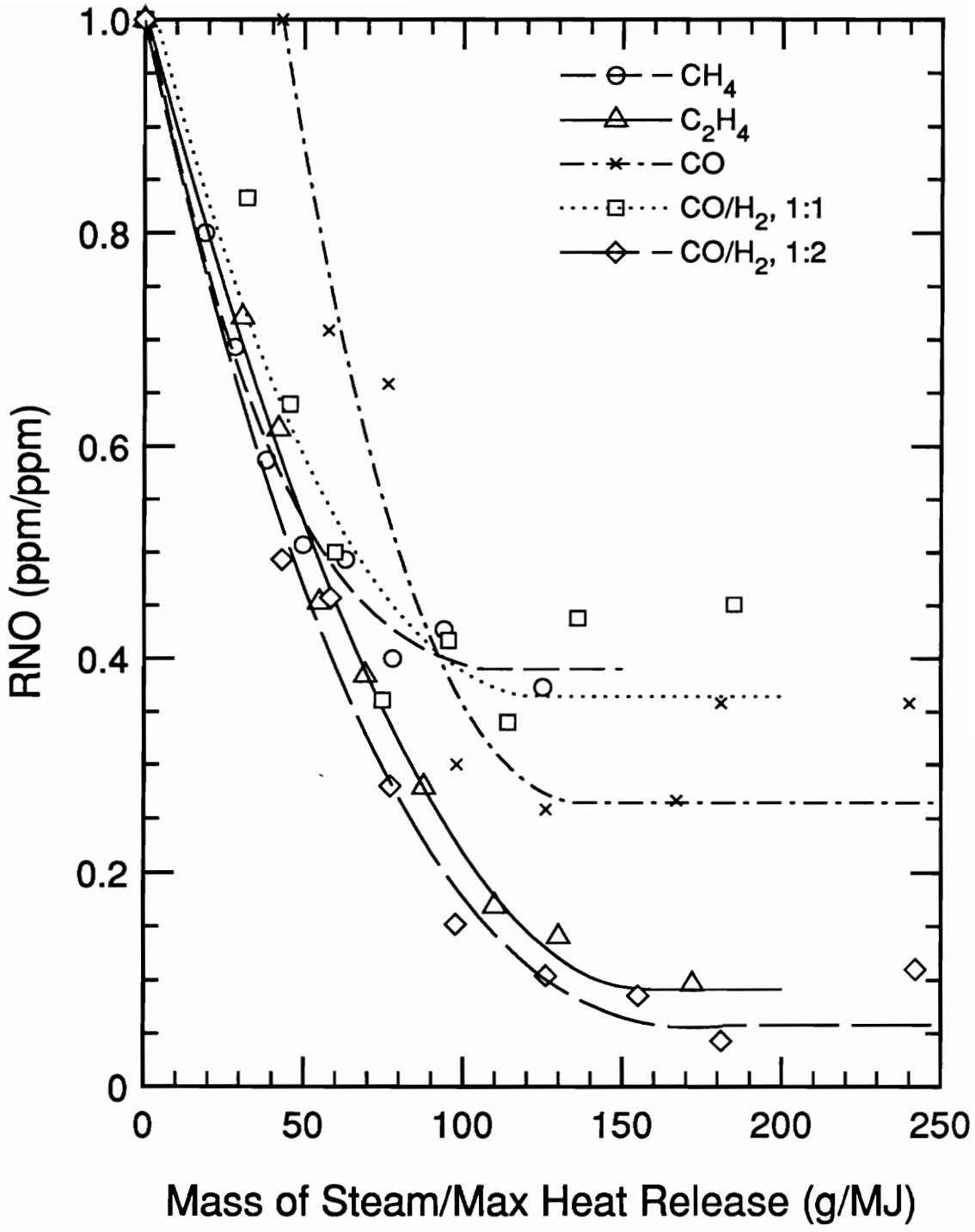

Figure 26. RNO for all fuels, with the clean nozzle.

Table 3.2. Comparison of NO and NO_x for Clean Nozzle

Fuel	Peak [NO] (ppm, dry)	Minimum RNO (ppm/ppm)	Peak [NO_x] (ppm, dry)	Minimum RNO_x (ppm/ppm)
CH_4	75	0.39	92	0.46
C_2H_4	86	0.09	98	0.31
CO	3	0.27*	11	0.41*
CO/H_2 (1:1)	36	0.36	46	0.32
CO/H_2 (1:2)	4.1	0.06	7.9	0.20

* These quantities are expressed as a percentage of data taken from a flame with a small amount of steam injection. This was the only way to stabilize this flame.

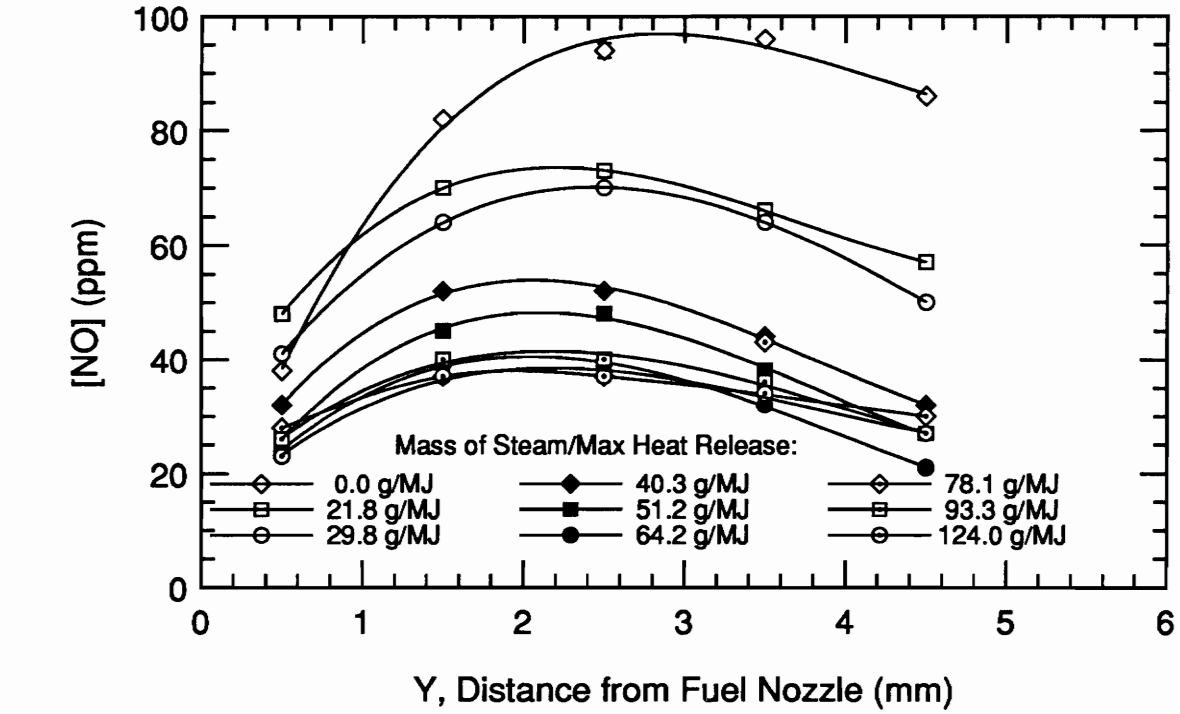

Figure 27(a). NO concentration profiles for various amounts of steam, CH_4 as a fuel, using the coked nozzle.

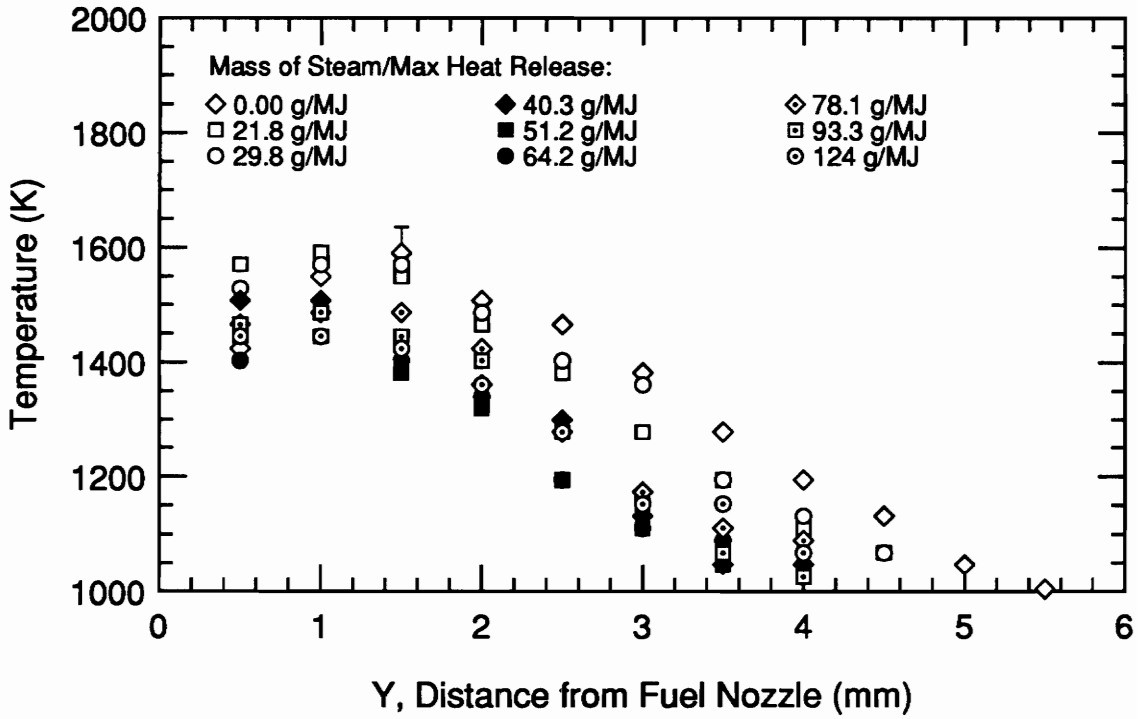

Figure 27(b). Temperature profiles for various amounts of steam, CH_4 as a fuel, using the coked nozzle.

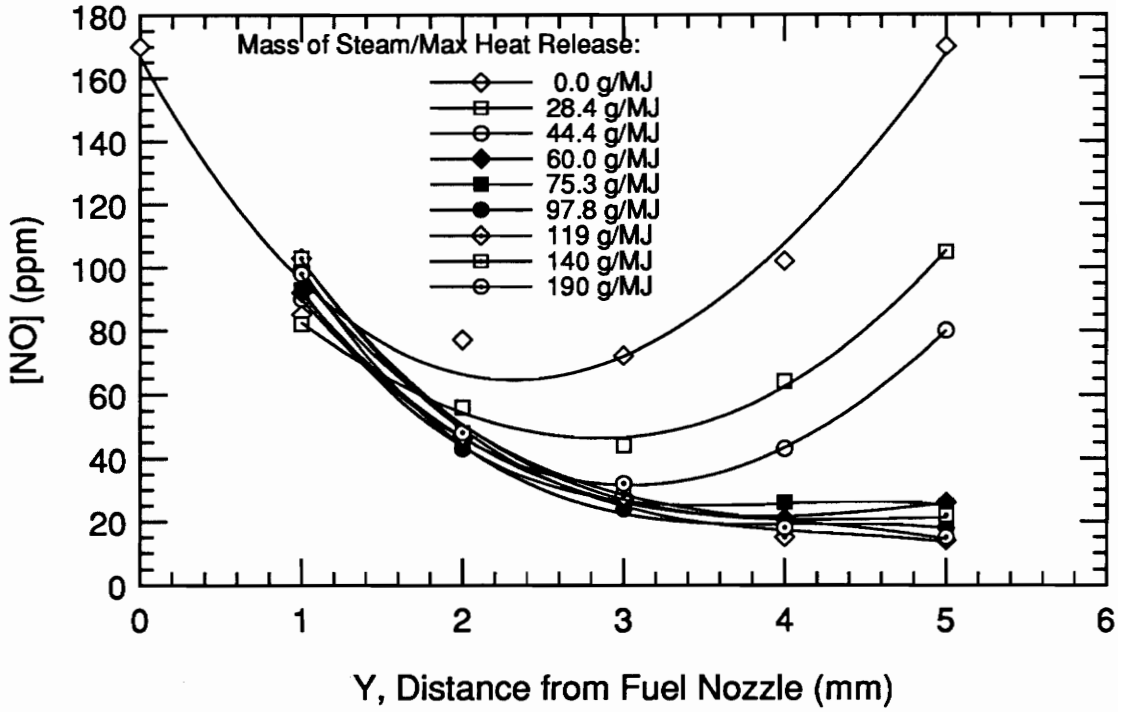

Figure 28(a). NO concentration profiles for various amounts of steam, C_2H_4 as a fuel, using the coked nozzle.

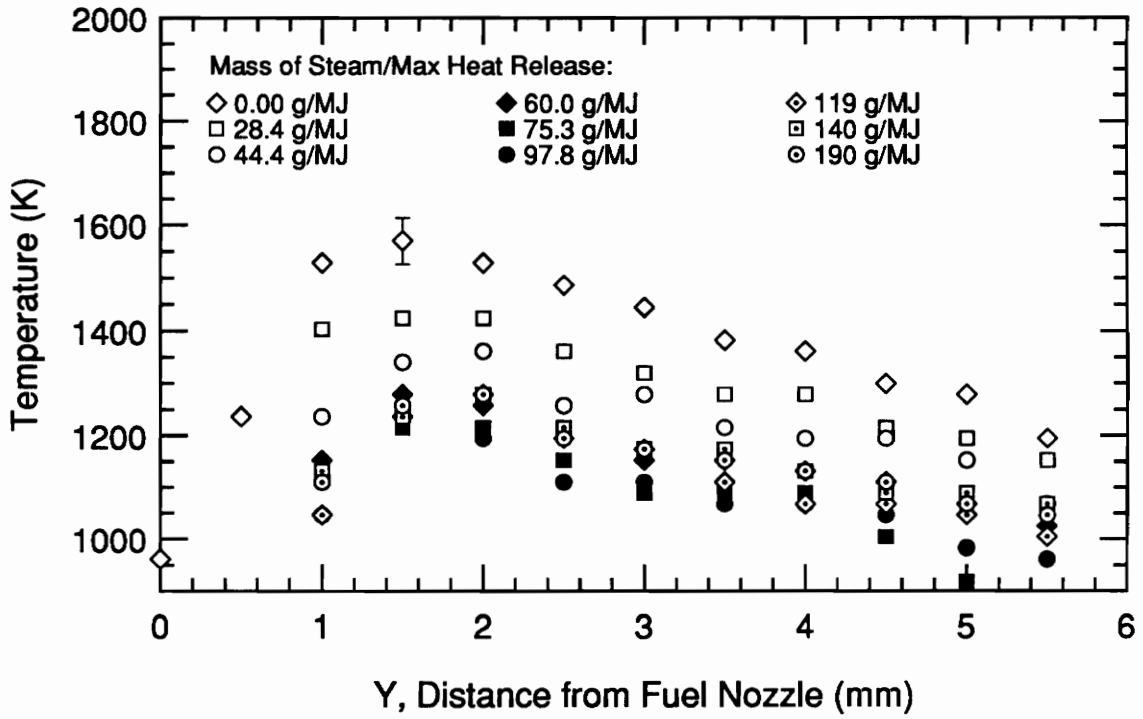

Figure 28(b). Temperature profiles for various amounts of steam, C_2H_4 as a fuel, using the coked nozzle.

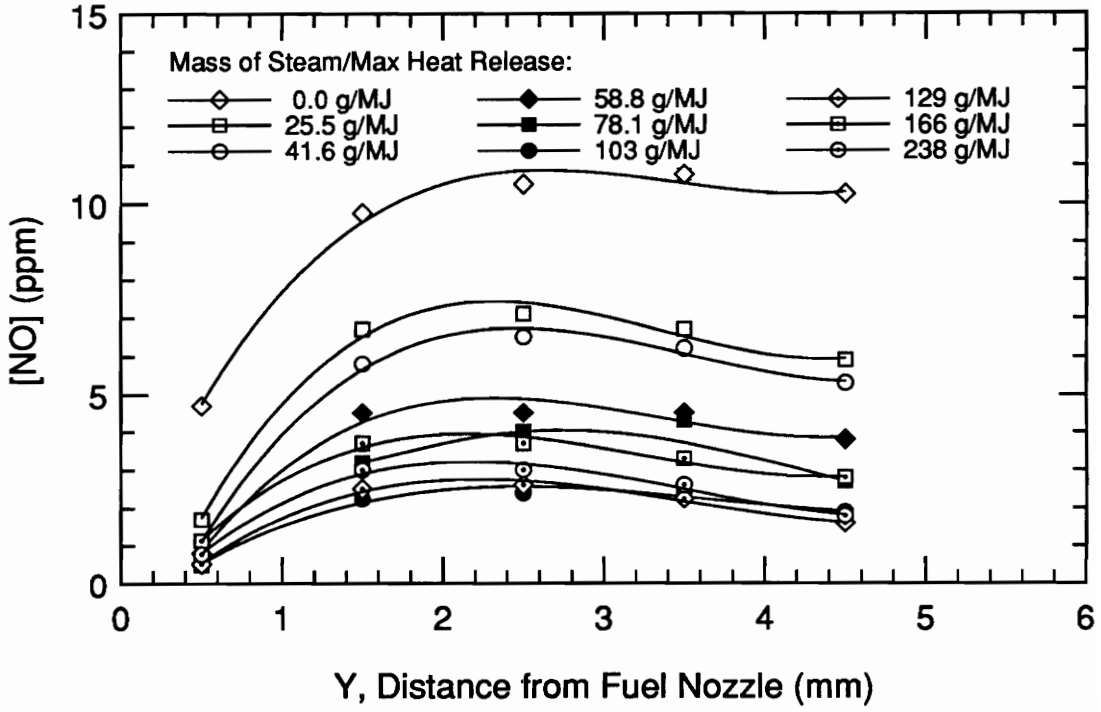

Figure 29(a). NO concentration profiles for various amounts of steam, CO as a fuel, using the coked nozzle.

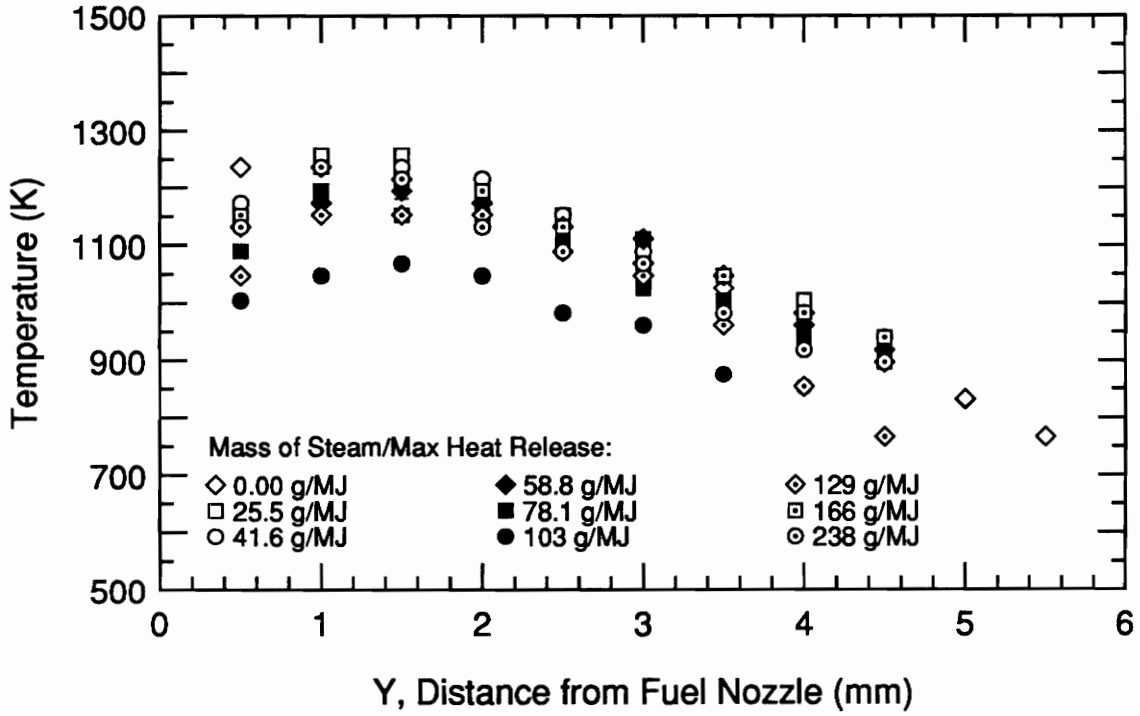

Figure 29(b). Temperature profiles for various amounts of steam, CO as a fuel, using the coked nozzle.

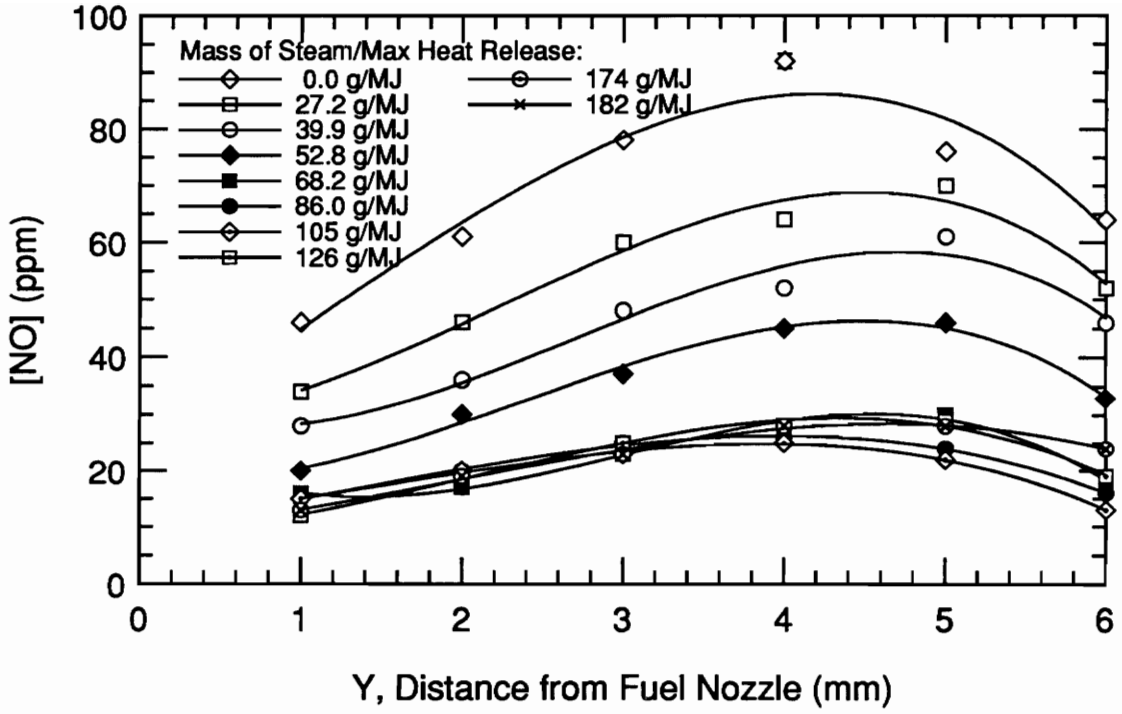

Figure 30(a). NO concentration profiles for various amounts of steam, CO/H_2 (1:1) as a fuel, using the coked nozzle.

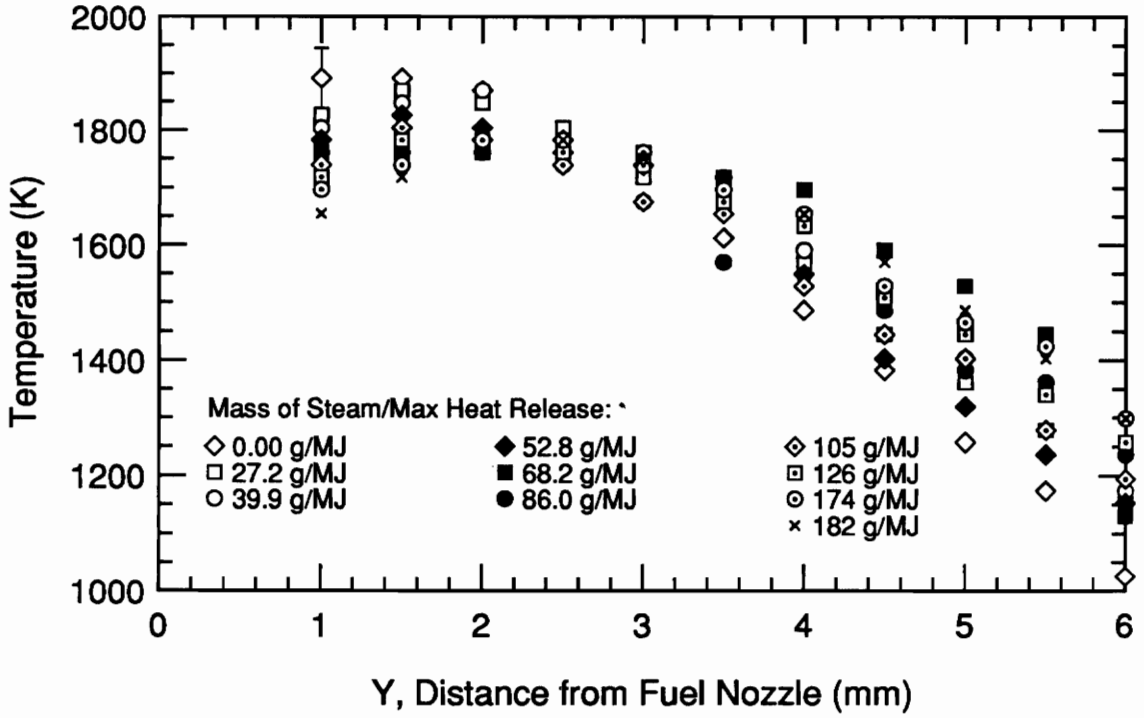

Figure 30(b). Temperature profiles for various amounts of steam, CO/H_2 (1:1) as a fuel, using the coked nozzle.

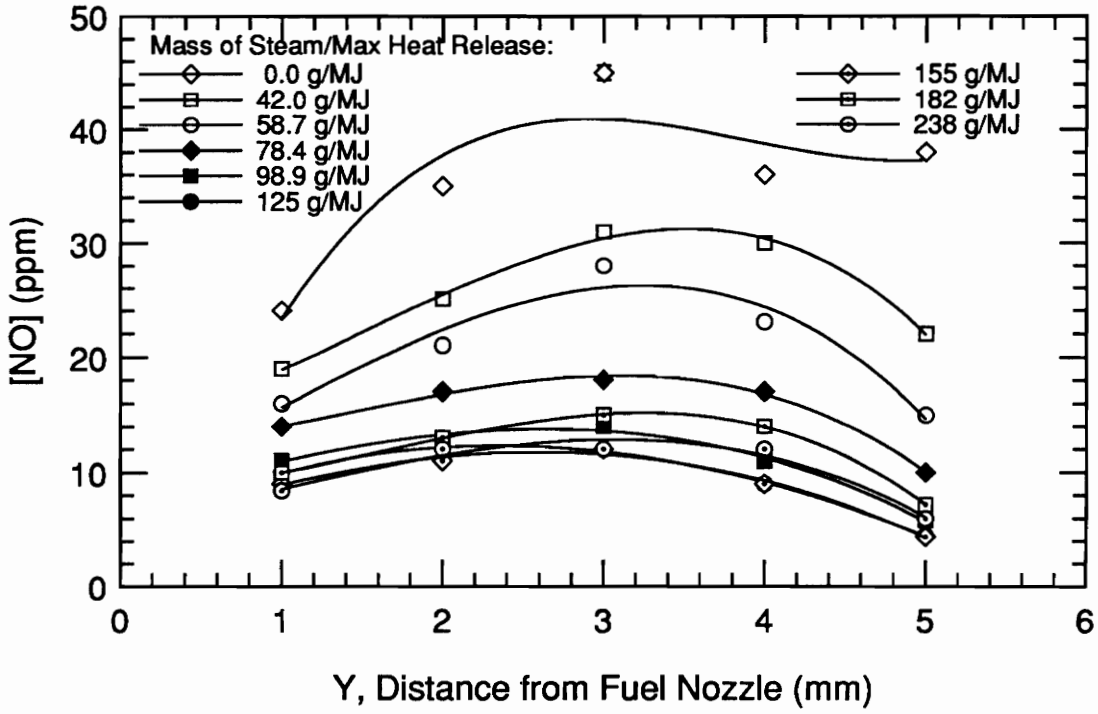

Figure 31(a). NO concentration profiles for various amounts of steam, CO/H_2 (1:2) as a fuel, using the coked nozzle.

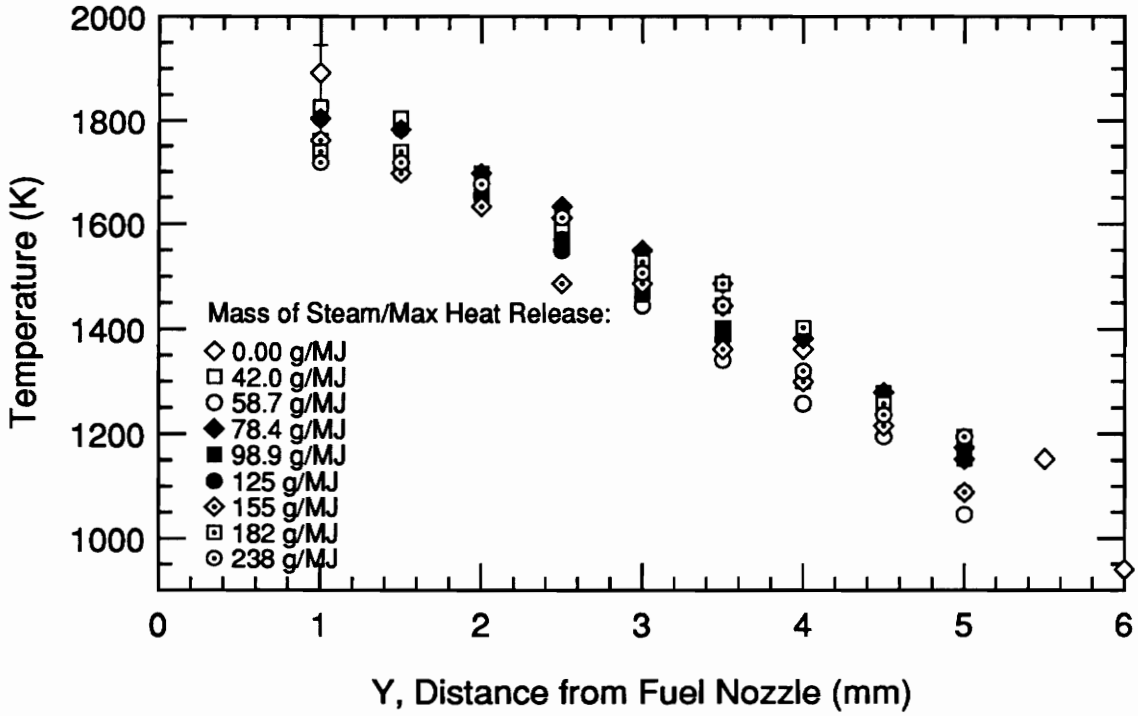

Figure 31(b). Temperature profiles for various amounts of steam, CO/H_2 (1:2) as a fuel, using the coked nozzle.

nozzle, there are some conflicting trends. Some significant differences in the results from the coked and clean nozzle will be presented in this section.

There is an interesting difference between the C_2H_4 data from the coked nozzle and that from the clean nozzle. The NO concentration profiles shown in Fig. 28(a) have different shapes from the profiles shown in Fig. 15 for the clean nozzle. For closer comparison, Fig. 32 shows NO concentration profiles for the C_2H_4 flame with no steam injection for both the clean and coked nozzle. With the clean nozzle, NO concentration is low on the fuel side of the burner, increases to a maximum of 86 ppm, and then decreases again on the air side of the burner. However, with the coked nozzle, the NO concentration is at a maximum of 170 ppm very close to the fuel nozzle and steadily decreases through the fuel side of the flame. The NO concentration peaks at the fuel nozzle, which is the exact location of the coking.

The CO flame also exhibited different behavior with the clean and coked nozzle. Unlike the CO flame with the clean nozzle, the CO flame with the coked nozzle was very stable. Steam addition was not necessary to keep the flame burning. The temperature profiles for the CO flame in the coked nozzle initially decrease but eventually increase, just like those from the clean nozzle.

3.6.2. Comparison of All Fuels

Figure 33 shows peak temperature as a function of the amount of steam for each fuel with the coked nozzle. Temperatures in the CH_4, C_2H_4, and CO/H_2 (1:1) flames "level off." Once again, temperature in the CO flames decreases to a minimum and then increases again. Temperature in the CO/H_2 (1:2) flame decreases until it reaches a minimum. All temperatures "level off" at a steam amount of 100-150 g/MJ. For the

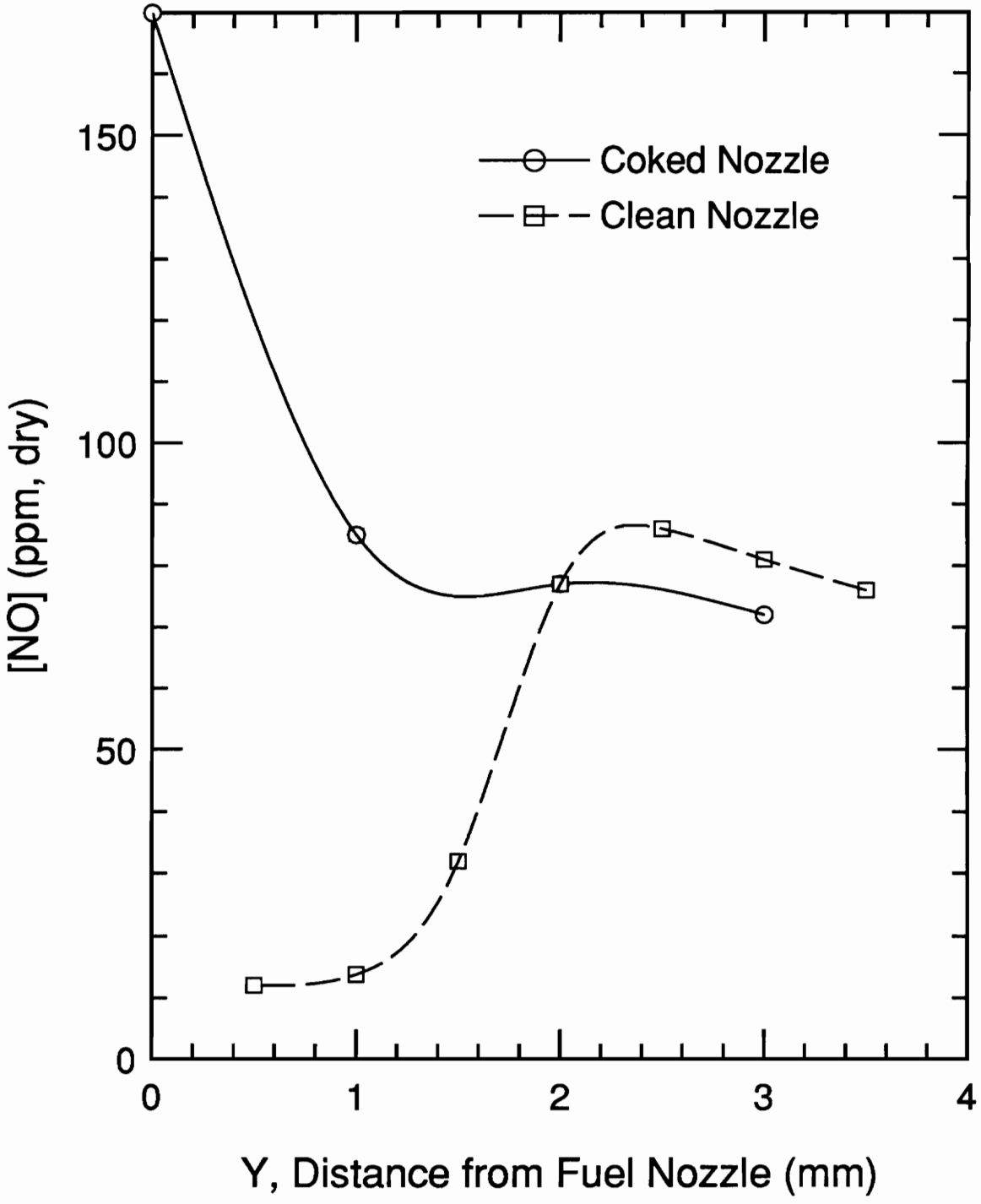

Figure 32. NO concentration profiles, no steam, C_2H_4, coked and clean nozzle.

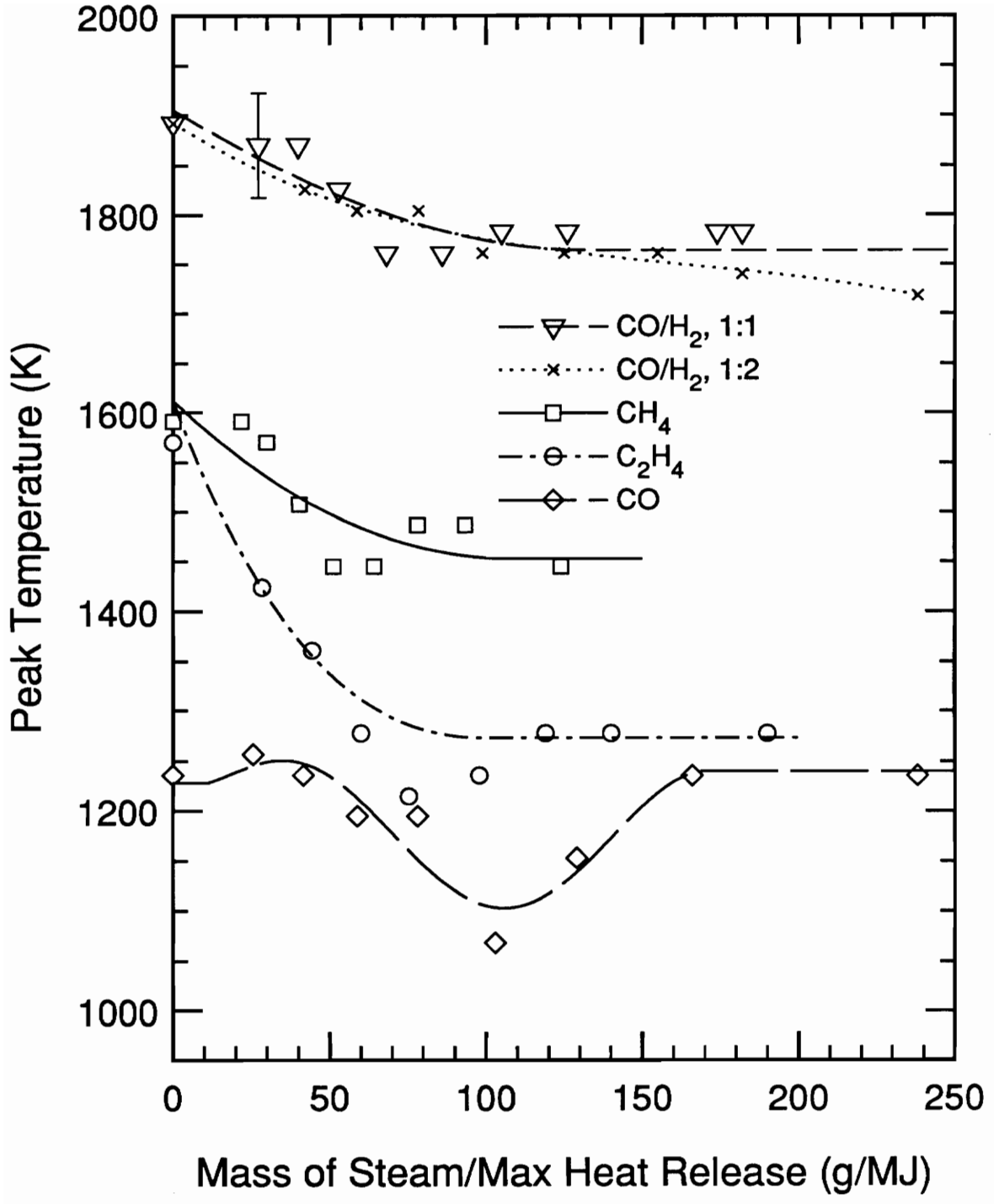

Figure 33. Peak temperatures for all fuels, using the coked nozzle.

hydrocarbon flames, peak temperatures are higher with the clean nozzle. In contrast, for the non-hydrocarbon flames, peak temperatures are higher with the coked nozzle.

Table 3.3 shows the total amount of temperature suppression provided by the range of steam amounts used in these experiments. Peak temperature, minimum temperature, and temperature drop are shown for each fuel with both the coked and clean nozzle. The temperature drop is also expressed as a percentage of the peak temperature in the flame. The data in Table 3.3 shows that there are varying amounts of temperature suppression for all of the fuels. There are also varying peak flame temperatures for all of the fuels. The smallest percent temperature drop is 1.1% in the CO/H_2 (1:1) flame with the clean nozzle; the largest percent temperature drop is 23% in the C_2H_4 flame with the coked nozzle.

Table 3.3 shows that for C_2H_4, the temperature drops by 23% with the coked nozzle, but that the temperature drop is only 8% with the clean nozzle. This fact deserves emphasis because the temperature profiles for the C_2H_4 flames with no steam injection are essentially the same for the coked and clean case. Temperatures peak at about 1600 K at a distance of about 1.5 mm away from the fuel nozzle. Thus, for the same initial C_2H_4 flame condition, there is more temperature suppression with the coked nozzle than with the clean nozzle. Table 4 shows that, with the exception of CO/H_2 (1:2), there is always a greater percentage of temperature suppression with the coked nozzle than with the clean nozzle.

Figure 34(a) and Fig. 34(b) show NO concentration as a function of the amount of steam with the coked nozzle. For clarity, results for the hydrocarbon fuels and the non-hydrocarbon fuels are shown on separate graphs. For this comparison, the peak NO concentrations for the C_2H_4 flame in the coked nozzle are taken from the flame area

Table 3.3. Temperature Suppression

Fuel	Peak Temperature (K)	Minimum Temperature (K)	Temperature Drop (K)	Percent Drop (%)
CH_4 (clean)	1722	1566	156	9.1
CH_4 (coked)	1591	1445	146	9.2
C_2H_4 (clean)	1618	1489	129	8.0
C_2H_4 (coked)	1570	1215	355	23
CO (clean)	1065	1023	42	3.9
CO (coked)	1236	1068	168	14
CO/H_2 (1:1) (clean)	1855	1834	21	1.1
CO/H_2 (1:1) (coked)	1892	1761	131	6.9
CO/H_2 (1:2) (clean)	1618	1345	273	17
CO/H_2 (1:2) (coked)	1892	1718	174	9.2

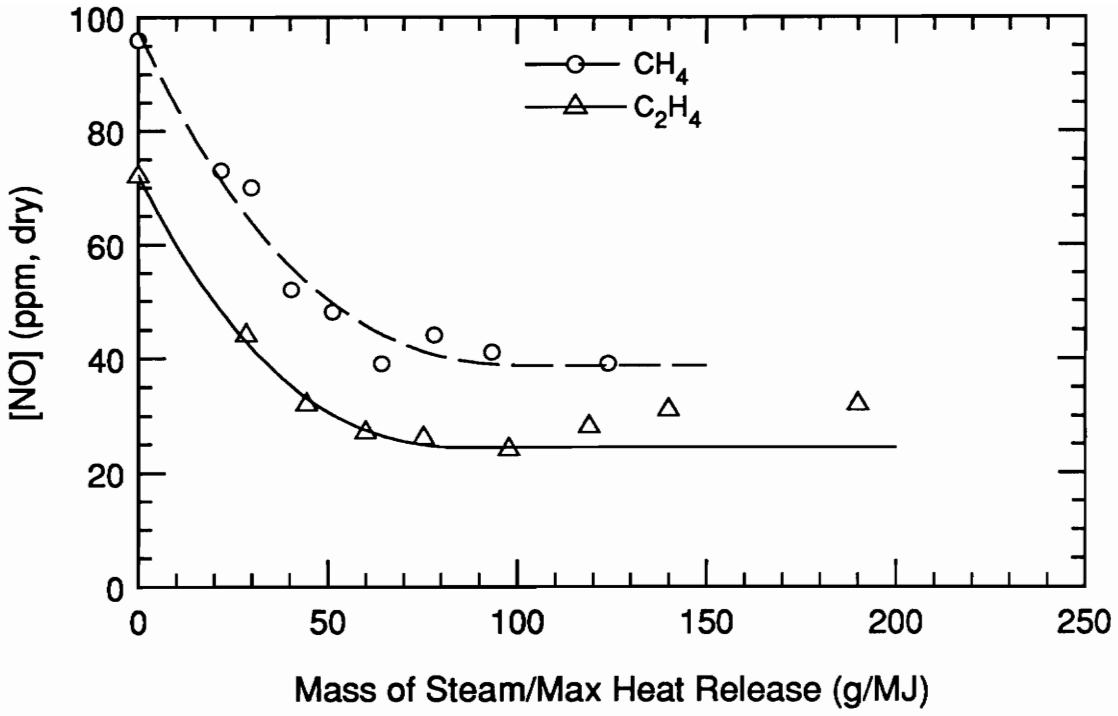

Figure 34(a). NO concentrations for hydrocarbon fuels, using the coked nozzle.

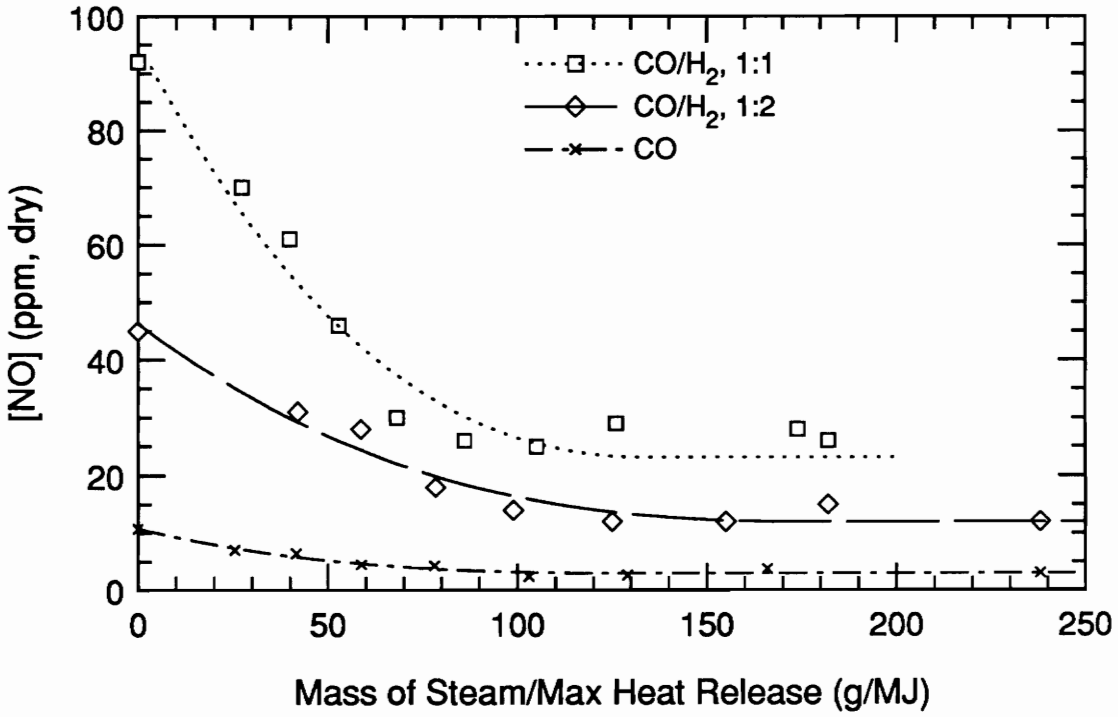

Figure 34(b). NO concentrations for non-hydrocarbon fuels, using the coked nozzle.

rather than from the location of the fuel nozzle. All of these NO concentrations "level off" at steam amounts of 100-150 g/MJ. This data shows that for the coked nozzle, NO concentrations "level off" at the highest amount for the CH_4 flame. These NO concentrations "level off" at intermediate amounts for the C_2H_4 and CO/H_2 (1:1) flame, and they "level off" at the lowest amounts for the CO and CO/H_2 (1:2) flames. For all fuels, peak NO concentrations are higher in the coked case than in the clean case.

Figure 35 shows RNO as a function of the amount of steam with the coked nozzle for all fuels. All of these curves "level off" at steam amounts of 100-150 g/MJ. These results show that with the coked nozzle, steam is slightly more effective at eliminating NO in the non-hydrocarbon flames than in the hydrocarbon flames. Because RNO "levels off" at values of 0.40 and less, these results show that with the coked nozzle, at least 60% of the NO was eliminated using steam injection.

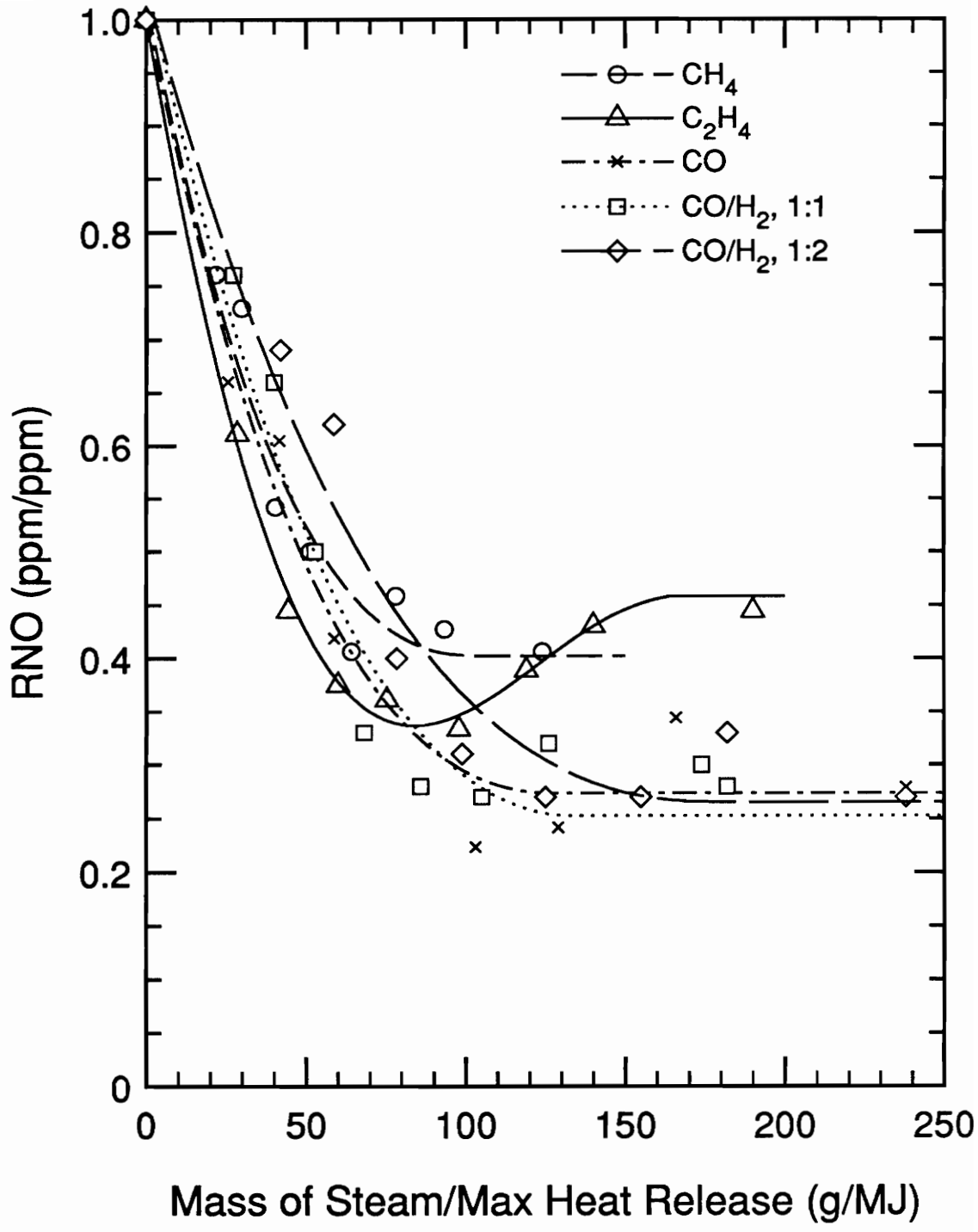

Figure 35. RNO for all fuels, using the coked nozzle.

CHAPTER 4: DISCUSSION

4.1. Introduction

The first section of this chapter discusses the thermal effect of steam addition seen in the results of these experiments. The next section compares the current study with the past studies of Touchton and Drake and Blint. The following section discusses evidence of a chemical effect of steam addition. Finally, the last section discusses several clues of the existence of Fenimore NO in these experiments.

4.2. Thermal Effect of Steam Addition

These experiments reproduced the "leveling off" of NO_x emissions with increasing steam addition that has been reported for industrial gas turbine combustors. The "leveling off" of NO_x emissions in these experiments coincided with a "leveling off" of peak flame temperatures.

Chemical equilibrium modeling was performed to predict the thermal effect of adding steam to a stoichiometric CH_4/Air flame and a stoichiometric CO/H_2/Air flame. This modeling was performed with the STANJAN computer program [40], using the assumption that the fuel, air, and steam were well mixed. Figure 36(a) shows the predicted temperature drop for both CH_4 and CO/H_2 flames with increasing steam amounts. Predicted temperature drops uniformly as steam injection increases. This predicted temperature drop is a result of the thermal effect of adding the heat capacity of the steam to the flame. Figure 36(b) shows the actual temperature drop for all fuels in the laboratory burner. The initial slopes of the actual temperature curves are much smaller than the slopes of the predicted temperature curves. This means that the actual temperature drops at a slower rate than the predicted temperature. This difference in rates

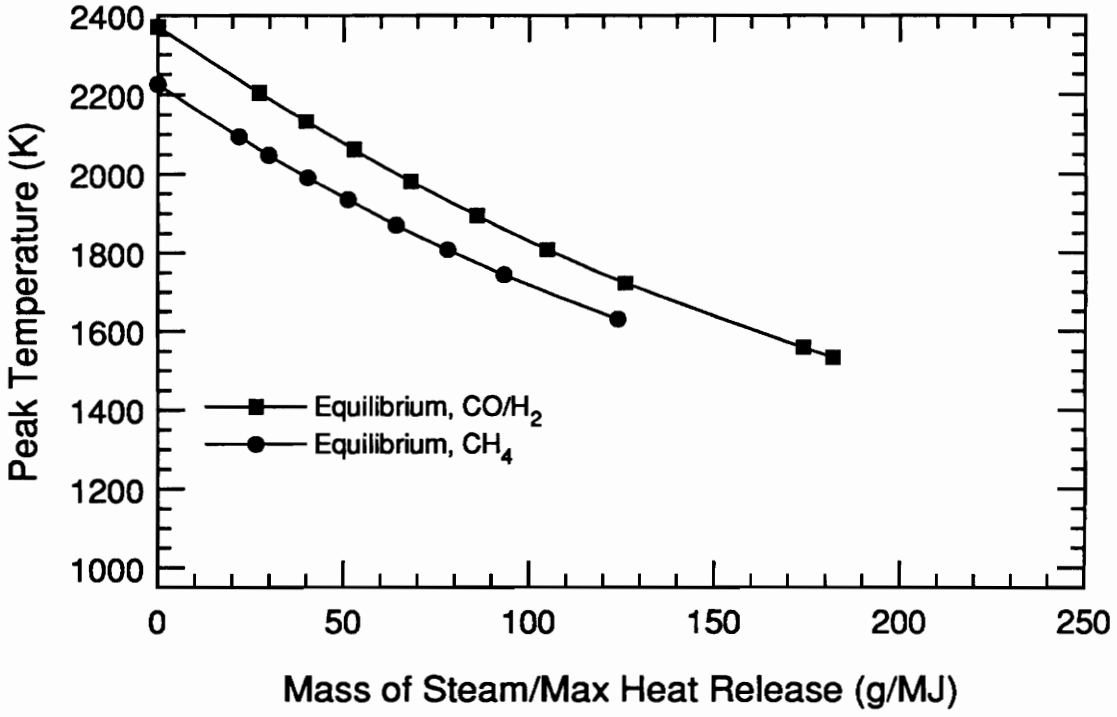

Figure 36(a). Peak temperatures for some fuels, equilibrium model.

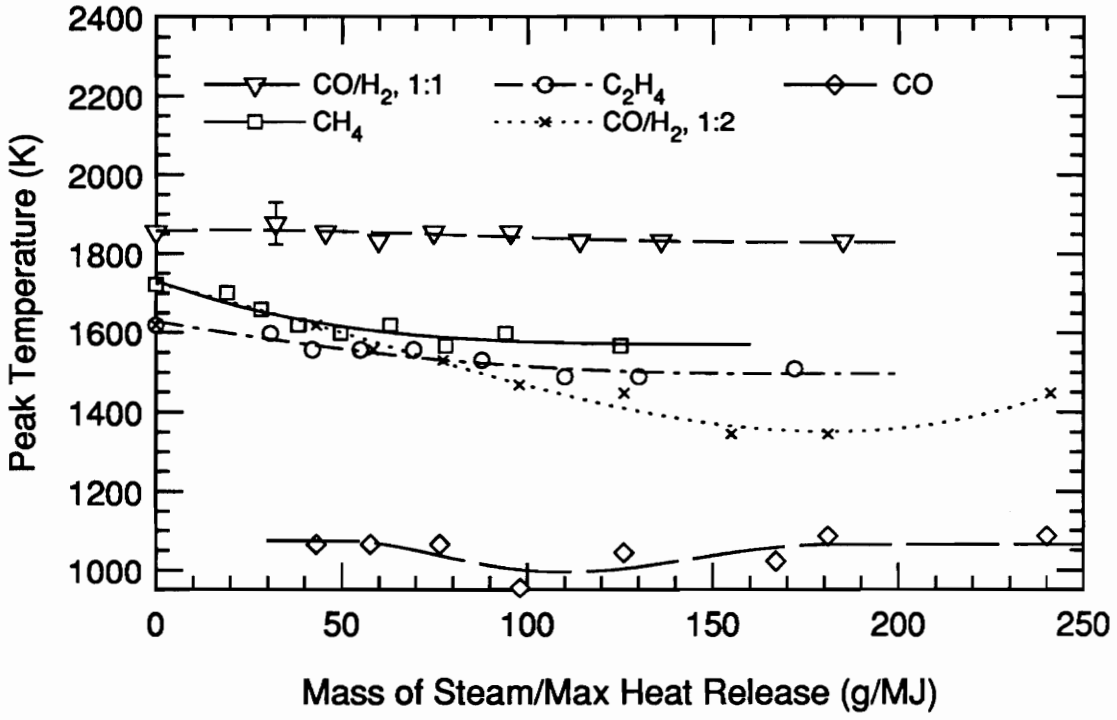

Figure 36(b). Peak temperatures for all fuels, using the clean nozzle.

is probably due to the fact that the steam, air, and fuel do not mix as uniformly in a diffusion flame as was assumed before executing the STANJAN computer program. The actual temperature also exhibits a "leveling off" trend; equilibrium modeling does not predict this trend.

If steam injection works entirely by the thermal effect of lowering temperature and slowing down the Zeldovich mechanism, equilibrium modeling should predict the trend in NO_X emissions with increasing steam addition. The quantity RNO_X is used to compare the measured and predicted results, since the actual NO_X concentrations in the laboratory flames did not reach the high NO_X concentrations predicted by the equilibrium model. Figure 37 shows actual and equilibrium RNO_X as a function of steam amount with the clean nozzle for all fuels. Interestingly, the predicted RNO_X for the CH_4 and CO/H_2 fuels collapse onto the same line. The equilibrium modeling shows that RNO_X should decrease uniformly to nearly zero at a steam amount of 150 g/MJ. The laboratory RNO_X decreases at a slower rate than the predicted RNO_X, and the actual data also "levels off" at values of 0.2 and above. Nonetheless, the trend in actual RNO_X seems to mimic the trend in the predicted RNO_X. If the actual temperature had been suppressed as quickly and as uniformly in the laboratory as the equilibrium model predicted that it should, RNO_X may have matched the equilibrium prediction exactly. Thus, equilibrium modeling suggests that the effects of steam injection could be thermal in nature, and these effects would be evident if the temperature could be suppressed uniformly in the burner.

There are at least two possible reasons that the temperature "leveled off" in the burner. First, the flames had the ability to move closer to the fuel nozzle. Since the nozzle was stainless steel, it conducted heat away from the flame. It is possible that the steam pushed the flame closer to the nozzle, and a point was reached where heat transfer to the nozzle dominated any thermal effect caused by the steam. This could have caused the

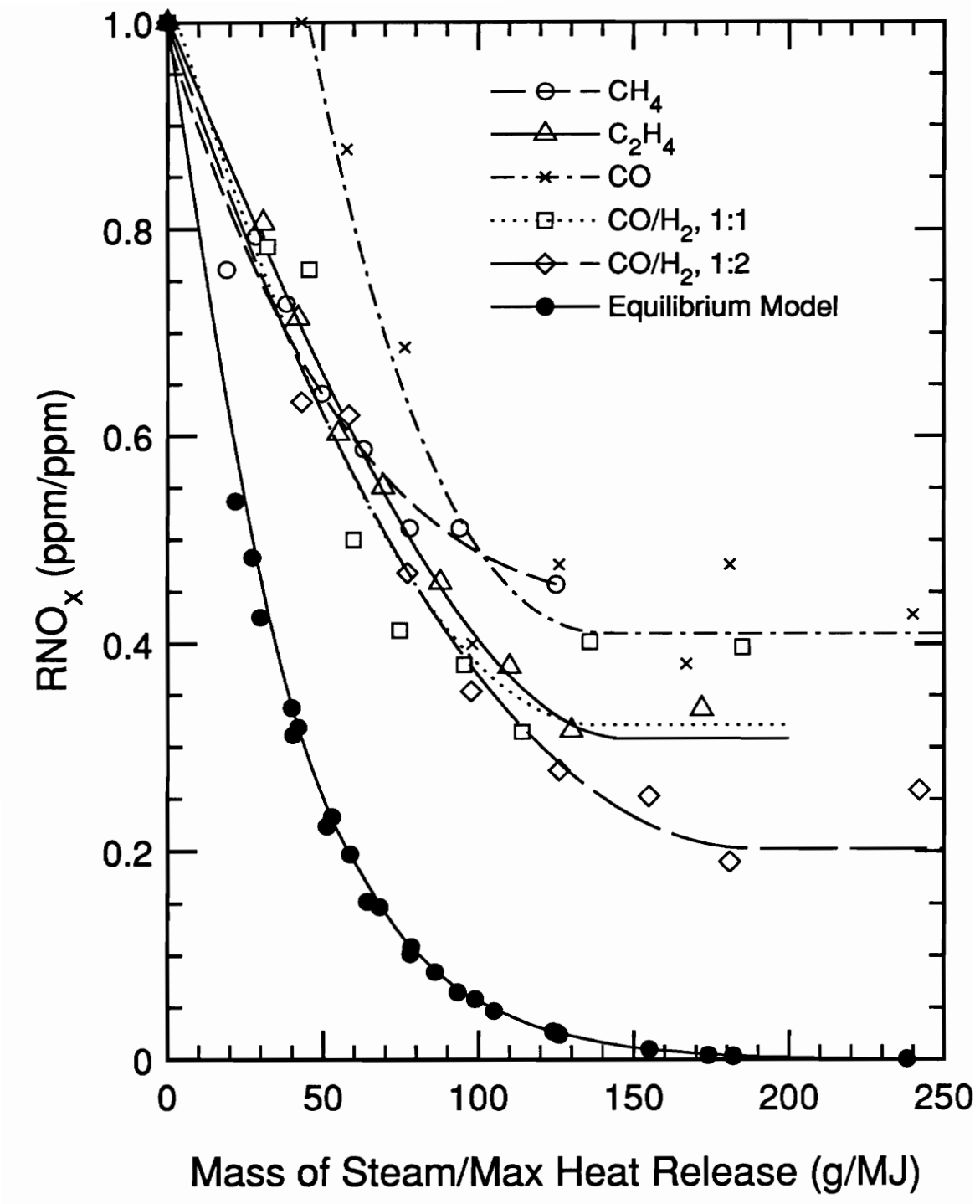

Figure 37. Actual and equilibrium RNO_x for all fuels, using the clean nozzle.

flame to remain at a constant temperature. This explanation is more likely to apply to the CH_4 flames than to the other flames, since the CH_4 flames moved the most. The second explanation for the "leveling off" of temperature is that there may be a limit to how much steam can diffuse into the chemically reactive zone of the flame. Once this limit is reached, a constant amount of steam contacts the flame, regardless of how much steam is injected into the burner. Thus, all data points collected after the steam diffusion limit is reached are actually the same data point. This would explain the "leveling off" of temperature and NO_X emissions in the burner. Thus, steam injection into nonpremixed flames may be a diffusion limited process.

The fact that the NO_X concentration always peaked on the air side of the temperature peak indicated that Zeldovich NO is important in opposed flow diffusion flames. It is well known that Zeldovich NO peaks in premixed flames that are slightly fuel lean. This is because the Zeldovich NO requires high oxygen concentrations in addition to the high temperatures associated with a stoichiometric mixture. Also, hydrocarbon fuel fragments that participate in the Fenimore mechanism are less likely to survive on the air side of the flame without being quickly oxidized. Thus, the NO_X peak on the air side of the flame emphasizes the importance of the Zeldovich mechanism.

4.3. Comparison of Results with Past Studies

There was not a strong enough difference in the data from the hydrocarbon and non-hydrocarbon fuels to draw a conclusion about the importance of the Fenimore mechanism in diffusion flames. It can be said, however, that the Zeldovich mechanism was responsible for at least 55% of the NO_X formed in these opposed flow diffusion flames. This was because 55% or more of the NO_X formed in all flames was eliminated with steam before the temperatures "leveled off." The "leveling off" of NO_X emissions

can be attributed to the fact that the temperatures "leveled off" and stopped slowing down the Zeldovich mechanism. It is not necessary to invoke the Fenimore mechanism to explain the "leveling off" of NO_X emissions.

These results do not clearly agree with either Touchton [9] or Drake and Blint [32]. Touchton stated that almost all of the NO_X formed in diffusion flames is Zeldovich NO and thus can be eliminated using steam injection; only 55% of the NO_X in the current study was eliminated by steam injection. Drake and Blint stated that less than 33% of the NO_X formed in diffusion flames is formed by the Zeldovich mechanism; at least 55% of the NO_X in the current study was formed by the Zeldovich mechanism.

The largest amount of steam used in Touchton's experiments corresponded to a mass of steam to mass of fuel ratio of 2.0. For the CH_4 fuel used by Touchton, this amount of steam corresponded to a mass of steam per maximum heat release ratio of 40 g/MJ. With steam amounts up to 40 g/MJ, the NO_X concentrations in the current study decreased uniformly, very much like the results compiled in Touchton's study. Thus, upon closer inspection, the results of the current study actually agree with the results of Touchton. However, Touchton assumed that the NO_X emissions would continue to decrease uniformly with addition of more steam. If Touchton had studied larger quantities of steam injection, he most likely would have observed that the NO_X emissions actually "level off," which was reported by Toof [6], and which was shown in the current study. Because the "leveling off" of NO_X concentrations coincided with the "leveling off" of temperatures in the current study, Touchton's conclusion that steam works by a thermodynamic effect may be correct. However, Touchton further concluded that almost all of the NO_X is formed by the Zeldovich mechanism, and thus can be eliminated using steam injection. The "leveling off" results of this study show that only a portion of the NO_X can be eliminated using steam addition. Thus, even though the results of this study

at low steam amounts agree with Touchton's results, the conclusion of this study is quite different from Touchton's conclusion.

The results of the current study did not show that the Fenimore mechanism is responsible for the "leveling off" of NO_x emissions with high amounts of steam. However, the results did not eliminate the possibility that Fenimore NO is important. Because of this, the conclusion of Drake and Blint that Fenimore NO is important in diffusion flames may be correct. However, the results of the current study show that there was a larger percentage of Zeldovich NO in opposed flow diffusion flames than was predicted by Drake and Blint. This discrepancy is at least partially due to differences between the flames studied by Drake and Blint and the flames of this study. First, the flames of Drake and Blint had strain rates of 42 s^{-1}, 70 s^{-1}, and 140 s^{-1}, which were much higher than the strain rate of 13 s^{-1} used in this study. Higher strain rates result in lower temperatures and shorter residence times. Since Zeldovich NO is proportional to both the peak temperature and the residence time, higher strain rates would make the contribution of the Zeldovich mechanism less important. Also, the experiments used in the study by Drake and Blint were performed with the fuels of $CO/H_2/N_2$ and CH_4/N_2. Addition of N_2 on the fuel side of the burner probably gave an exaggerated importance to the Fenimore mechanism. This is because the N_2 was available in the hot nozzle where the fuel pyrolyzed, which encouraged initiation of the Fenimore mechanism. Because Drake and Blint studied a specific type of diffusion flame, their conclusion that the Fenimore mechanism is important in all diffusion flames is not valid. In fact, the results of the current study prove that the conclusion of Drake and Blint does not even apply to the specific case of the laminar, opposed flow diffusion flame. Thus, the conclusion of the current study that at least 55% of the NO_x formed in laminar, opposed flow diffusion flames is Zeldovich NO contradicts the conclusion of Drake and Blint.

The findings of the current study do not clearly agree or disagree with the conclusions of Touchton or Drake and Blint. Instead, there are portions of each study which are supported by the current study, and there are portions of each study which are refuted by the current study. Touchton's conclusion that steam addition works by a thermodynamic effect is supported by these results. Touchton's assumption that most of the NO_X can be eliminated using steam injection is refuted by these results. The conclusion of Drake and Blint that Fenimore NO may be important is not proven wrong by these results. The conclusion of Drake and Blint that most of the NO_X in diffusion flames is Fenimore NO is refuted by these results.

4.4. Chemical Effect of Steam Addition

Although steam generally acted as a heat sink and suppressed temperatures in the flames, there was some evidence of a chemical effect of adding steam, particularly in the CO flame. Combustion of pure CO in air does not produce an active radical pool like that produced by combustion of hydrocarbon fuels. For this reason, the pure CO flame was difficult to stabilize. Addition of a small amount of steam added OH radicals to the flame, and helped with stability. Thus, the steam participated chemically in the oxidation of the CO. This chemical participation may explain the fact that temperatures decreased and then began to increase again in the CO flame. At high steam levels, there was enough OH to participate actively and make the temperature in the flame begin to rise.

This evidence of chemical participation in the CO flame must be considered cautiously. The temperature data may have been in error because the Pt/PtRh thermocouple was uncoated. Uncoated platinum is a catalyst for certain exothermic reactions, particularly the H atom recombination reaction. These exothermic reactions on the surface of the thermocouple cause the temperature reading to be higher than the

actual temperature being measured. Addition of steam increased H atom concentration. Thus, at high levels of steam addition, the increase in temperature in the CO flame was at least partially caused by excess H atom recombination reactions rather than the chemical effect of adding the steam. There was a slight increase in NO_x emissions when the temperature began to rise in the CO flames. This means that the temperature may have risen slightly, but not as dramatically as the temperature data indicated. Thus, there was a slight chemical effect of adding steam to the CO flame.

The fact that the temperature data remained "level" in the CO/H_2 (1:1) flame over the range of steam amounts provides further evidence of the error associated with using the uncoated thermocouple. In this flame, H_2 was present in the fuel, which may have increased the probability that exothermic recombination reactions would occur on the thermocouple. Total NO_x generally decreased with steam addition, in spite of the fact that the temperature remained "level" with steam addition. The NO_x trend leads to the conclusion that the temperature actually decreased, but that the thermocouple data was distorted. Thus, the trend in the temperature of the CO/H_2 (1:1) flame can be explained by exothermic chemical reactions on the surface of the thermocouple bead.

There is a possibility that steam acted in a chemical capacity in the C_2H_4 flames. The reason for this hypothesis is that there was a temperature suppression of 23% in the flame with the coked nozzle, whereas there was a temperature suppression of only 8% with the clean nozzle. Perhaps the thermal and chemical effects competed in the C_2H_4 flames. With the coked nozzle, the existence of the hydrocarbon coking when the fuel was pyrolyzing may have created more hydrocarbon radicals. These radicals may have acted to sustain combustion, while the added steam acted entirely as a heat sink. However, with the clean nozzle, some of the steam may have acted to oxidize the fuel and sustain combustion, instead of acting as a heat sink. It is also possible that there was

more soot with the coked nozzle, and that the steam addition encouraged the formation of even more soot. In this case, the large temperature drop with the coked nozzle may have been from increased radiative heat losses caused by the soot.

Another chemical effect that should be discussed is that the steam was most effective at eliminating NO_x in the CO/H_2 (1:2) flame. This is evidenced by the fact that in both the coked and clean case, RNO_x and RNO "leveled off" at the lowest amounts for the CO/H_2 (1:2) flame. Because this flame involved the addition of a large amount of H_2, this trend suggests that H_2 may have an effect on NO reduction. Further studies are needed to verify that this trend exists.

4.5. Hints of the Existence of Fenimore NO

Although these experiments did not show that the Fenimore mechanism is important for explaining the "leveling off" trend of NO_x emissions, there were some indications of the existence of Fenimore NO in these flames. First, comparison of RNO_x values indicated that steam was least effective at eliminating NO_x from CH_4 flames. Only about 55% of the NO_x was eliminated from CH_4 flames with the clean nozzle. For the non-hydrocarbon fuels and C_2H_4, 70%-80% of the NO_x was eliminated with steam injection. It is possible that some of the 45% of NO_x left in the CH_4 flame was Fenimore NO.

Another indicator of the existence of Fenimore NO was that absolute NO_x concentrations were much higher in the hydrocarbon flames of CH_4 and C_2H_4 than they were in the non-hydrocarbon flames of CO, CO/H_2 (1:1), and CO/H_2 (1:2). This was not merely a temperature effect, because the temperatures in the CH_4 and C_2H_4 flames were lower than those in the CO/H_2 (1:1) flame. The fact that the NO_x concentrations were higher in the hydrocarbon flames might possibly be explained by the participation of the

more active radical pool in the Zeldovich mechanism. However, another possible explanation for these higher NO_X amounts is that the Fenimore mechanism is significant in the hydrocarbon flames. If this is the case, the NO_X concentrations in the hydrocarbon flames were higher because they contained both Zeldovich and Fenimore NO, whereas the non-hydrocarbon flames only contained Zeldovich NO.

The differences in results from the coked and the clean nozzle also hint at the existence of Fenimore NO. The coking was a result of the partial pyrolysis of the hydrocarbon fuels in the hot nozzle. Thus, hydrocarbon fragments were deposited on the surface of the stainless steel beads in the fuel nozzle. This provided a supply of hydrocarbon fragments to participate in the Fenimore mechanism for all of the flames, even for those burned with non-hydrocarbon fuels.

There were several effects that proved that this coking added hydrocarbon fragments to the flames. First of all, the CO flame with no steam addition was very stable in the coked nozzle. The same flame would not stabilize in the clean nozzle. This means that some of the hydrocarbon fragments from the coked nozzle participated in the combustion reactions of the CO flame, and provided an active radical pool to keep the CO flame stable. This stability enhancement was evident in all of the non-hydrocarbon flames. Comparison of the NO concentration profiles in the coked and clean nozzle for the non-hydrocarbon fuels reveals that the NO concentration profiles were more smooth and uniform with the coked nozzle than with the clean nozzle. Thus, the hydrocarbon fragments had a positive effect on the stability of the non-hydrocarbon flames. The other effect that proved the existence of the hydrocarbon fragments in the nozzle was the temperature effect. In all cases, peak temperatures of the non-hydrocarbon flames were higher with the coked nozzle than they were with the clean nozzle. This was because the added hydrocarbon fragments had higher heating values than the non-hydrocarbon fuels.

Combustion of this higher heating value fuel produced hotter flame temperatures. Also, in all cases, peak temperatures of the hydrocarbon flames were lower with the coked nozzle than with the clean nozzle. This was because the coking produced soot in the flames, which increased the radiative heat losses of the flames.

The existence of the hydrocarbon coking influenced NO production in the flames. For all fuels, NO concentrations were dramatically higher when the nozzle was coked with hydrocarbons. These hydrocarbons may have contributed to Fenimore NO formation. This hypothesis is supported by the fact that in the C_2H_4 flame, with the coked nozzle, the peak NO concentrations were at the surface of the nozzle. This was the location of these hydrocarbon coked beads, and it was likely the location of excessive Fenimore NO formation.

The trend in RNO with the coked nozzle was that steam was slightly more effective at eliminating NO from the non-hydrocarbon flames than it was at eliminating NO from the hydrocarbon flames. The fact that the nozzle was coked made the Fenimore mechanism more important, which emphasized the differences in the types of fuels.

CHAPTER 5: SUMMARY, CONCLUSIONS, AND RECOMMENDATIONS

5.1. Summary

In summary, laboratory experiments were performed to try to reproduce the "leveling off" of NO_X emissions with high amounts of water injection which has been observed in industrial gas turbine diffusion flame combustors. The secondary goal of the study was to see if the "leveling off" of NO_X emissions can be attributed to the Fenimore NO formation mechanism. The experiments involved injecting steam into a laminar, opposed flow diffusion flame burner. The fuels used were the hydrocarbon fuels of CH_4 and C_2H_4, and the non-hydrocarbon fuels of CO, CO/H_2 (1:1), and CO/H_2 (1:2). Probe sampling and a chemiluminescent analyzer were used to determine NO concentrations and total NO_X concentrations in the flame front. An uncoated, radiation corrected Pt/Pt10%Rh thermocouple was used to measure flame temperatures.

The results of the laboratory experiments did reproduce the "leveling off" of NO_X emissions with high amounts of steam addition. Temperatures "leveled off" in the laboratory burner also. Temperatures and NO_X concentrations "leveled off" at about the same steam amount for all fuels. There was no significant difference in the results from the hydrocarbon fuels and those from the non-hydrocarbon fuels. At least 55% of the NO_X was eliminated from all of the flames using steam injection. There were important differences in results obtained from a hydrocarbon coked fuel nozzle and those obtained with a clean nozzle.

5.2. Conclusions

The first conclusion of this study was that the "leveling off" of NO_X emissions can be reproduced in the laboratory. The "leveling off" of NO_X emissions was attributed to

the "leveling off" of temperatures in the flames. The steam injected into the laboratory flames reduced NO_x emissions by suppressing the temperature. However, there was a limit to how low the temperature could be suppressed in this opposed flow burner using steam injection. Thus, there was a limit to how low the NO_x concentrations could be driven using steam injection. This contradicts the conclusion of Touchton that most of the NO_x in diffusion flames can be eliminated using steam addition. However, the current study supports Touchton's conclusion that steam injection works by a thermodynamic effect.

The second conclusion of this study was that there may be a limit to how much steam can diffuse into the chemically reactive zone of a nonpremixed flame. If steam injection is a diffusion limited process, once the diffusion limit is reached, further addition of steam will have no effect on how much steam contacts the flame. Thus, the temperature will remain constant. The fact that the temperature remained level in the laboratory burner suggests that this diffusion limit exists. Thus, steam addition may be a diffusion limited process.

The third conclusion of this study was that at least 55% of the NO_x formed in these laminar, opposed flow diffusion flames was formed by the Zeldovich mechanism. This conclusion was drawn because 55% or more of the NO_x was eliminated from all of the flames using steam injection. This contradicts the findings of Drake and Blint that more than 67% of the NO formed in laminar, opposed flow diffusion flames is formed via the Fenimore mechanism. However, the possibility that the Fenimore mechanism may be important in diffusion flames cannot be eliminated based on the results of the current study. Further temperature suppression in the flames is necessary to eliminate the Zeldovich NO and investigate the relative importance of the Fenimore mechanism.

The fourth conclusion of this study was that steam addition can have a chemical effect, in addition to the thermal effect, particularly in non-hydrocarbon flames. This was evidenced by the fact that the temperature in the CO flames initially decreased with steam injection but eventually began to increase again. Also, the fact that the non-hydrocarbon flames were more stable with the coked nozzle than with the clean nozzle reinforced this conclusion.

The fifth conclusion of this study was that the addition of H_2 to a non-hydrocarbon flame may increase the effectiveness of steam injection. This conclusion was drawn from the fact that the steam was most effective at reducing the NO_x emissions in the CO/H_2 (1:2) flame, which was the non-hydrocarbon flame with the most H_2 added. Eighty percent of the NO_x in these flames was reduced with steam injection.

The final conclusion of this study was that Fenimore NO was formed in some of the flames of this study, and that it can play a role in diffusion flames. The existence of the Fenimore mechanism was proven by the fact that the hydrocarbon coked nozzle encouraged the production of NO_x in all of the flames. Results from the coked nozzle also suggested that Fenimore NO might be likely to form at the locations of coked fuel nozzles or burner parts in industrial combustors.

5.3. Recommendations

In the future, efforts should be made to reduce the effects of the nozzle interfering with the flame. One way to do this is to eliminate the heat transfer to the nozzle by using a ceramic fuel nozzle instead of a stainless steel nozzle. Another way to eliminate the heat transfer and coking effects of the nozzle is to add an inert diluent other than N_2 on the fuel side of the flame. This will increase fuel velocities and enable the flame to

stabilize farther away from the fuel nozzle. If the nozzle effects are eliminated, the ability of steam to diffuse into the flame front can be studied more carefully.

It would be important to quantify how much of the injected steam actually contacts the flame front. Flow visualization may be used to approximate this amount. A more accurate way to know how much of the steam contacts the flame is to inject steam on the fuel side of the burner. This will ensure that all of the steam injected contacts the flame front.

The burner should be modified so that a greater range of strain rates can be obtained. One way to do this is to use a smaller fuel nozzle and a smaller chimney for the air flow. The results of these high strain rate tests could then be more readily compared with those of Drake and Blint.

The stability limits of the burner need to be expanded. If the flames were more stable, a wider range of fuel flow rates would be possible in the burner. This would mean that all tests could be performed with approximately the same flame temperatures. Analysis of the results would then be easier because the temperature effect could be eliminated. One way to make the flames more stable might be to turn the burner upside down, and allow the fuel to flow upward while the air is flowing downward.

One way to improve the accuracy of the data collected in these experiments would be to use a coated Pt/PtRh thermocouple. This would eliminate the exothermic reactions on the surface of the thermocouple, which would give more accurate temperature data. However, coated thermocouples should be used with caution. The coating may introduce errors in the radiation correction because the emissivity of a coated thermocouple is difficult to determine. Also, the bead of a coated thermocouple is larger than that of an

uncoated thermocouple, which makes an accurate radiation correction even more difficult.

Another improvement would be to measure CO concentrations in the flames. Observing the way that the CO emissions behave with respect to the NO_X emissions will give more insight into the combustion process. The use of optical measurements would eliminate the flow disturbance that is created by the sample probe and thermocouple.

Data analysis would be more meaningful if the distance from the fuel nozzle were normalized based on flame front location. In this case, the NO_X profiles for the different fuels could be compared readily. One way to normalize this distance would be to convert it to a residence time. This could be accomplished by making velocity measurements using the laser doppler velocimetry (LDV) technique. Residence time could then be calculated using distance and velocity.

Another advantage of using LDV would be that the measured velocities could be converted to a strain rate. The use of the actual velocity would make the calculation of strain rate more accurate than use of the current technique of estimating an average velocity from the flow rate of the air and the size of the chimney.

REFERENCES

1. Davis, L.B., "Gas Turbine Combustion and Emissions," GER-3568, GE Turbine Reference Library.

2. Dibelius, N.R., M.B. Hilt, and R.H. Johnson, "Reduction of Nitrogen Oxides from Gas Turbines by Steam Injection," ASME Paper No. 71-GT-58, March, 1971.

3. Shaw, H., "The Effects of Water, Pressure, and Equivalence Ratio on Nitric Oxide Production in Gas Turbines," ASME Paper 73-WA/GT-1, July 1974.

4. Hilt, M.B., and J. Waslo, "Evolution of NO_x Abatement Techniques Through Combustor Design for Heavy-Duty Gas Turbines," Journal of Engineering for Gas Turbines and Power, October 1984, Vol. 106, pp. 825-832.

5. Correa, Sanjay, "Current Problems of Gas Turbine Combustion," Presented at the 1990 Fall Technical Meeting of the Eastern Section of the Combustion Institute, Orlando, Florida, December 1990.

6. Toof, J.L., "A Model for the Prediction of Thermal, Prompt, and Fuel NO_x Emissions From Combustion Turbines," ASME Paper 85-GT-29, July 1985.

7. Zeldovich, J., "The Oxidation of Nitrogen Combustion and Explosions," Acta Physicochimica, URSS, Vol. 21, p. 577, 1946.

8. Bowman, Craig T., "Kinetics of Nitric Oxide Formation in Combustion Processes," Fourteenth Symposium (International) on Combustion, The Combustion Institute, 1972, pp. 729-738.

9. Touchton, G.L., "Influence of Gas Turbine Combustor Design and Operating Parameters on Effectiveness of NO_x Suppression by Injected Steam or Water," Transactions of the ASME, Vol. 107, July 1985, pp. 706-713.

10. Miyauchi, T., Y. Mori and T. Yamaguchi, "Effect of Steam Addition on NO Formation," Eighteenth Symposium (International) on Combustion, The Combustion Institute, pp. 43-51, 1981.

11. Fenimore, C.P., "Formation of Nitric Oxide in Premixed Hydrocarbon Flames," Thirteenth Symposium (International) on Combustion, The Combustion Institute, 1971.

12. Hayhurst, A.N., and I.M. Vince, "The Origin and Nature of "Prompt" Nitric Oxide in Flames," Combustion and Flame, Vol. 50, pp. 41-57, 1983.

13. Bachmaier, F., K.H. Eberius, and Th. Just, "The Formation of Nitric Oxide and the Detection of HCN in Premixed Hydrocarbon-Air Flames at 1 Atmosphere," Combustion Science and Technology, Vol. 7, pp. 77-84, 1973.

14. Heberling, P.V., " "Prompt NO" Measurements at High Pressures," Sixteenth Symposium (International) on Combustion, The Combustion Institute, 1977.

15. Blauwens, Joanna, Brun Smets, and Jozef Peeters, "Mechanism of "Prompt" NO Formation in Hydrocarbon Flames," Sixteenth Symposium (International) on Combustion, The Combustion Institute, 1976, pp. 1055-1064.

16. Duterque, Jean, Nicole Avezard, and Roland Borghi, "Further Results on Nitrogen Oxides Production in Combustion Zones," Combustion Science and Technology, Vol. 25, pp. 85-95, 1981.

17. Sarofim, A.F., and J.H. Pohl, "Kinetics of Nitric Oxide Formation in Premixed Laminar Flames," Fourteenth Symposium (International) on Combustion, The Combustion Institute, pp. 739-754, 1973.

18. Iverach, David, Nikolas Y. Kirov, and Brian S. Haynes, "The Formation of Nitric Oxide in Fuel-Rich Flames," Combustion Science and Technology, Vol. 8, pp. 159-164, 1973.

19. Miyauchi, T., Y. Mori, and A. Imamura, "A Study of Nitric Oxide Formation in Fuel-Rich Hydrocarbon Flames: Role of Cyanide Species, H, OH and O," Sixteenth Symposium (International) on Combustion, The Combustion Institute, pp. 1073-1082, 1976.

20. Matsui, Yasuji, and Tamotsu Nomaguchi, "Spectroscopic Study of Prompt Nitrogen Oxide Formation Mechanism in Hydrocarbon-Air Flames," Combustion and Flame, Vol. 32, pp. 205-214, 1978.

21. Sanders, W.A., C.Y. Lin, and M.C. Lin, "On the Importance of the Reaction CH_2 + N_2 = HCN + NH as a Precursor for Prompt NO Formation," Combustion Science and Technology, Vol. 51, pp. 103-108, 1987.

22. Heard, Dwayne E., Jay B. Jeffries, Gregory P. Smith, and David R. Crosley, "LIF Measurements in Methane/Air Flames of Radicals Important in Prompt-NO Formation," Combustion and Flame, Vol. 88, pp. 137-148, 1992.

23. Bilger, R.W., and R.E. Beck, "Further Experiments on Turbulent Jet Diffusion Flames," Fifteenth Symposium (International) on Combustion, The Combustion Institute, 1974, pp. 541-552.

24. Lavoie, George A., and Albert F. Schlader, "A Scaling Study of NO Formation in Turbulent Diffusion Flames of Hydrogen Burning in Air," Combustion Science and Technology, Vol. 8, pp. 215-224, 1974.

25. Takagi, Toshimi, Mitsunobu Ogasawara, Kenichi Fujii, and Masahito Daizo, "A Study on Nitric Oxide Formation in Turbulent Diffusion Flames," Fifteenth Symposium (International) on Combustion, The Combustion Institute, pp. 1051-1059, 1975.

26. Peters, N. and S. Donnerhack, "Structure and Similarity of Nitric Oxide Production in Turbulent Diffusion Flames," Eighteenth Symposium (International) on Combustion, The Combustion Institute, pp. 33-42, 1981.

27. Drake, M.C., S.M. Correa, R.W. Pitz, W. Shyy, and C.P. Fenimore, "Superequilibrium and Thermal Nitric Oxide Formation in Turbulent Diffusion Flames," Combustion and Flame, Vol. 69, pp. 347-365, 1987.

28. Peters, N., "Laminar Flamelet Concepts in Turbulent Combustion," Twenty-first Symposium (International) on Combustion, The Combustion Institute, pp. 1231-1250, 1986.

29. Drake, Michael C., Robert W. Pitz, and Marshall Lapp, "Laser Measurements on Nonpremixed H_2-Air Flames for Assessment of Turbulent Combustion Models," Vol. 24, No. 6, June 1986.

30. Tsuji, Hiroshi, "Counterflow Diffusion Flames," Progress in Energy and Combustion Science, Vol. 8, pp. 93-119, 1982.

31. Kee, Robert J., James A. Miller, and Gregory H. Evans, "A Computational Model of the Structure and Extinction of Strained, Opposed Flow, Premixed Methane-Air Flames," Twenty-Second Symposium (International) on Combustion, The Combustion Institute, pp. 1479-1494, 1988.

32. Drake, Michael C., and Richard J. Blint, "Relative Importance of Nitric Oxide Formation Mechanisms in Laminar Opposed-flow Diffusion Flames," Combustion and Flame, Vol. 83, pp. 185-203, 1991.

33. Valenti, Michael, "Coal Gasification: An Alternative Energy Source is Coming of Age," Mechanical Engineering, January 1992, pp. 39-47.

34. Mitchell, R.E., Private Communication.

35. Puri, I.K., and K. Seshadri, "Extinction of Diffusion Flames Burning Diluted Methane and Diluted Propane in Diluted Air," Combustion and Flame, Vol. 65, pp. 137-150.

36. Schlichting, H., "Boundary Layer Theory," 6th Edition, McGraw-Hill, 1968.

37. Drake, M.C., "Kinetics of Nitric Oxide Formatiion in Laminar and Turbulent Methane Combustion," Gas Research Institue Report GRI-85/0271, December 1985.

38. Hargreaves, K.J.A., R. Harvey , F.G. Roper, and D.B. Smith, "Formation of NO_2 by Laminar Flames," Eighteenth Symposium (International) on Combustion, The Combustion Institute, 1981, pp. 133-142.

39. Hori, Morio, Naoki Matsunaga, and Philip C. Malte, "The Effect of Hydrocarbons on the Conversion of Nitric Oxide to Nitrogen Dioxide," Presented at the 1992

Spring Meeting of the Western States Section of the Combustion Institute, Corvallis, Oregon, March 1992.

40. Reynolds, W.C., "The Element Potential Method for Chemical Equilibrium Analysis: Implementation in the Interactive Program STANJAN," Version 3, Department of Mechanical Engineering, Stanford University, January 1986.

41. Roby, R.J., "A Study of Fuel-Nitrogen Reactions in Rich, Premixed Flames," Ph.D. Thesis, Stanford University, December 1987.

APPENDIX A:
SHOP DRAWINGS OF THE BURNER

AIR SIDE HOUSING

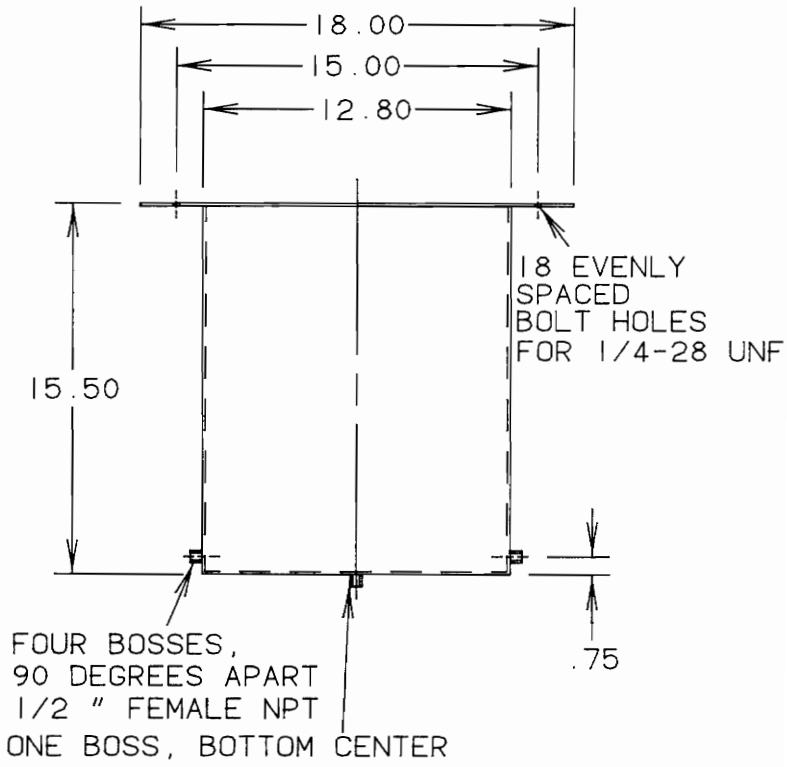

SCALE: 1 = 8

MATERIAL: 22 GUAGE SHEET METAL

ALL DIMENSIONS IN INCHES

FLOW STRAIGHTENER SPACERS

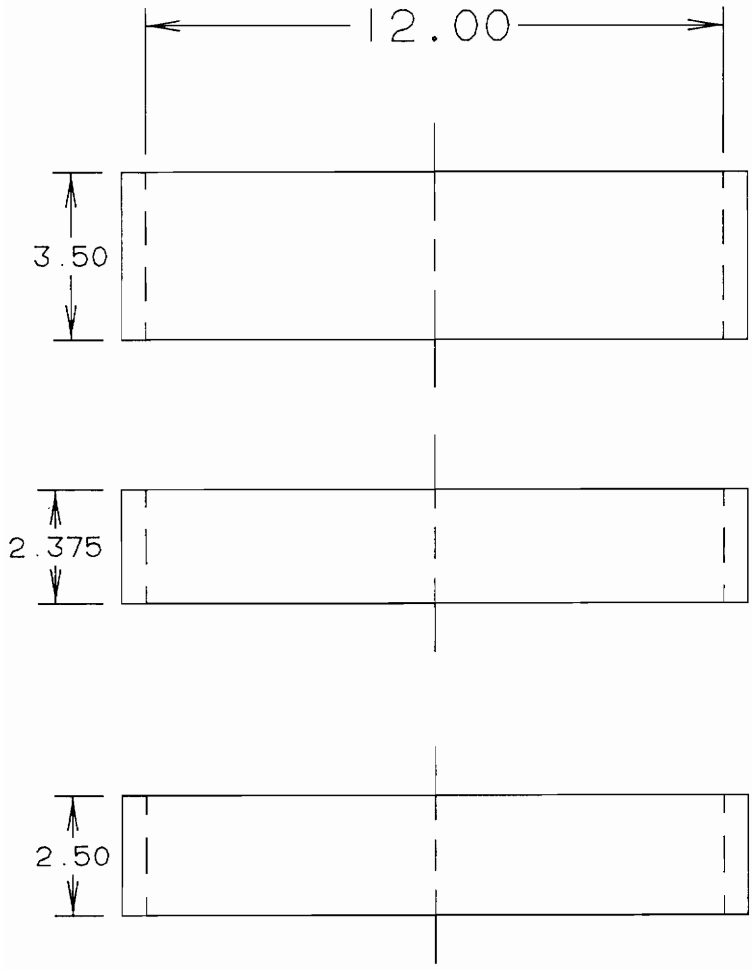

MATERIAL: PVC PIPE
SCALE: 1 = 4
DIMENSIONS IN INCHES

AIR INLET PIECE

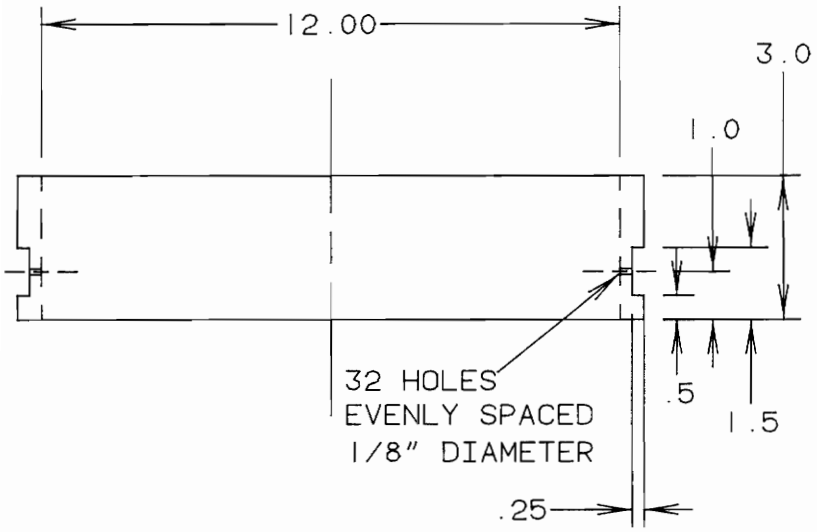

MATERIAL: PVC PIPE
SCALE: 1 = 4
ALL DIMENSIONS IN INCHES

CHIMNEY FLANGE

TOP VIEW

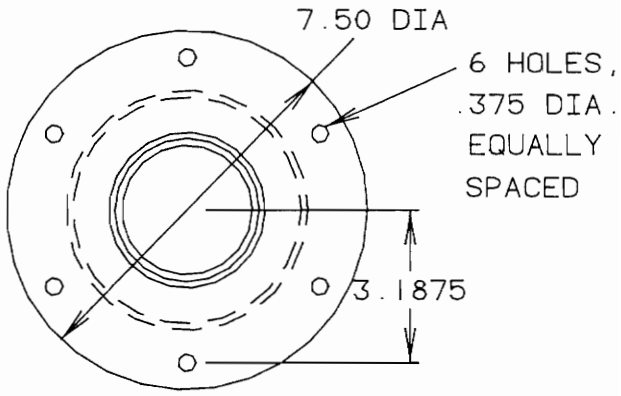

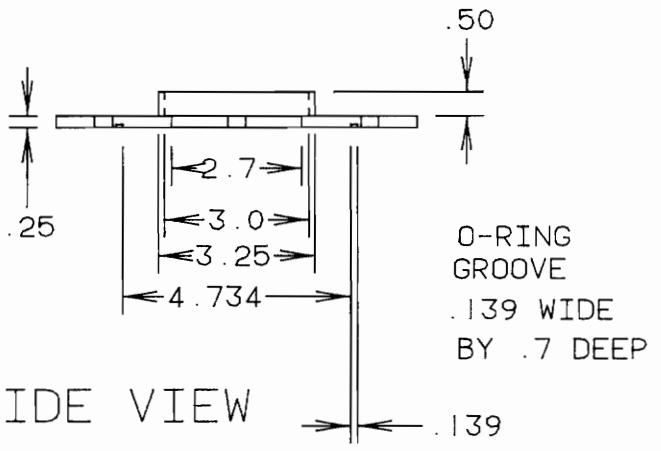

SIDE VIEW

MATERIAL: ALUMINUM

1. FUEL NOZZLE UPPER PLATE

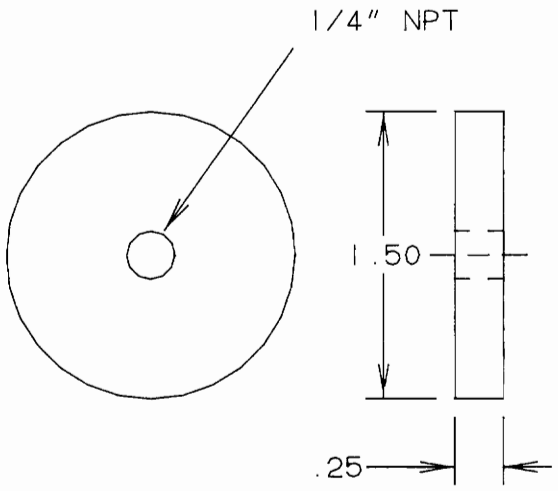

2. FUEL NOZZLE LOWER PLATE

FOR HOLE PATTERN,
SEE ATTACHED SKETCH.

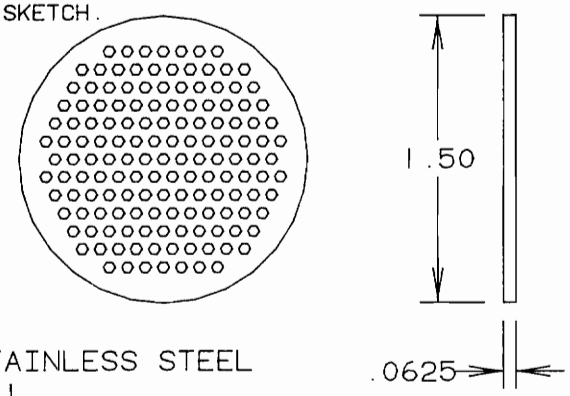

MATERIAL: STAINLESS STEEL
SCALE: 1 = 1

WELD UPPER AND LOWER PLATES TO NOZZLE BODY.

ALL DIMENSIONS IN INCHES

3. NOZZLE BODY

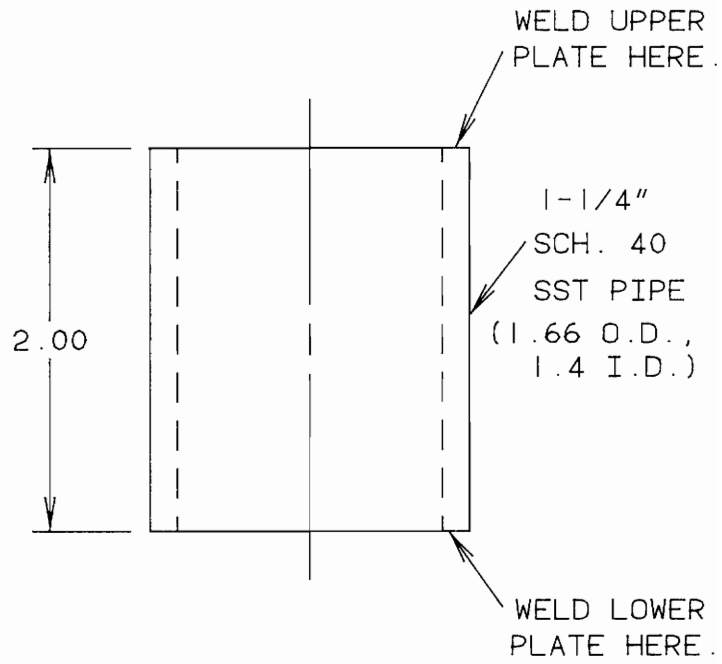

MATERIAL: SST PIPE
SCALE: 1 = 1
ALL DIMENSIONS IN INCHES

4. LOWER PLATE HOLE PATTERN

SCALE: 2 = 1
147 HOLES
HOLES 1/16" IN DIAMETER
3/32" CENTER TO CENTER SPACING
ONLY 1/4 OF PLATE SHOWN
ALL DIMENSIONS IN INCHES

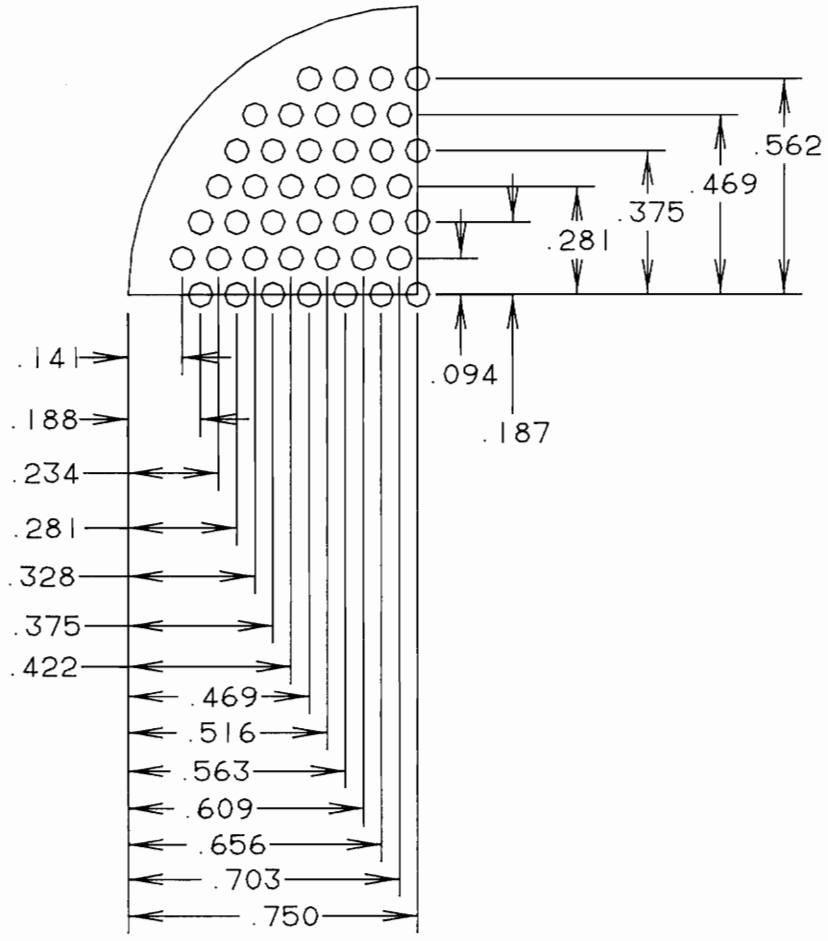

CONDENSATE TRAP

ALL DIMENSIONS IN INCHES

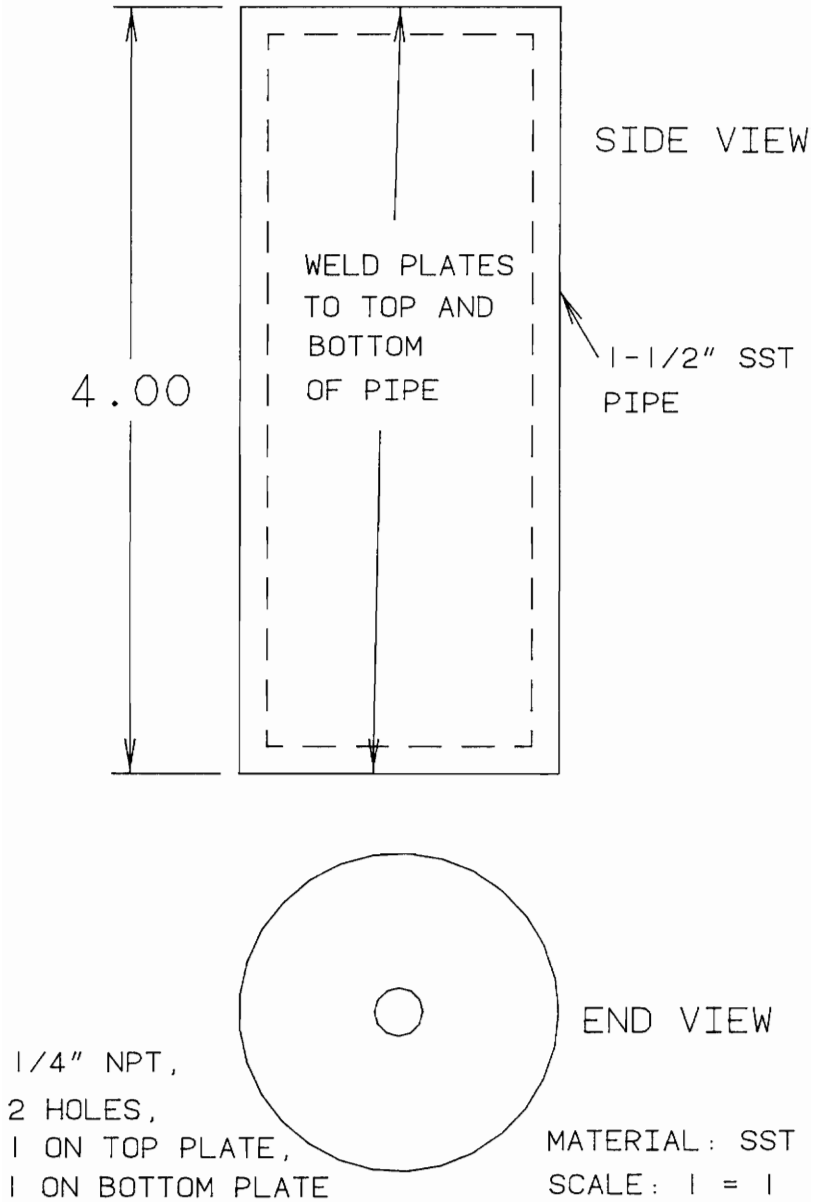

APPENDIX B:
CALIBRATION CURVES

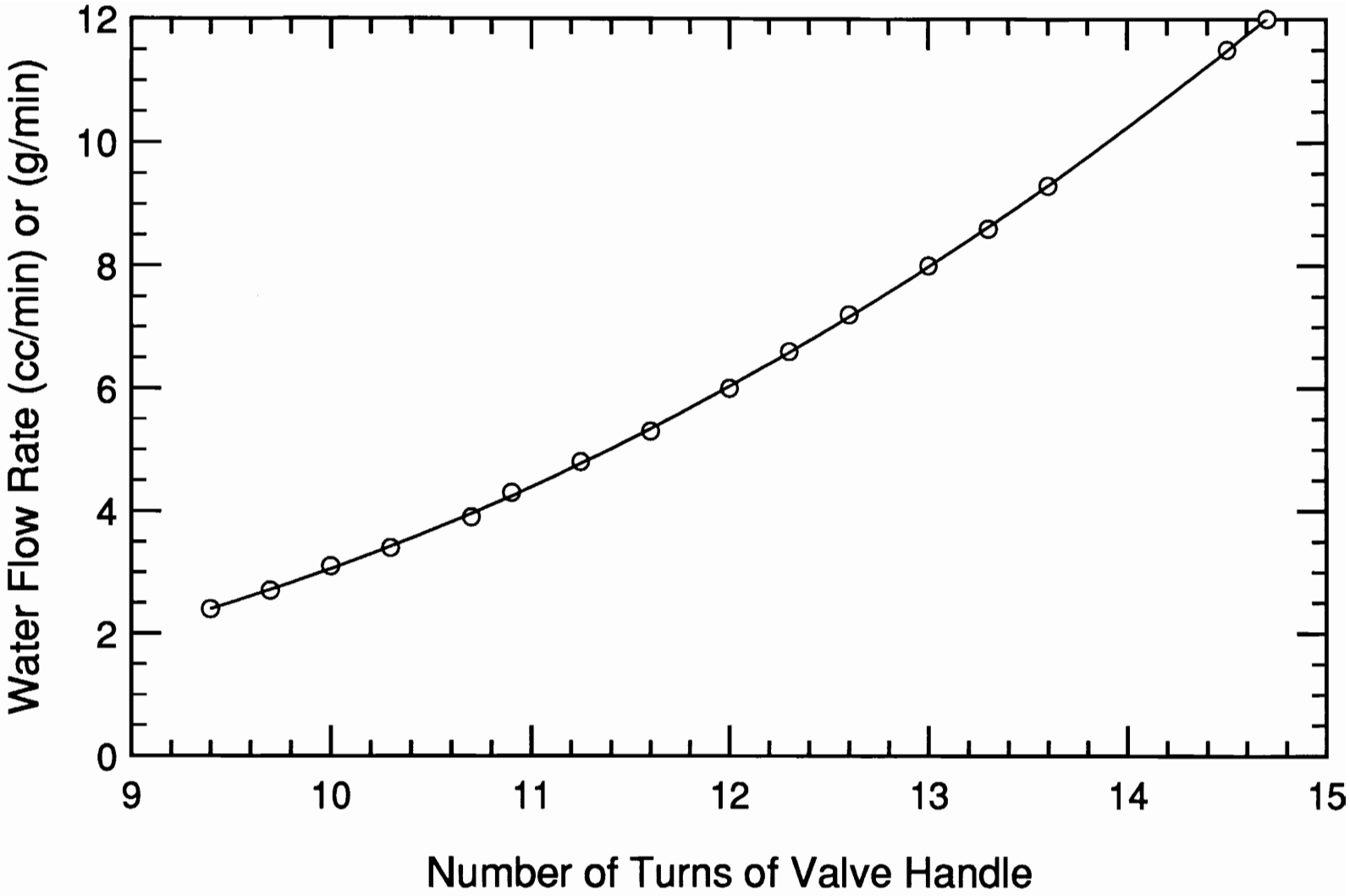

Figure 38. Calibration curve for fine metering valve.

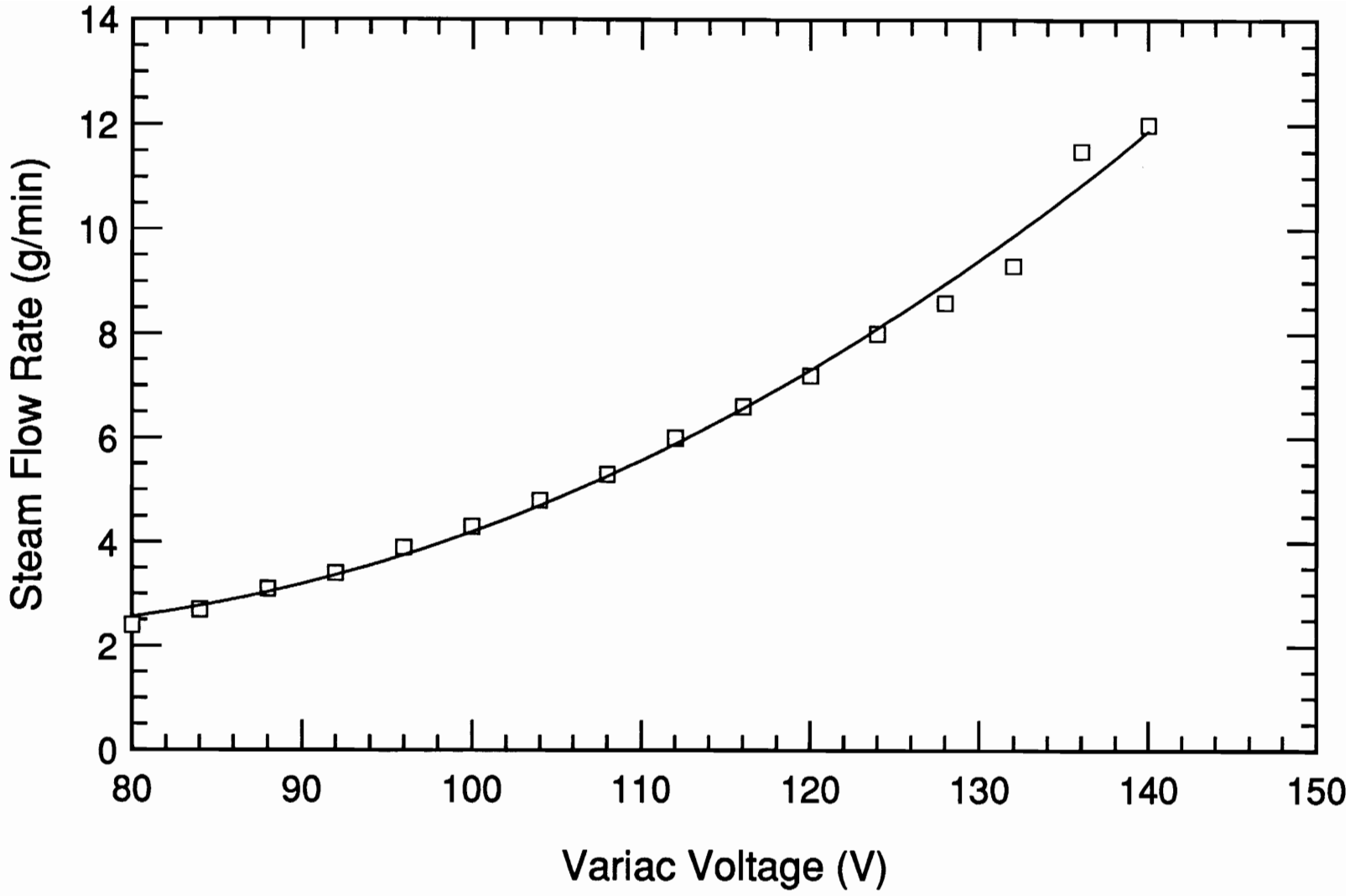

Figure 39. Calibration curve for variac.

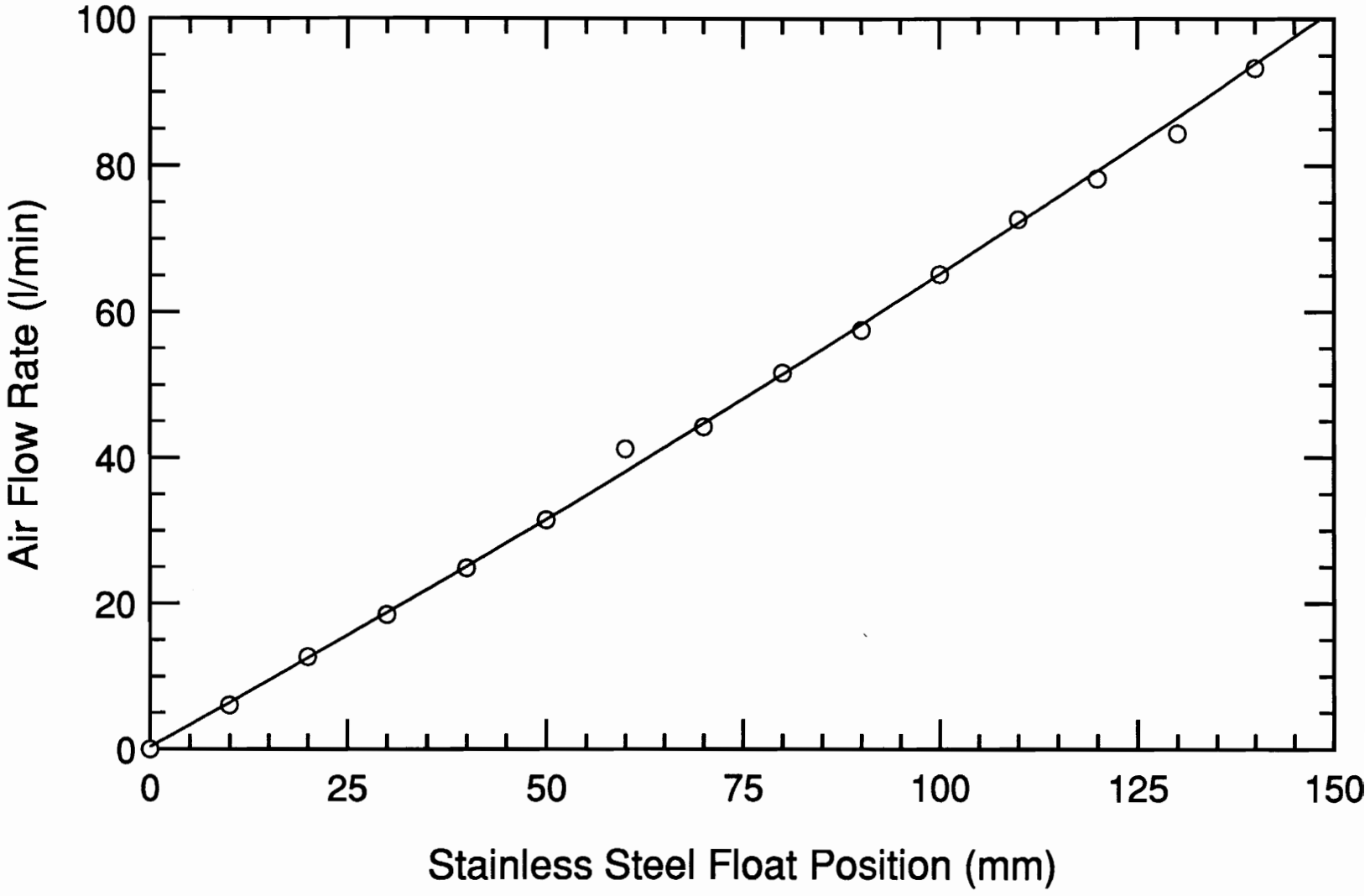

Figure 40. Calibration curve, air, Matheson 605 tube, 550 KPa or 80 psig.

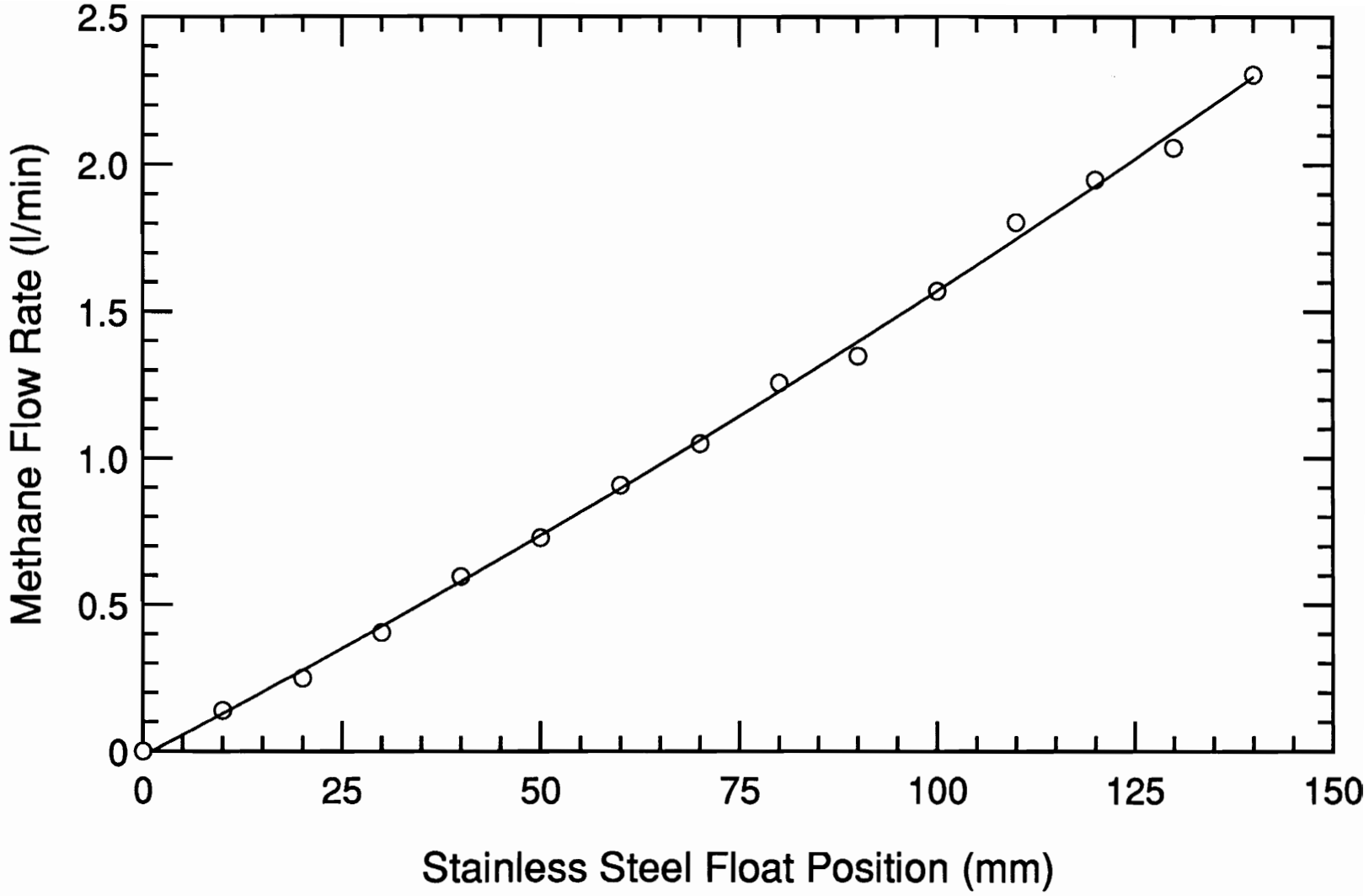

Figure 41. Calibration curve, CH_4, Matheson 602 tube, 280 KPa or 40 psig.

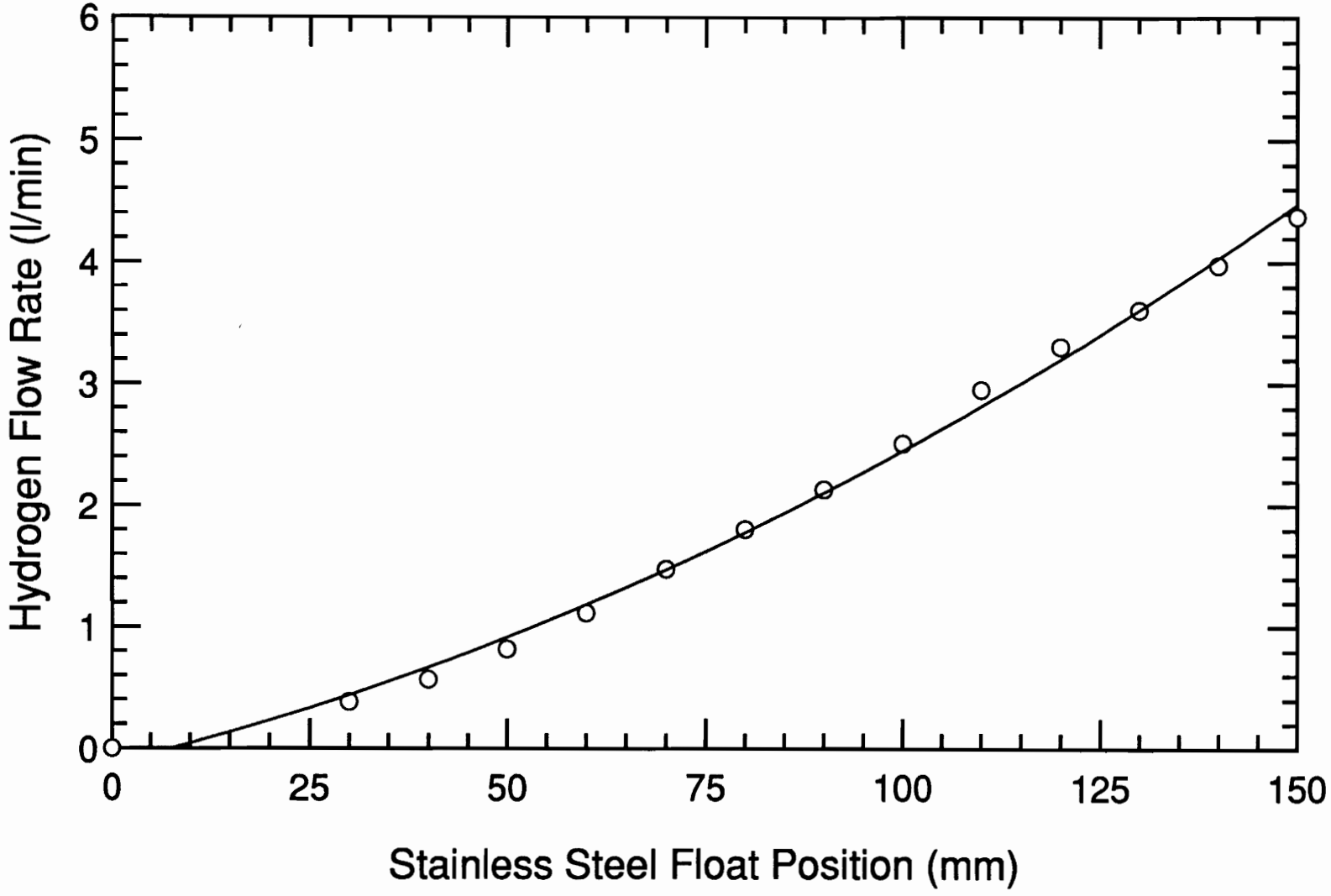

Figure 42. Calibration curve, H_2, Matheson 602 tube, 140 KPa or 20 psig.

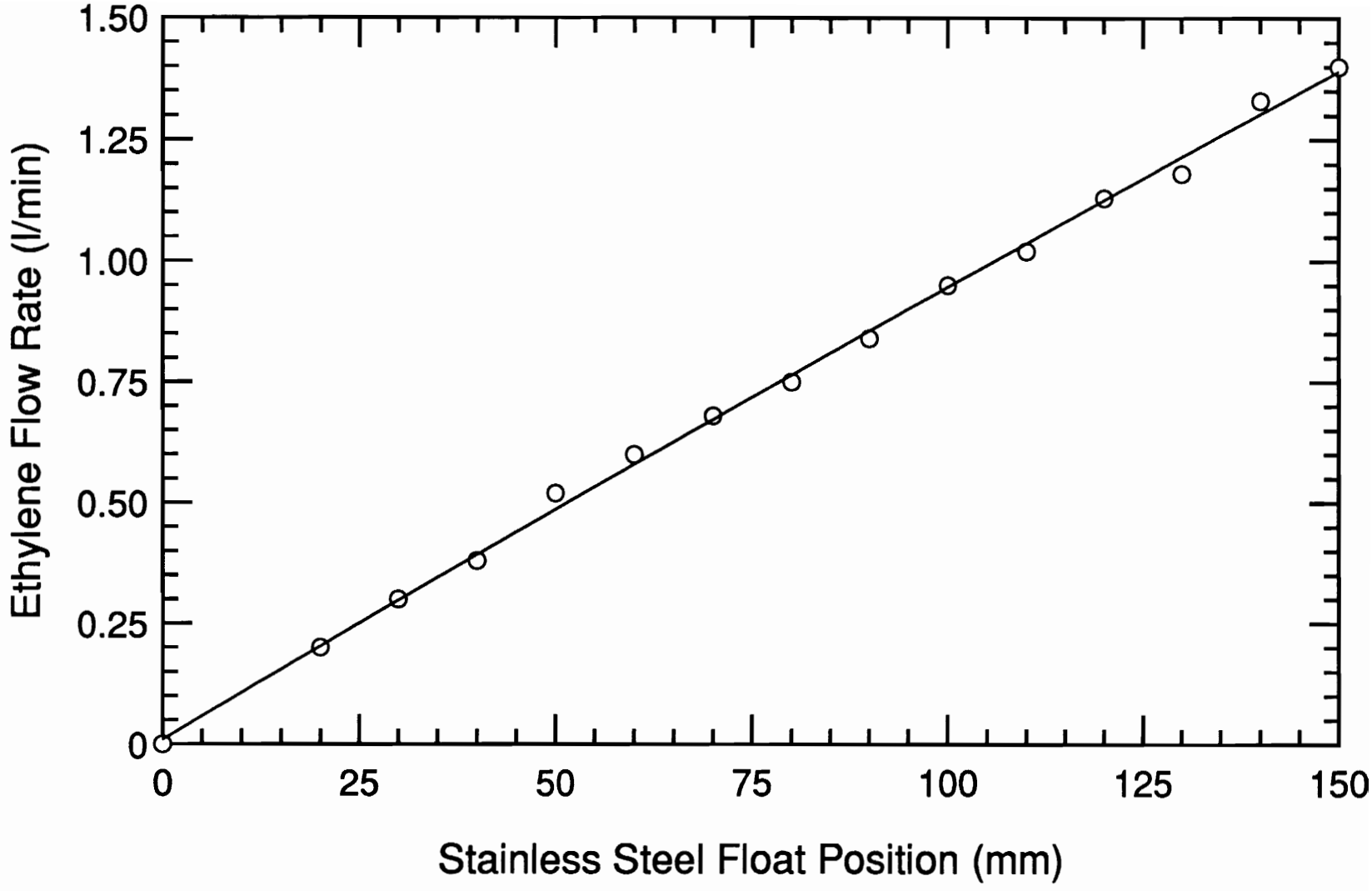

Figure 43. Calibration curve, C_2H_4, Matheson 602 tube, 140 KPa or 20 psig.

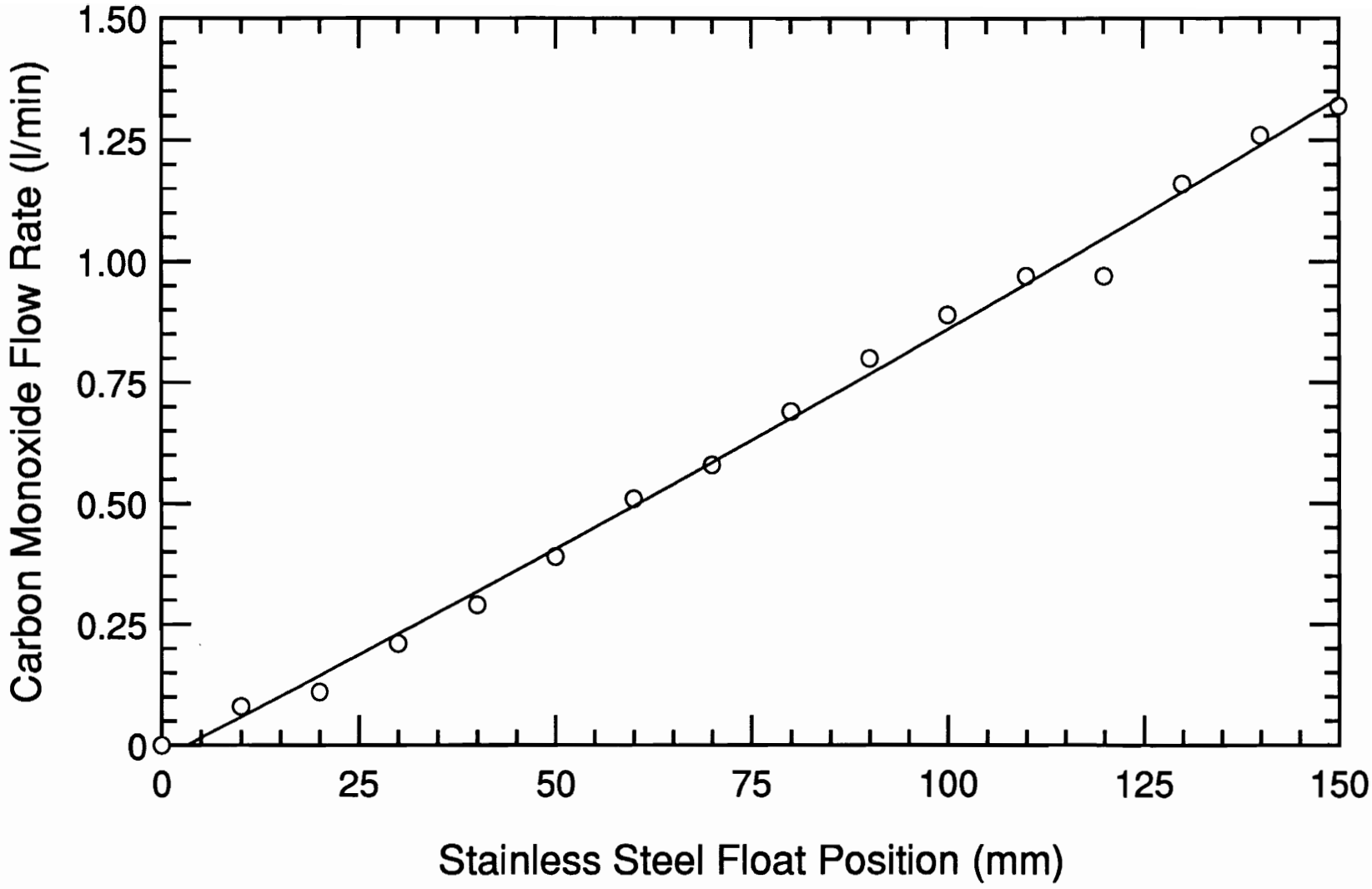

Figure 44. Calibration curve, CO, Matheson 602 tube, 140 KPa or 20 psig.

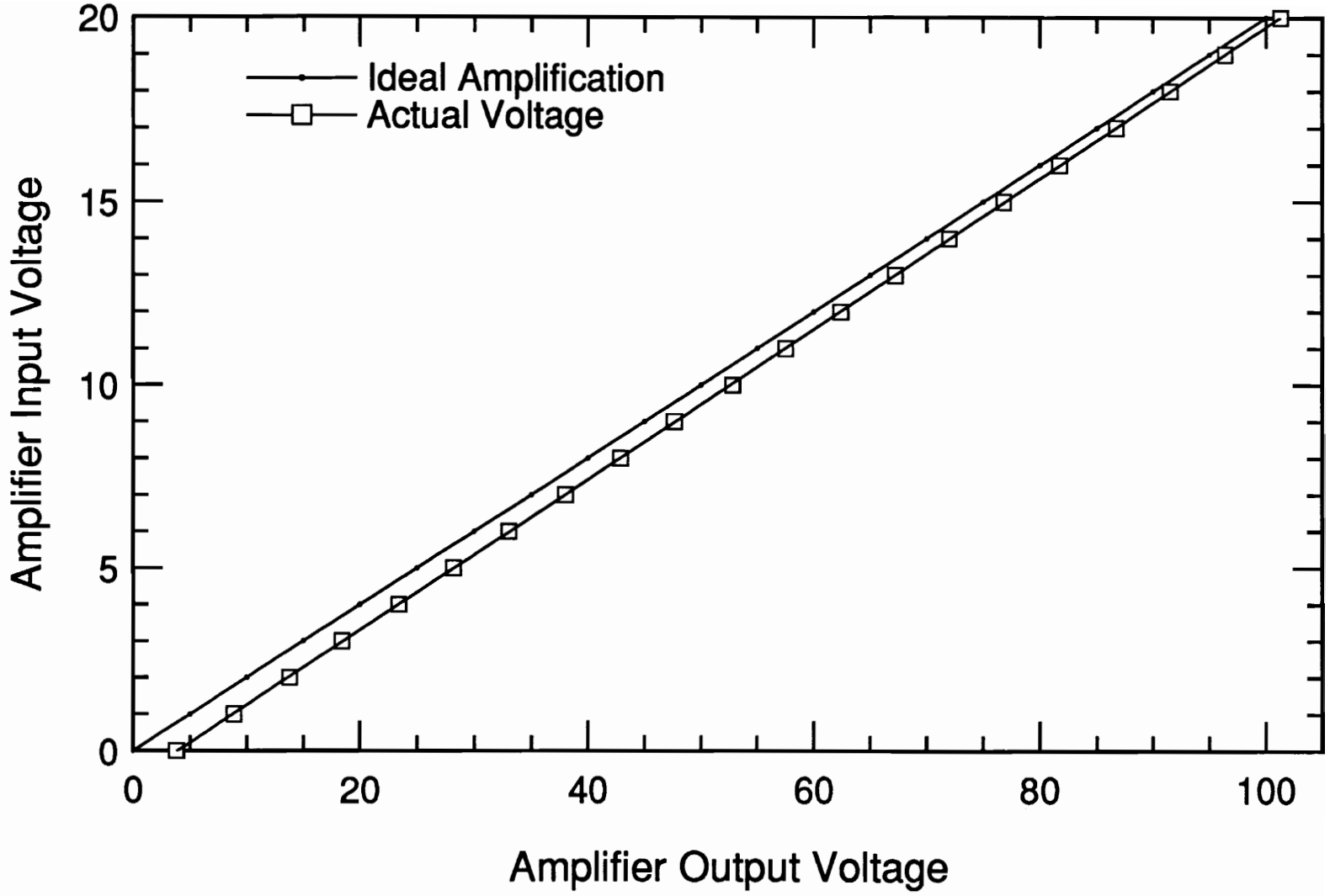

Figure 45. Calibration curve, OMEGA OMNI II-A millivolt amplifier.

APPENDIX C:
THERMOCOUPLE RADIATION CORRECTION PROGRAM

```
C THIS ROUTINE DETERMINES THE GAS TEMP. AT THE LOCATION
C OF A Pt/Pt10%Rh THERMOCOUPLE BEAD BY MAKING A RADIATION
C CORRECTION TO THE THERMOCOUPLE BEAD TEMPERATURE.
C
C TG = TC + SIGMA*EMISS*D*(TC**4-TW**4)/LAMDA/NU
C
C WHERE: TC    = THERMOCOUPLE BEAD TEMPERATURE
C       SIGMA = STEFAN-BOLTZMANN CONSTANT,
C                                  CAL/SQCM/SEC/K
C       EMISS = THERMOCOUPLE WIRE EMISSIVITY
C       D     = BEAD DIAMETER, CM
C       TW    = TEMPERATURE OF SURROUNDINGS
C       LAMDA = GAS THERMAL CONDUCTIVITY,
C                                  CAL/CM/SEC/K
C       NU    = NUSSELT NUMBER OF THE BEAD
C
C DECLARATION OF VARIABLES
      REAL LAMDA,NU
      INTEGER FLAG
C
C OPENING OF DATA FILE
C
      OPEN (7,FILE = 'tt.dat')
      OPEN (8,FILE = 'tt2.dat')
C
C ASSIGNMENT OF VALUES TO CONSTANTS
C
      SIGMA = 1.355E-12
      EMISS = 0.3
      NU = 2.0
      FLAG = 0
C
C WRITING OF DATAFILE TITLES
C
      WRITE (7,100)
  100 FORMAT (22X,'THERMOCOUPLE CORRECTION DATA',/,13X,
     $'(TEMPERATURES IN KELVIN; DISTANCES IN MM)',//)
      WRITE (7,110)
  110 FORMAT (5X,'  Y  ',4X,' MV  ', 3X,'BEAD TEMP',6X,
     $'CORRECTED GAS TEMP',/)
C
C CHECK FOR SERIES TYPE DATA
C
      WRITE (*,120)
  120 FORMAT (5X,'WILL BEAD DIAMETER AND SURROUNDINGS
TEMPERATURE',/,5X,
     $'BE THE SAME FOR ALL INPUT (Y OR N)?',\)
      READ (*,130) IYY
  130 FORMAT (A1)
  135 FORMAT (F10.6)
      IF (IYY.EQ.'Y') THEN
```

```
        FLAG = 1
        WRITE (*,140)
 140      FORMAT (/15X,'ENTER SURROUNDINGS TEMPERATURE (C): '\)
        READ (*,135) TW
        WRITE (*,150)
 150      FORMAT (15X,'ENTER BEAD DIAMETER (MM): '\)
        READ (*,135) D
        TW = TW + 273.0
        D = D / 10.
     ENDIF
C
C WRITING OF DESCRIPTION OF PROGRAM FUNCTION
C
     WRITE (*,160)
 160  FORMAT (/3X'THIS CODE MAKES RADIATION CORRECTIONS TO A
THERMOCOUPL
    $E BEAD TEMPERATURE'/)
C
C READING IN OF THERMOCOUPLE AND TEMPERATURE DATA
C
 300  CONTINUE
     IF (FLAG.NE.1) THEN
        WRITE (*,140)
        READ (*,135) TW
        WRITE (*,150)
        READ (*,135) D
        TW = TW + 273.0
        D = D / 10.
     ENDIF
     WRITE(*,169)
 169  FORMAT (15X,'ENTER DISTANCE FROM BURNER (MM): '\)
     READ (*,135) ST
     WRITE(*,170)
 170  FORMAT (15X,'ENTER THERMOCOUPLE READING (MV): '\)
     READ (*,135) V
     V = V / 1000.
     C0 = 0.927763167
     C1 = 169526.5150
     C2 = -31568363.94
     C3 = 8990730663.
     C4 = -1.63565E12
     C5 = 1.88027E14
     C6 = -1.37241E16
     C7 = 6.17501E17
     C8 = -1.56105E19
     C9 = 1.69535E20
     TC = C0+V*(C1+V*(C2+V*(C3+V*(C4+V*(C5+V*(C6+V*(C7+V*(C8+V*C9))))
    $))))
     TC = TC + 273.0
C
C THERMAL CONDUCTIVITY IS THAT FOR A MIXTURE OF EQUILIBRIUM
```

```
C PRODUCTS OF A LEAN (PHI=0.80) METHANE/OXYGEN/NITROGEN FLAME.
C LAMDA SHOULD BE EVALUATED AT TGAS.  AN ITERATIVE PROCESS IS
C SUGGESTED.  EXPERIENCE SHOWS THAT ONLY 3 TO 6 ITERATIONS
C ARE NEEDED.
C
      TG = TC
      DO 400 ITER = 1,6
         LAMDA = 5.0E-5*(TG/273.)**0.94
         TCORR = SIGMA*EMISS*D*(TC**4-TW**4)/LAMDA/NU
         TG = TC + TCORR
 400  CONTINUE
      ERROR = 0.2*TCORR
C
C PRESENTATION OF OUTPUT
C
      WRITE (*,180)
 180  FORMAT (//,20X,'CALCULATION OF TGAS'/20X'----------'/)
      WRITE (*,190) TC
 190  FORMAT(15X,'THERMOCOUPLE BEAD TEMPERATURE:  ',F6.1,' K')
      WRITE (*,200) TW
 200  FORMAT (15X,'SURROUNDINGS TEMPERATURE:  ',5X,F6.1,' K')
      D = D * 10.
      WRITE (*,210) D
 210  FORMAT (15X,'THERMOCOUPLE BEAD DIAMETER:  ',3X,F6.2,' MM')
      WRITE (*,220) TG,ERROR
 220  FORMAT (15X,'CORRECTED GAS TEMPERATURE:  ',4X,F6.1,' +/- ',F6.1,'
     $K')
C
C INQUIRY TO USER IF THERE ARE MORE CASES TO RUN
C
      V = V * 1000.
      WRITE (8,229) ST,V,TG,ERROR
 229  FORMAT (3X,F6.2,3X,F6.2,3X,F6.1,3X,F6.1)
      WRITE (7,230) ST,V,TC,TG,ERROR
 230  FORMAT (5X,F6.2,4X,F6.2,5X,F6.1,9X,F6.1,'+/-',F6.1)
      IF (FLAG.EQ.1) D = D / 10.
      WRITE(*,240)
 240  FORMAT (/15X,'ARE THERE MORE CASES TO RUN, Y OR N?'\)
      READ (*,250) IYY
 250  FORMAT (A1)
     WRITE (*,*)
      IF (IYY.NE.'N') GOTO 300
      CLOSE (7)
      CLOSE (8)
      END
```

APPENDIX D:
UNCERTAINTY ANALYSIS

Introduction

This appendix presents a brief uncertainty analysis for the experimental quantities of NO and NO_X concentrations, flame temperatures, and distances from the fuel nozzle. The method used to combine multiple errors associated with a single measurement was the root mean square addition technique described by Roby [41]. This method assumes that the errors are independent of each other, and that they are normally distributed. In this analysis, the quantity dx/X represents the total uncertainty of a measurement.

Uncertainty Analysis

The error in the NO and NO_X concentrations was 1.4%. This was determined by combining the error associated with reading the strip chart recorder and the uncertainty of the analyzer. The recorder had 50 divisions, which represented 0.2 V per division. It was assumed that the chart could be read in increments of one half of a division, which represented 0.1 V. Since the full scale output of NO_X analyzer was 10 V, one half of a division translated into 1% of the full scale reading. Thus, the error associated with reading the strip chart recorder was 1%. The uncertainty of the chemiluminescent analyzer was 1%, and was provided by the manufacturer. The following equation shows how these two errors were combined:

$$dx/X = [(0.01)^2 + (0.01)^2]^{1/2} = 0.014$$

Thus, the total error in the NO and NO_X concentration measurements was 1.4%.

Since the span gas used was only accurate to 240 ppm +/- 4.8 ppm, the absolute magnitude of all NO and NO_X measurements had a systematic error of +/- 4.8 ppm. This error was the same for all measurements, so that even though the absolute magnitudes

may have been slightly in error, the relative magnitudes of the measurements were accurate.

The flame temperature measurements were known within 2.8%. This accuracy was obtained by combining the error associated with reading the strip chart recorder and the error associated with the thermocouple radiation correction program. The thermocouple output voltage was amplified five times. The recorder had 50 divisions, which represented 2 mV per division. It was assumed that the chart could be read in increments of one half of a division, which represented 1 mV. A 1 mV error in the amplified signal corresponded to a 0.2 mV error in the original thermocouple reading. From the thermocouple temperature table, 0.2 mV corresponded to an uncertainty of +/- 2% in the range of temperatures measured in these experiments. Thus, the error associated with reading the strip chart recorder was 2%. The error of the thermocouple radiation program was 20% of the difference between the measured temperature and the corrected temperature. In the range of temperatures studied, this error corresponded to about 2% of the temperature reading. Thus, the error of the radiation correction program was 2%. The following equation shows how these two errors were combined:

$$dx/X = [(0.02)^2 + (0.02)^2]^{1/2} = 0.028$$

Thus, the total error in the temperature measurements was 2.8%.

The distance from the fuel nozzle was known to within 0.5 mm. This accuracy was a result of the ability to read the scale on the translation stage. The stage was marked in 1 mm increments. It was assumed that the scale could be read in increments of one half of a division. This meant that the accuracy was +/- 0.5 mm.

VITA

Linda Gail Akers Blevins was born February 11, 1966, in San Angelo, Texas. Because her father was in the United States Air Force, she grew up in Germany, Turkey, and the U.S.A. Her stateside homes were in Texas, Louisiana, Florida, and Alabama.

Linda graduated from Robert E. Lee High School in Montgomery, Alabama, in May 1984. She received a Bachelor of Science degree in Mechanical Engineering from the University of Alabama in December 1989. While attending the University of Alabama, Linda obtained professional experience by participating in the co-operative education program with Tennessee Eastman Company in Kingsport, Tennessee.

After graduation from the University of Alabama, Linda pursued a Master of Science degree in Mechanical Engineering from Virginia Polytechnic Institute and State University. Her graduate school funding was provided by a National Science Foundation Fellowship.

Linda's current plans are to pursue a Doctor of Philosophy in Mechanical Engineering at Purdue University. She will continue working in the field of combustion.

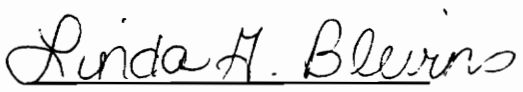

Linda G. Blevins